

**THE EFFECTS OF EXISTING WATER-ERODED CHANNELS ON WATER  
EROSION AND TILLAGE EROSION, AND THE INTEGRATION OF THESE  
EFFECTS INTO MODELS OF TOTAL SOIL EROSION**

by

FANGZHOU ZHENG

Thesis submitted to the Faculty of Graduate Studies of  
The University of Manitoba  
in partial fulfillment of the requirements of the degree of

DOCTOR OF PHILOSOPHY

Department of Soil Science  
University of Manitoba  
Winnipeg

Copyright © 2023

## **ABSTRACT**

Water erosion creates rills and gullies. These water-eroded channels are focal points for water, wind, and tillage erosion processes as they can function as pathways for sediment transport, sources or traps of sediments and topography features that alter the nature of soil redistribution by tillage. The linkages and interactions of different erosion processes around the channel area are complex and dynamic, not only during the period when the channel is created but also after it is created. There are many studies focusing on the generation and development of channels during water erosion events. However, their effects on subsequent water and tillage erosion events and their contribution to total soil erosion have not been examined. To fill this knowledge gap, we carried out three studies, focusing on the role of channels in water and tillage erosion processes and the assessment of total soil erosion.

In the first study, we examined the effects of a channel on tillage translocation. In this plot experiment, we used point tracers to track soil movement and measured tillage translocation under three tillage treatments: downslope tillage (DT), upslope tillage (UT), and contour tillage (CT) with three channel treatments: no channel, 10-cm-by-10-cm channel, and 20-cm-by-20-cm channel. We found that for DT, the presence of a channel reduced total translocation, whereas, for UT, it increased total translocation. This trend was attributed to a decrease in forward translocation under DT and an increase in forward translocation under UT with the presence of channels, while lateral translocation was not significantly affected by the presence of channels. For CT, the presence of a channel increased both forward and lateral soil

translocation and, therefore, total translocation. Process-wise, we found that the patterns of tillage translocation can be well explained by the relative importance of the trapping effect (channel functions like a trap for moving soil) versus the energy-intensity-increase effect (greater energy intensity due to less soil being moved with the presence of a channel). Soil movement decreases when the trapping effect dominates and increases when the energy-intensity-increase effect dominates.

In the second study, we used another plot experiment to examine the effects of an existing channel and tillage on water erosion. There were four treatments: no channel- no tillage (as the control); with a channel-no tillage; no channel-with tillage; and with a channel-with tillage. We found that with an existing channel, runoff discharge and sediment export have increased, whereas, with tillage, runoff discharge and sediment export have decreased. When an existing channel was tilled, the effects of tillage dominated, while the existing channel only demonstrated some minor impacts.

In the third study, a modeling procedure was developed to integrate the Raster-RUSLE2 (RUSLER), Ephemeral Gully Erosion Estimator (EphGEE) and Modified Directional Tillage Erosion Model (ModDirTilLEM) for simulating sheet and rill erosion, gully erosion and tillage erosion, respectively. In particular, knowledge gained from previous studies on the effects of channels on water and tillage erosion were incorporated into the models to reflect the linkages and interactions between different erosion processes. The modeling results were validated against field measurements on two sites in Atlantic Canada. We found that individual models provide reasonable estimations for the individual erosion processes. The integrated model was

able to provide accurate estimations of total soil erosion for most parts of the fields. However, around the ephemeral gully areas, errors and uncertainties were high. This situation could be due to the dynamic erosion processes in these areas, or the low resolution and accuracy of the model input data, indicating that the gully area is a weak point for soil erosion modeling, which calls for detailed investigation in the future.

## **ACKNOWLEDGEMENTS**

I would like to acknowledge the Agricultural and Agri-Food Canada and the Canadian Natural Science and Engineering Research Council (NSERC) for funding.

I would like to thank my Advisory Committee members: Dr. Genevieve Ali, Dr. Philip Owens, Dr. Fan-rui Meng, and in particular, my supervisors, Dr. David Lobb and Dr. Sheng Li, for their support and thoughtful advice for my studies at the University of Manitoba.

I would like to thank Zhisheng Xing, Yulia Kupriyanovich, Yefang Jiang, Sylvie Lavoie, Jacques Williams, Alyre Godin, Meagan Betts, Tegan Smith, Joyce Wang, Samantha Soubasis, Michael Colford, Brian Murray and Kang Liang for their help with the field experiments and/or lab analyses.

Especially, I would also like to thank my wife, Aanran Chen, my baby girls, Olivia (Weimiao) and Amelia (Wei-xiao) and my parents (Qinfeng and Lan) back in China for their tremendous moral support.

# TABLE OF CONTENTS

<b>ABSTRACT</b> .....	<b>I</b>
<b>ACKNOWLEDGEMENTS</b> .....	<b>IV</b>
<b>TABLE OF CONTENTS</b> .....	<b>V</b>
<b>LIST OF TABLES</b> .....	<b>VIII</b>
<b>LIST OF FIGURES</b> .....	<b>X</b>
<b>1. INTRODUCTION</b> .....	<b>1</b>
1.1 GENERAL BACKGROUND ON SOIL EROSION AND THE INTERACTIONS BETWEEN DIFFERENT EROSION PROCESSES .....	1
1.2 EFFECTS OF A WATER-ERODED CHANNEL ON TILLAGE TRANSLOCATION .....	6
1.3 EFFECTS OF CHANNEL REFILLING ACTION BY TILLAGE ON SUBSEQUENT WATER EROSION .....	7
1.4 MODELING OF TOTAL EROSION, INCLUDING INTERACTION EFFECT IN CULTIVATED FIELDS .....	8
1.5 REFERENCES.....	12
<b>2. A PLOT STUDY ON THE EFFECTS OF WATER-ERODED CHANNELS ON TILLAGE TRANLSOCATION</b> .....	<b>18</b>
CONTRIBUTIONS OF AUTHORS .....	18
2.1 ABSTRACT.....	18
2.2 INTRODUCTION.....	20
2.3 MATERIALS AND METHOD .....	23
2.3.1 <i>Study area and plot layout</i> .....	23
2.3.2 <i>Tracer installation and plot setup</i> .....	24
2.3.3 <i>Tillage equipment</i> .....	25
2.3.4 <i>Tillage operation and tracer sampling</i> .....	27
2.3.5 <i>Data Analysis</i> .....	29
2.4 RESULTS.....	33
2.4.1 <i>Tracer recovery, tillage speed and depth</i> .....	33
2.4.2 <i>Tillage translocation for DT and UT</i> .....	34
2.4.3 <i>Tillage translocation for CT</i> .....	43
2.5 DISCUSSION.....	46
2.5.1 <i>Mechanism of soil movement around channels</i> .....	46

2.5.2 <i>Implication for conservation tillage practices</i> .....	54
2.5.3 <i>Experimental errors and uncertainties</i> .....	56
2.5.4 <i>Future studies</i> .....	58
2.6 CONCLUSION .....	59
2.7 ACKNOWLEDGEMENTS .....	61
2.8 REFERENCES.....	61
2.9 NOMENCLATURE .....	67
<b>3. SHORT-TERM EFFECTS OF AN EXISTING CHANNEL, A SINGLE PASS OF TILLAGE AND THEIR INTERACTION ON THE GENGERATION OF RUNOFF AND SEDIMENT .....</b>	<b>69</b>
CONTRIBUTIONS OF AUTHORS .....	69
3.1 ABSTRACT.....	69
3.2 INTRODUCTION.....	70
3.3 MATERIALS AND METHODS.....	74
3.3.1 <i>Study area and plot layout</i> .....	74
3.3.2 <i>Plot setup</i> .....	76
3.3.3 <i>Rainfall simulation and data collection</i> .....	78
3.3.4 <i>Data analysis</i> .....	79
3.4 RESULTS.....	82
3.4.1 <i>Runoff</i> .....	82
3.4.2 <i>Sediment</i> .....	84
3.5 DISCUSSION.....	89
3.5.1 <i>Runoff and sediment generations on a bare soil surface</i> .....	89
3.5.2 <i>Effects of an existing channel</i> .....	90
3.5.3 <i>Effects of tillage</i> .....	91
3.5.4 <i>Effects of tilling an existing channel</i> .....	93
3.5.5 <i>Implications for soil and water conservation in Atlantic Canada</i> .....	94
3.5.6 <i>Future studies</i> .....	96
3.6. CONCLUSION .....	97
3.7. ACKNOWLEDGEMENTS .....	98
3.8 REFERENCES.....	98
3.9 NOMENCLATURE .....	105
<b>4. INTEGRATING WATER AND TILLAGE EROSION MODELS TO SIMULATE TOTAL SOIL EROSION IN CULTIVATED FIELDS.....</b>	<b>106</b>
CONTRIBUTIONS OF AUTHORS .....	106
4.1 ABSTRACT.....	106

4.2 INTRODUCTION .....	107
4.3 MATERIALS AND METHODS.....	111
4.3.1 <i>Study area</i> .....	111
4.3.2 <i>Integration of erosion models</i> .....	115
4.3.3 <i>Validation</i> .....	132
4.4 RESULTS .....	139
4.4.1 <i>Modeling water erosion, tillage erosion and their interactions</i> .....	139
4.4.2 <i>Model Validation</i> .....	145
4.5 DISCUSSION.....	154
4.5.1 <i>Erosion processes</i> .....	154
4.5.2 <i>Model performance based on Cs-137</i> .....	156
4.5.3 <i>Model performance based on other validation methods</i> .....	159
4.5.4 <i>Further studies</i> .....	161
4.6 CONCLUSION .....	162
4.7 ACKNOWLEDGEMENTS .....	163
4.8 REFERENCES.....	164
4.9 NOMENCLATURE .....	174
<b>5. GENERAL CONCLUSIONS .....</b>	<b>176</b>
5.1 THE CONTEXT OF THE RESEARCH.....	176
5.2 MAJOR FINDINGS .....	176
5.3 IMPLICATIONS FOR SOIL AND WATER CONSERVATION.....	179
5.4 SUGGESTIONS FOR FUTURE STUDIES .....	182
<b>APPENDIX.....</b>	<b>185</b>

## LIST OF TABLES

Table 2.1 Results of the linear regression analyses between absolute lateral translocation (y) and forward translocation (x). .....	39
Table 3.1 The Latin Square experimental design used in this study. Time and field were used as row and column factor to block temporal and spatial variations on experimental conditions, respectively. The treatments (i.e., NN, CN, NT, CT) were allocated to specific time and field based on a random selected Latin square .....	76
Table 3.2 The mean and coefficient of variation for runoff flow rate (RFR), runoff discharge (RD), runoff coefficient (RC), sediment yield (SY), total sediment export (TSE), and sediment concentration (SC) at 15, 30, 45 and 60 min after rainfall simulation started.....	86
Table 4.1 The input parameters used for RUSLER modeling .....	117
Table 4.2 The crop management operations for the 5-year crop rotation (grain-hay-grain-hay-potato) used for the PEI site .....	118
Table 4.3 The crop management operations for 3-year crop rotation (potato-potato-grain) for the NB site.....	120
Table 4.4 The crop management operations for 2-year crop rotation (potato-grain) used for the NB site.....	122
Table 4.5 The tillage translocation parameters ( $\alpha$ , $\beta$ , $\gamma$ and lateral throw direction) used in the ModDirTilLEM with different sites, crop rotations, and tillage tools .....	125
Table 4.6 The channel adjusting function applied for the channel cell in ModDirTilLEM with different tillage directions, channel directions (the distance ratio and mass ratio are obtained from the experiment described in Chapter 2, and the channel adjusting function is obtained from the calculation of distance ratio $\times$ mass ratio) .....	130
Table 4.7 The average soil erosion rate and its associated standard deviation (SD) obtained from different erosion models for overall and different landform positions for both of the PEI and NB sites.....	141

Table 4.8 The differences ( $\text{Mg ha}^{-1} \text{ yr}^{-1}$ ) between erosion estimates obtained from sampling points for overall and different landform positions for both of the PEI and NB sites ( $H_0$ : difference = 0,  $H_a$ : difference  $\neq$  0).....152

Table 4.9 Correlation coefficients for different erosion estimates obtained from all sampling points for both of the PEI and NB sites.....153

## LIST OF FIGURES

Figure 1.1. A schematic outlining how the chapters of this thesis are linked.....	11
Figure 2.1. The layout of point tracers dyed with four different colours in: a) downslope tillage, b) upslope tillage, and c) contour tillage plots. Squares indicate point tracers.....	26
Figure 2.2. a) The tillage equipment with sweeps (McKay 50 - 12 K) installed, and b) the targeted layout of the sweep arrangement with the downslope tillage and upslope tillage plots.....	27
Figure 2.3. Tillage translocation measurements for all three channel sizes under all three tillage direction treatments. a) DT, total translocation; b) DT, forward translocation; c) DT, absolute lateral translocation; d) UT, total translocation; e) UT, forward translocation; f) UT, absolute lateral translocation; g) CT, total translocation; h) CT, forward translocation; and i) CT, absolute lateral translocation. Capital letters indicate the comparisons between downslope and upslope tillage treatments, and lower-case letters indicate the comparisons between channel sizes within each chart. Mean values with different letters are significantly different from each other at $P < 0.10$ based on the Tukey test.....	36
Figure 2.4. The three parameters ( $P_{all}$ : the percentage of soil being moved into the channel area as oppose to outside of the channel area, $P_{loc}$ : the percentage of soil in each source area being moved into the channel area, and $P_{con}$ : the contribution of different source area to soil being moved into the channel area) calculated to indicate individual tracer movement relative to the channel. a) $P_{all}$ for DT; b) $P_{loc}$ for DT; c) $P_{con}$ for DT; d) $P_{all}$ for UT; e) $P_{loc}$ for UT and f) $P_{con}$ for UT. Capital letters indicate the comparisons between source areas and lower-case letters indicate the comparisons between channel sizes. Mean values with different letters are significantly different from each other at $P < 0.10$ based on the Tukey test. Only significant comparisons are denoted. ....	40
Figure 2.5. The total soil translocation of individual tracers under Contour Tillage treatment (CT) with channels in three different sizes (C0, C10 and C20). The shaded areas are NCAs before and after the channel area. Capital letters indicate the comparisons between different areas (within a chart) and lower-case letters indicate the comparisons between channel sizes (across different charts). Mean values with different letters are significantly different from each other at $P < 0.10$ based on the Tukey test. ....	45

Figure 2.6. Illustration of Zone of Influence (ZoI) for a tillage tool under different channel conditions and tillage directions. a) to d), e) to h) and i) to l) are for downslope, upslope and contour tillage, respectively. a) no channel, forward > lateral; b) sweep going through the channel, forward > lateral; c) sweep close to the channel, forward > lateral; d) sweep within impact range of the channel, forward > lateral; e) no channel, forward < lateral; f) sweep going through the channel, forward < lateral; g) sweep close to the channel, forward < lateral; h) sweep within impact range of the channel, forward < lateral; i) no channel, forward > lateral; j) sweep before the channel; k) sweep going across the channel; and l) sweep passed the channel. Circles are iso-intensity lines. Soil particles theoretically move in directions perpendicular to the iso-intensity lines. The thickness of the line indicates the degree of influence (decreases from the centre to outside).....48

Figure 3.1. a) a CN treatment plot before tillage (the red line delineates the boundary of the plot); b) the tractor hooked with a chisel plow used in this study; c) an NT treatment plot during the rainfall simulation experiment; and d) an NT treatment plot after rainfall simulation.....77

Figure 3.2. The runoff initiation time (minute) for different treatments (NN, CN, NT and CT). For each treatment, the four dots represent the four repeats and the triangle represents average values of the four repeats. ....83

Figure 3.3. Changes of: a) runoff flow rate ( $\text{mm hr}^{-1}$ ); b) runoff discharge (mm); c) runoff coefficient (%); d) sediment yield ( $\text{kg m}^{-2} \text{hr}^{-1}$ ); e) total sediment export (kg); and f) sediment concentration ( $\text{g L}^{-1}$ ) with time for the four treatments. ....85

Figure 4.1. The location of the PEI site is within the watershed near Harrington, PEI..... 113

Figure 4.2. a) The topography of the PEI site within the watershed near Harrington, PEI; b) the topography of the NB site near Grand Falls, NB..... 114

Figure 4.3. The grid points (red cross) along the tillage directions are generated for the tillage erosion modeling for the PEI site..... 124

Figure 4.4. a) The locations (black dot) of sampling points (n=50) in the PEI site; b) the locations (black dot) of sampling points (n=67) in the NB site..... 135

Figure 4.5. a) The predicted soil loss rate ( $\text{Mg ha}^{-1} \text{yr}^{-1}$ ) from RUSLER for the PEI site; b) the predicted soil loss rate ( $\text{Mg ha}^{-1} \text{yr}^{-1}$ ) from RUSLER for the NB site (the green/blue and dark colour indicate soil accumulation, whereas the brown and light colour indicate soil loss). .... 140

Figure 4.6. a) The predicted soil loss rate ( $\text{Mg ha}^{-1} \text{ yr}^{-1}$ ) from EphGEE for the PEI site, with the average soil erosion rate of 936.0 and 243.4  $\text{Mg ha}^{-1} \text{ yr}^{-1}$  for the G1 and G2, respectively; b) the predicted soil loss rate ( $\text{Mg ha}^{-1} \text{ yr}^{-1}$ ) from EphGEE for the NB site, with the average soil erosion rate of 606.5 and 236.2  $\text{Mg ha}^{-1} \text{ yr}^{-1}$  for the G1 and G2, respectively (the green/blue and dark colour indicate soil accumulation, whereas the brown and light colour indicate soil loss. G1 indicates the main channel and G2 indicates the tributary channel). ..... 142

Figure 4.7. a) The predicted soil loss rate ( $\text{Mg ha}^{-1} \text{ yr}^{-1}$ ) from DirTillem for the PEI site; b) the predicted soil loss rate ( $\text{Mg ha}^{-1} \text{ yr}^{-1}$ ) from DirTillem for the NB site (the green/blue and dark colour indicate soil accumulation, whereas the brown and light colour indicate soil loss). ..... 143

Figure 4.8. a) The predicted soil loss rate ( $\text{Mg ha}^{-1} \text{ yr}^{-1}$ ) from ModDirTillem for the PEI site; b) the predicted soil loss rate ( $\text{Mg ha}^{-1} \text{ yr}^{-1}$ ) from ModDirTillem for the NB site (the green/blue and dark colour indicate soil accumulation, whereas the brown and light colour indicate soil loss). ..... 144

Figure 4.9. a) The predicted soil loss rate ( $\text{Mg ha}^{-1} \text{ yr}^{-1}$ ) from the combination of RUSLER + EphGEE + ModDirTillem for the PEI site; b) the predicted soil loss rate ( $\text{Mg ha}^{-1} \text{ yr}^{-1}$ ) from the combination of RUSLER + EphGEE + ModDirTillem for the NB site (the green/blue and dark colour indicate soil accumulation, whereas the brown and light colour indicate soil loss). ..... 145

Figure 4.10. The drone-derived photo for the PEI site in 2018 after snow melting (the blue lines are the predicted ephemeral gully using EphGEE, and the red dash circled area is the sediment accumulation caused by rill erosion)..... 146

Figure 4.11. The drone-derived photo for the NB site in 2017 after snow melting (the blue lines are the predicted ephemeral gully using EphGEE, and the red dash circled area is the sediment accumulation caused by ephemeral gully erosion). ..... 147

Figure 4.12. a) The estimated soil loss rate ( $\text{Mg ha}^{-1} \text{ yr}^{-1}$ ) based on Cs-137 inventory using Proportional Model for the PEI site; b) the estimated soil loss rate ( $\text{Mg ha}^{-1} \text{ yr}^{-1}$ ) based on Cs-137 inventory using Proportional Model for the NB site (the green/blue and dark colour indicate soil accumulation, whereas the brown and light colour indicate soil loss, and the black dots indicate soil sampling points. The reference Cs-137 level is 1877  $\text{Bq m}^{-2}$  and 1448  $\text{Bq m}^{-2}$  for PEI and NB site, respectively)..... 150

# **1. INTRODUCTION**

## **1.1 General background on soil erosion and the interactions between different erosion processes**

Soil is the skin of the Earth that interacts with the lithosphere, the hydrosphere, the atmosphere, and the biosphere (Brady and Weil, 2016). More importantly, soil provides a medium for crop growth, supporting every human being's life. Historically, soil erosion refers to the wearing away of topsoil by natural agents such as water and wind (Brady and Weil, 2016). The studies of water erosion and wind erosion started in the 1930s, with the establishment of the Universal Soil Loss Equation (USLE) (Wischmeier and Smith, 1965) and Wind Erosion Prediction Equation (WEQ) (Chepil et al., 1962) as the respective milestones. In recent decades, it has been documented that soil erosion is also caused by another erosive agent (i.e., tillage), which moves soil downslope progressively, resulting in soil loss from hilltops and soil accumulation at the bottom of slopes (Lobb et al., 1995; Lobb and Kachanoski, 1999). The recognition of the erosive power of tillage can be dated back to the 1920s (Aufrère, 1929).

Previously, studies of soil erosion have mainly focused on a single erosion process and mostly at the plot scale (i.e. water, wind, and tillage erosion, separately) (Lal, 2001). Knowledge gained from these studies has been used to develop soil conservation practices, often targeted at a type of erosion. Therefore, these measures only work well when the targeted

erosion process dominates (Chow et al., 1999; Schnepf and Cox, 2006). However, these measures might not work well for the cultivated fields suffering multiple erosion processes (Lobb, 2003). Many fields in Canada are subject to the risk of more than one type of erosion process. For example, the potato fields in Atlantic Canada suffer water and tillage erosion due to the humid coastal climate, rolling landscape and the high soil disturbance associated with potato cropping (Chow et al., 1990). When both processes work together, they can result in high rates of total soil erosion (Li et al., 2007; 2008a). Furthermore, it should be noted that the frequency of incorporating potato cultivation within crop rotations exerts a substantial influence on the extent of soil erosion. Primarily, the cultivation of potato crops necessitates intensive tillage practices, a direct contributor to the phenomenon of tillage erosion. A higher frequency of potato cultivation within crop rotations increases susceptibility to tillage erosion. Additionally, in the context of tuber crops like potatoes, the process of crop harvesting can yield notable soil loss, with rates ranging from 1.0 to 14.0 Mg ha<sup>-1</sup> yr<sup>-1</sup> across spatial and temporal dimensions. This variability is depending upon factors encompassing soil characteristics, agronomic methodologies, harvesting techniques, and post-harvest interventions (Poesen, 2018). Hence, the higher frequency of potato cultivation escalates the potential for soil loss resulting from crop harvesting activities.

Usually, different erosion forms do not occur simultaneously in one event, but they can occur in a successive sequence (e.g. a rainfall event after a tillage operation followed by a wind storm event), resulting in possible linkage and interaction effects between different erosion processes (Lobb et al., 2003; Poesen et al., 2003). The linkage refers to the additive effects

among different processes. For example, on the upslope positions in fields, the processes of all water, tillage and wind erosion could cause and reinforce the soil loss. On the contrary, in the midslope or lowerslope positions, some processes cause soil loss while others cause soil accumulation. The three erosion processes together could cancel each other, resulting in no net soil loss or, potentially, resulting in net accumulation.

The interaction effects occur when one erosion process delivers sediment for another erosion process to act upon or when one erosion process changes the landscape erodibility for another erosion process. Firstly, the interaction can occur between water and wind erosion. In arid or semi-arid areas that suffer from wind erosion, soil particles can be transported to hillslopes or channels by the wind. These loose soil particles provide the materials to flush away the following water erosion event (Zhao et al., 2006). In addition, wind erosion leads to the loss of fine particles and the increase in soil coarseness and dryness (Zhao et al., 2006), increasing the potential for scouring by water flow (Gómez and Nearing, 2005; Römken et al., 2002). As a result, water erosion is reinforced. On the other hand, constant scouring by water flow can prevent the formation of crust layer on the soil surface. Therefore, the wind erosion is reinforced without the soil crust on the surface. Overall, the process of soil particle transportation by water erosion can be accelerated by wind erosion and wind erosion can be enhanced by water erosion as well (Erpul et al., 2002; Pedersen and Hasholt, 1995).

Secondly, the interaction can occur between tillage and wind erosion. Tillage erosion can redistribute soil within a landscape, moving soil from upslope to lowerslope areas. For the upslope area, where soil loss occurs, tillage erosion exposes more highly erodible subsoil,

which can lead to the high rates of wind erosion (Hevia et al., 2003; Six et al., 2000). In addition, For the lowerslope area, where soil accumulation occurs, the loose soil transported by tillage is highly erodible, which can result in high rates of wind erosion as well.

Lastly, interactions can occur between water and tillage erosion around the channel area. Channels (rills and ephemeral gullies) can be created in water erosion events, which are often filled or smoothed in the subsequent tillage operation. These channels are hollow spaces, reshaping the local topography and thereby affecting tillage erosion. On the other hand, tillage-induced accumulation usually occurs in contourly concave slopes. This area is subjected to strong channelized water erosion. Therefore, tillage erosion transports soil materials for water erosion to act upon (Lobb et al., 1995, 2003). Such interactions between tillage erosion and water erosion could be a major contributor to the total soil erosion in cultivated landscapes of humid climate regions like Atlantic Canada. This thesis centers on investigating the manifestations of water and tillage erosion, a focus driven by the experimentation carried out in the region of Atlantic Canada, where the water and tillage erosion contributed significantly towards total erosion. It is important to note that this thesis constitutes an initial stride in the broader exploration of erosion phenomena. Subsequent phases of research will encompass an examination of wind erosion, thus expanding the scope and depth of the study's investigation. Consequently, it is important to delineate that wind erosion, while integral to the research, does not command primary focus in this thesis.

In the previous total erosion studies, the total erosion is usually modeled as the sum of different erosion forms (Li et al., 2008a; Van Oost et al., 2000). This approach only considers

the linkage, not the interactions among different erosion processes. Why are the interactions ignored in most total erosion assessments? One reason is probably that the impact of one erosion process may have been partially accounted for in evaluating the effect of another. For example, in water erosion modeling (USLE), tillage as part of field management has been considered a factor affecting the estimation of water erosion rate (Renard, 1997; Wischmeier and Smith, 1965). Such argument may apply at the plot scale, with slope gradient being one of the dominant controlling factors. However, this argument may not apply at the field or landscape scale because of the tillage-induced soil redistribution. The pattern of soil erosion on a field scale can be very different from that estimated from topography alone. In addition, for water erosion experiments conducted at the plot scale, ephemeral gully erosion was not included in the experiments. As a result, the interactions between water erosion and tillage erosion around the ephemeral gully areas have not been accounted for.

In recent years, many researchers have used the interactions to explain the pattern of soil redistribution and soil properties observed (Li et al., 2008a; Poesen et al., 2003; VandenBygaert et al., 2012). However, studies on process interactions are still rare, particularly for the interaction between water erosion and tillage erosion (Dai et al., 2020; Zhang et al., 2014). There is a lack of field experiments on the interactions between water erosion and tillage erosion, especially on the critical roles channels may play.

Overall, for the cultivated fields subjected to substantial levels of both water erosion and tillage erosion (e.g., potato fields in Atlantic Canada), the current total erosion assessment misses an essential component – interactions between water erosion and tillage erosion. To

obtain a better understanding and estimation of the total erosion in cultivated fields, there is a need to examine, characterize and quantify the interactions between water erosion and tillage erosion processes. Since the interactions between these two erosion processes mainly occur around the water-eroded channel area, examining the roles channels may play for the water erosion and tillage erosion in cultivated fields is necessary.

The general objectives of this study were: firstly, to examine the effects of water-eroded channels on tillage erosion; secondly, to examine the effects of water-eroded channels refilling action by tillage on subsequent water erosion; and lastly, to model and validate the total erosion (including interactions) (Fig. 1.1). In this thesis, each data chapter tries to achieve the corresponding objective, respectively.

## **1.2 Effects of a water-eroded channel on tillage translocation**

Tillage erosion is a predominant erosion form causing soil loss in many cultivated fields (Li et al., 2008a). The result of soil displacement by tillage is called tillage translocation. Tillage erosion occurs when tillage operations translocate more soil out of an area than into that area (Van Oost et al., 2006). The local topography primarily impacts the pattern of tillage translocation and tillage erosion (Govers et al., 1994).

In cultivated lands, water-eroded channels are usually smoothed out by tillage operation. Since the locations of gullies are generally defined by topography, these gullies will reappear at roughly the same location after a major water erosion event. In the subsequent tillage operations, these gullies will be refilled by tillage again. Tillage translocation studies have been

focusing on the impacts of different tillage implements. The presence of gullies changes the soil surface's morphology, affecting tillage translocation and erosion. However, no study has been carried out to examine the tillage translocation in the presence of a water-eroded channel.

In the first data chapter of this thesis, plot experiments of tillage translocation were carried out at the Fredericton Research and Development Centre (FRDC) in New Brunswick. Tillage translocation under the combinations of three different tillage directions (downslope, upslope and contour) and three different channel conditions (no channel, 10-cm-by-10-cm channel, 20-cm-by-20-cm channel) was investigated. The movements of point tracers before and after the tillage operation were used to measure tillage translocation.

Overall, this study aimed to characterize and quantify the effects of tillage translocation under different tillage directions and channel sizes.

### **1.3 Effects of channel refilling action by tillage on subsequent water erosion**

When a channel is tilled over, it is deformed and filled. This is a form of tillage erosion as the soil has been redistributed by the action of tillage. The result of this form of tillage erosion can affect the subsequent water erosion event. Firstly, channel filling could block the pathway for sediment transport, reducing runoff and water erosion. Secondly, the newly deposited soil is easily erodible, increasing the potential risk of water erosion. Further investigation is required to determine the overall resultant effects of channel infilling by tillage on subsequent water erosion.

In recent years, a few studies have been carried out to investigate the interaction between tillage and channelized erosion. Wang et al. (2016) reported that tillage erosion increases soil erodibility and delivers the soil into rills for water erosion to act. Dai et al. (2020) reported that tillage erosion could increase the sediment yield of channelized water erosion on a hillslope. However, in these studies, the effects of tillage on water erosion were not quantified. Therefore, there is a knowledge gap on how existing channels and tillage individually affect water erosion and how an existing channel can link and interact with tillage in a water erosion event.

In the second data chapter of this thesis, rainfall simulation plot experiments were carried out in FRDC to quantify the effects of channels, tillage and their interactions on water erosion events. Four treatments: no channel, no-tillage; with a channel, no-tillage; no channel, with tillage; and with a channel, with tillage, were examined. Runoff and sediment samples collected from experimental plots were used to investigate the effects of different treatments.

Overall, this study aimed to characterize and quantify the effects of: a) an existing channel, b) a single pass of tillage, and c) a single pass of tillage filling an existing channel on the generation of runoff and sediment in a water erosion event.

#### **1.4 Modeling of total erosion, including interaction effect in cultivated fields**

Many water and tillage erosion models have been developed based on field studies. Sheet and rill erosions are often modeled with the Universal Soil Loss Equation (USLE) and its revised version RUSLE, RUSLE2, or the hillslope version of the Water Erosion Prediction Project (WEPP) (Flanagan and Nearing, 1995; Renard, 1997; Wischmeier and Smith, 1965).

For ephemeral gully erosion, Woodward (1999) developed Ephemeral Gully Erosion Model (EGEM) to simulate this specific erosion process. Several efforts have been made to integrate models for all water erosion forms (e.g., watershed version WEPP, Annual Agricultural Non-Point Source (AnnAGNPS), The Chemicals Runoff and Erosion from Agricultural Management Systems (CREAMS), Raster-based RUSLE2 and Ephemeral Gully Erosion Estimator (RUSLER & EphGEE)) (Bingner et al., 2003; Dabney et al., 2015; Flanagan and Nearing, 1995; Gordon et al., 2007; Knisel and Foster, 1981).

Tillage erosion can be modeled along hillslopes using Tillage Erosion Prediction (TEP) or Tillage Translocation Model (TillTM) (Li et al., 2008b; Lindstrom et al., 2000). At the field scale, tillage erosion can be modeled using Soil Redistribution by Tillage (SORET), Tillage Erosion model (TilLEM) and its upgraded version, Directional Tillage Erosion Model (DirTilLEM) (De Alba, 2003; Li et al., 2008b; Li et al., 2009).

However, not many attempts have been made to model both water erosion and tillage erosion together. Water and Tillage Erosion (WaTEM) attempted to sum the erosion rates from different types to calculate the total erosion rates at each grid node, accounting for the linkage effects between water and tillage erosion rates (Van Oost et al., 2000). WaTEM only considers the sheet, rill and tillage erosion forms. However, the ephemeral gully erosion is not included in the model. Clearly, no existing model considers all primary erosion forms (sheet, rill, ephemeral gully, and tillage erosion) in cultivated lands together with the interaction effects between channelized erosion and tillage erosion. To better design conservation measures for cultivated fields, a better estimation of total erosion is necessary. Therefore, it is necessary to

link the models accounting for three primary erosion forms in cultivated lands and to model the interaction effect between channelized erosion and tillage erosion.

In the third data chapter of this thesis, three computer programs – RUSLR, EphGEE, and DirTillem were used to estimate rates of different erosion forms in two cultivated field sites near Grand Falls, NB and Harrington, PE, respectively. The interactions between ephemeral gully erosion and tillage erosion were incorporated into the original erosion models (DirTillem). The model-predicted erosion patterns and rates were validated against air photos, topographic features and their evolutions obtained using photogrammetry, manually measured gully cross sections, runoff and sediment yield monitored at the outlet of the catchment, and Cs-137 derived erosion rates from two sites, respectively.

Overall, the objectives of this study were, firstly, to model the total erosion in cultivated fields considering all erosion processes and effects among different erosion processes using the knowledge gained from the first two data chapters, and secondly, to validate the total erosion model using different methods.

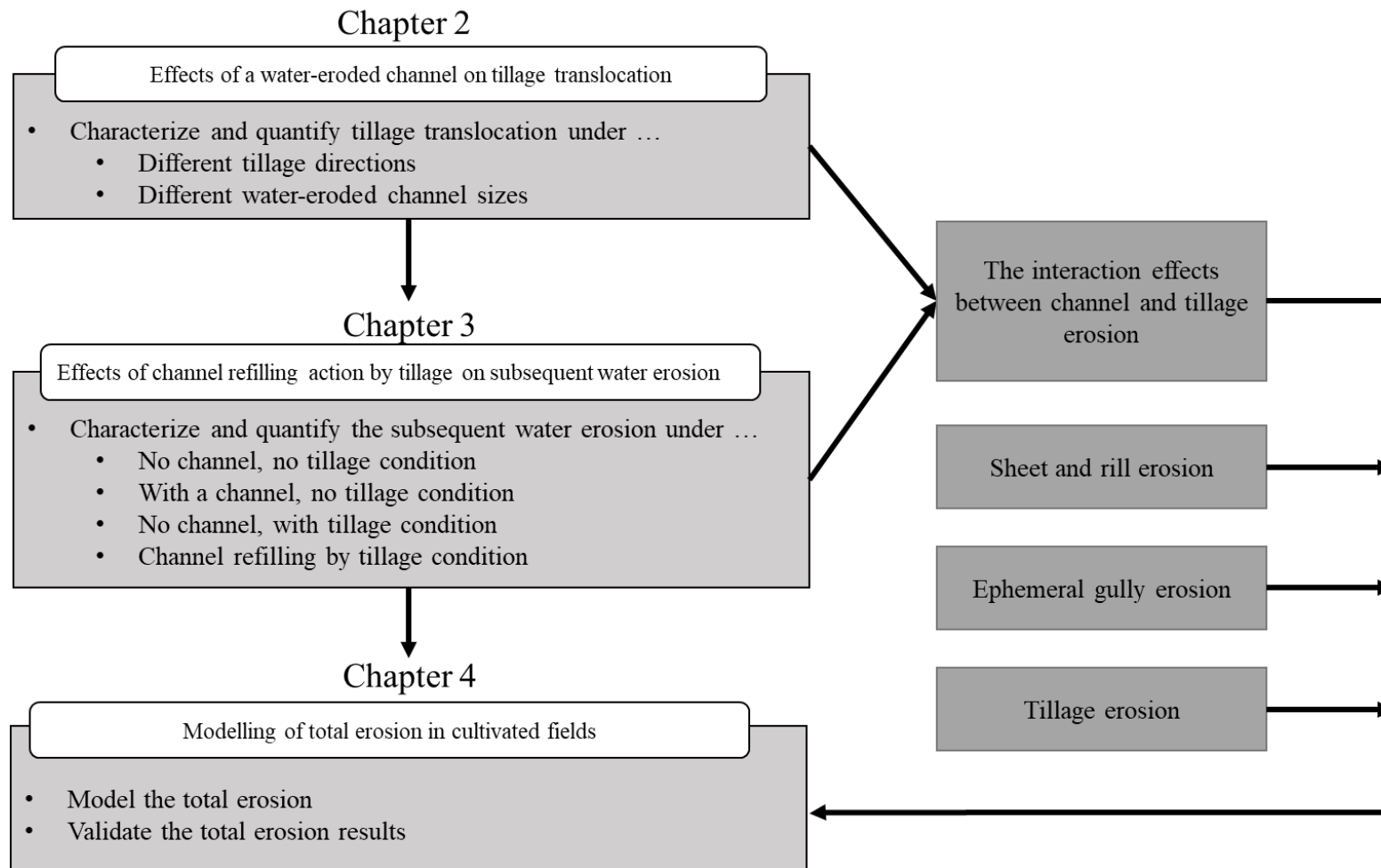


**Figure 1.1.** A schematic outlining how the chapters of this thesis are linked.

## 1.5 References

- Aufrère, L., 1929. Les rideaux: étude topographique, 216 ed. JSTOR, pp. 529-560.
- Bingner, R.L., Theurer, F.D., Yuan, Y., 2003. AnnAGNPS technical processes. USDA-ARS, Washington, D.C.
- Brady, N.C., Weil, R.R., 2016. The nature and properties of soils, 15 ed. Pearson, Columbus, Ohio.
- Chepil, W.S., Siddoway, F.H., Armbrust, D.V., 1962. Climatic factor for estimating wind erodibility of farm fields. *J. Soil Water Conserv.*
- Chow, T. L., Cormier, H., Daigle, J. L., Ghanem, I., 1990. Effects of potato cropping practices on water runoff and soil erosion. *Can. J. Soil Sci.* 70, 137-148. <https://doi.org/10.4141/cjss90-016>
- Chow, T.L., Rees, H.W., Daigle, J.L., 1999. Effectiveness of terraces/grassed waterway systems for soil and water conservation: A field evaluation. *J. Soil Water Conserv.* 54, 577-583
- Dabney, S.M., Vieira, D.A.N., Yoder, D.C., Langendoen, E.J., Wells, R.R., Ursic, M.E., 2015. Spatially distributed sheet, rill, and ephemeral gully erosion. *J. Hydrol. Eng.* 20, C4014009. [https://doi.org/10.1061/\(ASCE\)HE.1943-5584.0001120](https://doi.org/10.1061/(ASCE)HE.1943-5584.0001120).
- Dai, J., Zhang, J., Zhang, Z., Jia, L., Xu, H., Wang, Y., 2020. Effects of water discharge rate and slope gradient on runoff and sediment yield related to tillage erosion. *Archives of Agronomy and Soil Science*, 1-13. <https://doi.org/10.1080/03650340.2020.1766676>.

- De Alba, S., 2003. Simulating long-term soil redistribution generated by different patterns of mouldboard ploughing in landscapes of complex topography. *Soil Tillage Res.* 71, 71-86. [https://doi.org/10.1016/S0167-1987\(03\)00042-4](https://doi.org/10.1016/S0167-1987(03)00042-4).
- Erpul, G., Norton, L.D., Gabriels, D., 2002. Raindrop-induced and wind-driven soil particle transport. *CATENA* 47, 227-243. [https://doi.org/10.1016/S0341-8162\(01\)00182-5](https://doi.org/10.1016/S0341-8162(01)00182-5).
- Flanagan, D.C., Nearing, M.A., 1995. USDA-Water Erosion Prediction Project: Hillslope profile and watershed model documentation. Nserl Rep 10, 1-123
- Gómez, J.A., Nearing, M.A., 2005. Runoff and sediment losses from rough and smooth soil surfaces in a laboratory experiment. *CATENA* 59, 253-266. <https://doi.org/10.1016/j.catena.2004.09.008>.
- Gordon, L.M., Bennett, S.J., Bingner, R.L., Theurer, F.D., Alonso, C.V., 2007. Simulating ephemeral gully erosion in AnnAGNPS. *Transactions of the ASABE* 50, 857-866. <https://doi.org/10.13031/2013.23150>.
- Govers, G., Vandaele, K., Desmet, P., Poesen, J., Bunte, K., 1994. The role of tillage in soil redistribution on hillslopes. *Eur. J. Soil Sci.* 45, 469-478. <https://doi.org/10.1111/j.1365-2389.1994.tb00532.x>.
- Hevia, G.G., Buschiazzo, D.E., Hepper, E.N., Urioste, A.M., Antón, E.L., 2003. Organic matter in size fractions of soils of the semiarid Argentina. Effects of climate, soil texture and management. *Geoderma* 116, 265-277. [https://doi.org/10.1016/S0016-7061\(03\)00104-6](https://doi.org/10.1016/S0016-7061(03)00104-6).

- Knisel, W.G., Foster, G.R., 1981. CREAMS [Chemicals, runoff, and erosion from agricultural management systems]: a system for evaluating best management practices [Mathematical models, pollution].
- Lal, R., 2001. Soil degradation by erosion. *Land Degrad. Dev.* 12, 519-539. <https://doi.org/10.1002/ldr.472>.
- Li, S., Lobb, D.A., Lindstrom, M.J., Farenhorst, A., 2008a. Patterns of water and tillage erosion on topographically complex landscapes in the North American Great Plains. *J. Soil Water Conserv.* 63, 37-46. <https://doi.org/10.2489/jswc.63.1.37>.
- Li, S., Lobb, D.A., Lindstrom, M.J., Farenhorst, A., 2007. Tillage and water erosion on different landscapes in the northern North American Great Plains evaluated using <sup>137</sup>Cs technique and soil erosion models. *CATENA* 70, 493-505. <https://doi.org/10.1016/j.catena.2006.12.003>.
- Li, S., Lobb, D.A., Lindstrom, M.J., Papiernik, S.K., Farenhorst, A., 2008b. Modeling tillage-induced redistribution of soil mass and its constituents within different landscapes. *Soil Sci Soc Am J.* 72, 167-179. <https://doi.org/10.2136/sssaj2006.0418>.
- Li, S., Lobb, D.A., Tiessen, K.H.D., 2009. Modeling tillage-induced morphological features in cultivated landscapes. *Soil Tillage Res.* 103, 33-45. <https://doi.org/10.1016/j.still.2008.09.005>.
- Lindstrom, M.J., Schumacher, J.A., Schumacher, T.E., 2000. TEP: A tillage erosion prediction model to calculate soil translocation rates from tillage. *J. Soil Water Conserv.* 55, 105-108

- Lobb, D.A., Kachanoski, R.G., Miller, M.H., 1995. Tillage translocation and tillage erosion on shoulder slope landscape positions measured using  $^{137}\text{Cs}$  as a tracer. *Can. J. Soil Sci.* 75, 211–218. <https://doi.org/10.4141/cjss95-029>.
- Lobb, D.A., Kachanoski, R.G., 1999. Modeling tillage erosion in the topographically complex landscapes of southwestern Ontario, Canada. *Soil Tillage Res.* 51, 261–277. [https://doi.org/10.1016/S0167-1987\(99\)00042-2](https://doi.org/10.1016/S0167-1987(99)00042-2).
- Lobb, D.A., Lindstrom, M.J., Schumacher, T.E., 2003. Soil erosion processes and their interactions: implications for environmental indicators, *Agricultural Impacts on Soil Erosion and Soil Biodiversity: Developing Indicators for Policy Analysis*. Proceedings from an OECD Expert Meeting—Rome, Italy, March, pp. 325-336.
- Pedersen, H.S., Hasholt, B., 1995. Influence of wind speed on rainsplash erosion. *CATENA* 24, 39-54. [https://doi.org/10.1016/0341-8162\(94\)00024-9](https://doi.org/10.1016/0341-8162(94)00024-9).
- Poesen, J., 2018. Soil erosion in the Anthropocene: Research needs. *Earth Surf. Process. Landforms* 43, 64-84. <https://doi.org/10.1002/esp.4250>.
- Poesen, J., Nachtergaele, J., Verstraeten, G., Valentin, C., 2003. Gully erosion and environmental change: importance and research needs. *CATENA* 50, 91-133. [https://doi.org/10.1016/S0341-8162\(02\)00143-1](https://doi.org/10.1016/S0341-8162(02)00143-1).
- Renard, K.G., 1997. Predicting soil erosion by water: a guide to conservation planning with the Revised Universal Soil Loss Equation (RUSLE). United States Government Printing.

- Römken, M.J.M., Helming, K., Prasad, S.N., 2002. Soil erosion under different rainfall intensities, surface roughness, and soil water regimes. *CATENA* 46, 103-123. [https://doi.org/10.1016/S0341-8162\(01\)00161-8](https://doi.org/10.1016/S0341-8162(01)00161-8).
- Schnepf, M., Cox, C., 2006. Environmental benefits of conservation on cropland: the status of our knowledge. Soil and Water Conservation Society. Ankeny, Iowa, USA.
- Six, J., Paustian, K., Elliott, E.T., Combrink, C., 2000. Soil structure and organic matter I. Distribution of aggregate-size classes and aggregate-associated carbon. *Soil Sci Soc Am J.* 64, 681-689. <https://doi.org/10.2136/sssaj2000.642681x>.
- USDA-NRCS, 1997. America's Private Land, A Geography of Hope. USDA-NRCS, Washington, DC.
- Van Oost, K., Govers, G., De Alba, S., Quine, T.A., 2006. Tillage erosion: a review of controlling factors and implications for soil quality. *Prog Phys Geogr: Earth and Environment* 30, 443-466. <https://doi.org/10.1191/0309133306pp487ra>.
- Van Oost, K., Govers, G., Desmet, P., 2000. Evaluating the effects of changes in landscape structure on soil erosion by water and tillage. *Landscape Ecol.* 15, 577-589. <https://doi.org/10.1023/A:1008198215674>.
- VandenBygaart, A.J., Kroetsch, D., Gregorich, E.G., Lobb, D.A., 2012. Soil C erosion and burial in cropland. *Global Change Biol.* 18, 1441-1452
- Wang, Y., Zhang, J.H., Zhang, Z.H., Jia, L.Z., 2016. Impact of tillage erosion on water erosion in a hilly landscape. *Sci. Total Environ.* 551-552, 522-532. <https://doi.org/10.1016/j.scitotenv.2016.02.045>.

Wischmeier, W.H., Smith, D.D., 1965. Predicting rainfall-erosion losses from cropland east of the Rocky Mountains.

Woodward, D.E., 1999. Method to predict cropland ephemeral gully erosion. CATENA 37, 393-399. [https://doi.org/10.1016/S0341-8162\(99\)00028-4](https://doi.org/10.1016/S0341-8162(99)00028-4).

Zhang, J.H., Wang, Y., Zhang, Z.H., 2014. Effect of terrace forms on water and tillage erosion on a hilly landscape in the Yangtze River Basin, China. Geomo 216, 114-124. <https://doi.org/10.1016/j.geomorph.2014.03.030>.

Zhao, H.L., Yi, X.Y., Zhou, R.L., Zhao, X.Y., Zhang, T.H., Drake, S., 2006. Wind erosion and sand accumulation effects on soil properties in Horqin Sandy Farmland, Inner Mongolia. CATENA 65, 71-79. <https://doi.org/10.1016/j.catena.2005.10.001>.

## **2. A PLOT STUDY ON THE EFFECTS OF WATER-ERODED CHANNELS ON TILLAGE TRANSLLOCATION**

Zheng, F., Lobb, D.A. and Li, S., 2021. A plot study on the effects of water eroded channels on tillage translocation. *Soil Tillage Res.*, 213, p.105118.

Received 28 February 2021; Received in revised form 7 June 2021; Accepted 12 June 2021; Available online 23 June 2021.

### **Contributions of authors**

The authors confirm contribution to the paper as follows: 1. study conception and design: Zheng, F, Lobb, D.A. and Li, S.; 2. resources provided: Lobb, D.A. and Li, S.; 3. data collection: Zheng, F.; 4. data analysis: Zheng, F.; 5. data visualization: Zheng, F.; 6. data interpretation: Zheng, F., Lobb, D.A. and Li, S., 7. writing—original draft preparation: Zheng, F.; 8. writing—review and editing: Lobb, D.A. and Li, S.; 9. funding: Lobb, D.A. and Li, S.. The author confirms sole responsibility for the following: study conception and design, data collection, analysis, and paper preparation.

### **2.1 Abstract**

A major feature of water erosion is the formation of channels such as rills and gullies. The creation of these channels changes the local topography and, therefore, may affect soil movement during tillage operations. To quantify such interaction between water and tillage erosion, a plot experiment was conducted and point tracers were used to measure tillage translocation under three tillage treatments: downslope (DT), upslope (UT), and contour tillage

(CT) with three channel treatments: no channel (C0), 10-cm-by-10 cm channel (C10), and 20-cm-by-20-cm channel (C20). Forward and lateral translocation, and their resultant total translocation, were calculated by comparing the tracer locations before and after tillage. The results indicate that for DT, the presence of a channel reduced total translocation, whereas for UT, it increased total translocation. This trend was attributed to a decrease in forward translocation under DT and an increase in forward translocation under UT with the presence of channels, while lateral translocation was not significantly affected by the presence of channels. For CT, the presence of a channel increased both forward and lateral soil translocation, and therefore total translocation. These observed patterns of tillage translocation can be well explained by the relative importance of the trapping effect (channel functions like a trap for moving soil) versus the energy-intensity-increase effect (greater energy intensity due to less soil being moved with the presence of a channel). Soil movement decreases when the trapping effect dominates, and it increases when the energy-intensity-increase effect dominates. At the process level, the relative importance of the trapping effect and the energy-intensity-increase effect is determined by the shape and size of the tillage tool's zone of influence (ZoI), which is affected by the location and orientation of the channel, and the direction of tillage. Overall, our results suggest that if channels are formed by water erosion, CT would be better than DT and UT in reducing tillage translocation and filling the channel. The knowledge gained from this study can be used to improve water and tillage erosion modeling.

## 2.2 Introduction

Globally, water erosion on agricultural lands has been recognized as a severe threat to the sustainability of the agricultural industry and the environment (Lal, 2001; Morgan, 2009). Water erosion can be in the forms of sheet, rill and gully erosion (Morgan, 2009). Both rill and gully erosion are channelized erosion. There is not a quantitative definition to differentiate rill and gully. Conceptually, rills are usually small parallel channels running straight down the face of a hillslope. They can be smoothed out easily by tillage and normally do not reoccur at the same locations in the next year (Li et al., 2013). Gullies are larger in size, resulting from the concentration of surface runoff from across a land surface. Those can be smoothed out by tillage operations are termed ephemeral gullies whereas those cannot be eliminated by tillage operations are termed classical gullies (Poesen et al., 2003). The locations of gullies are usually determined by the topography of the landform and, therefore, they will reoccur at roughly the same locations after being smoothed out by tillage operation. Channelized water erosion is common on agricultural lands. Poesen et al. (2003) reported that, in some areas, as high as 94 % of total soil loss by water erosion was caused by channelized erosion. The significance of channelized erosion has also been reported by many other researchers all over the world (Chen and Cai, 2006; Foster, 1986; Nachtergaele and Poesen, 1999; Poesen, 1996; Poesen et al., 2011).

Another major form of erosion on agricultural lands is tillage erosion (Govers et al., 1999; Van Oost et al., 2006). Tillage erosion is defined as the net downslope tillage translocation, and is typically observed as soil loss on convexities and soil accumulation in concavities or as

soil loss on the downslope side of a field boundary and soil accumulation on the upslope side of a field boundary (Li et al., 2009). Tillage translocation and, therefore, tillage erosion are determined by two factors: the erosivity of the tillage operation and the erodibility of the landscape (Lobb and Kachanoski, 1999). The erosivity of the tillage operation is affected by characteristics of the tillage equipment (e.g., type and size of tillage tools and shanks) and operational parameters such as tillage depth and speed. The erodibility of the landscape is affected by the topographic properties of the landscape such as slope gradient and slope curvature, and soil condition such as soil texture, structure and moisture content (Lobb and Kachanoski, 1999; Novak and Hůla, 2017a, b).

Historically, soil erosion studies have been carried out with a focus on a single erosion process, wind, water or tillage erosion (Lal, 2001). It may be possible to justify the separation of wind and water erosion studies, but in cultivated land, tillage erosion will occur in addition to wind and water erosion. On land subjected to water and tillage erosion, it is necessary to examine both processes in order to provide a comprehensive estimate of soil erosion. There are linkages and interactions between these two erosion processes (Li et al., 2007b; Lobb et al., 2003). Linkages refer to the simple additive effects between different erosion processes, whereas interactions between different erosion processes occur when one erosion process changes the erodibility of the landscape for another erosion process, or when one process works as a delivery mechanism for another erosion process. Interactions between tillage and water erosion are likely strong around areas with channels, especially ephemeral gullies, because it is a common practice to use tillage to eliminate ephemeral gullies. On one hand, the presence

of a channel alters the local surface topography and, therefore, the erodibility of the landscape through tillage translocation. On the other hand, since ephemeral gullies are mostly topographically controlled and usually reoccur at roughly the same locations after being smoothed out by tillage, tillage operation serves as a delivery mechanism to transport soil into the channels to be eroded by ephemeral gully erosion.

Recently, the interaction between channelized erosion and tillage erosion has drawn a lot of attention (Li et al., 2007b; Lobb et al., 1995; Van Oost et al., 2005; Zhang et al., 2019, 2014). Wang et al. (2016) conducted a rainfall simulation experiment to examine the impact of tillage erosion on hydrological characteristics, such as flow velocity and runoff depth, and soil erodibility. The results indicated that tillage erosion increased soil erodibility and provided sediment for the subsequent runoff event, accelerating water erosion. Dai et al. (2020) also reported that tillage erosion altered the hydrologic process, increasing the sediment yield and runoff, thereby accelerating water erosion. However, no study to date has been carried out to examine the influence of channels caused by water erosion on tillage erosion. Therefore, the objective of this study was to quantify the effect of channels on tillage translocation. Knowledge on such effect will lead to a better understanding on the interactions between water and tillage erosion, help the development of more efficient and better erosion control measures, which ultimately will contribute to the enhancement of soil quality in agricultural fields.

## **2.3 Materials and Method**

### **2.3.1 Study area and plot layout**

The study was conducted at the experimental farm of the Fredericton Research and Development Centre (FRDC) in New Brunswick, Canada. The soil at the study site is classified as a Fredericton Orthic Humo-Ferric Podzol developed on a coarse loamy ancient fluvial deposit over coarse loamy morainal lodgement till, which has a podzolic B horizon of at least 10 cm thick and is well-drained. The topsoil is friable, yellowish brown (10 YR) sandy loam with 10 - 25 % angular cobbles and gravels, while the subsoil is firm, dark brown (7.5 YR) sandy loam with 10 - 20 % angular gravels and some cobbles (Rees and Fahmy, 1984). Three tillage treatments - downslope tillage (DT), upslope tillage (UT), and contour tillage (CT) - and three channel size treatments - no channel (C0), 10-cm-wide-by-10-cm-deep channel (C10), and 20-cm-wide-by-20-cm-deep channel (C20) - were examined in this study. A total of six small, narrow fields (6 m wide and 80 m long) were used. Four fields were used for DT and UT experiments and these fields were oriented along the slope (slope gradient  $\approx 10\%$ ). Another two fields were used for CT and these fields were oriented along the contour lines but with a small angle (slope gradient along the path of tillage  $\approx 3\%$  and across the path of tillage  $\approx 7\%$ ). It is a common practice for CT to have a small angle with the contour lines for the purpose of enhancing surface water drainage. Tillage was conducted along the length of each field. Normally, a set of three plots were situated within a field at any one time. The positions of the plots within the field were randomly selected, but there was at least 10 m distance between

plots and an additional at least 10 m was left in either end of the plots to allow for the acceleration and deceleration of the tractor and tillage implement. There was a total of nine treatment combinations and with four replicates, for a total of 36 plots.

### **2.3.2 Tracer installation and plot setup**

Tillage translocation was measured with tracers. These tracers were made from concrete mix and were moulded in a 20-cm-by-20-cm tray into 1 cm<sup>3</sup> cement cubes. These cubes were then dyed with four different colours for easy identification, and labelled with a unique ID number with an engraving tool.

For the DT and UT treatments, the plots were 1 m wide and 3 m long (Fig. 2.1). The width of the plot was designed to equal three times of the width of the tillage tool used, a sweep, because three sweeps formed the repeating pattern in the arrangement of tools for the implement (Li et al., 2007a). The 3 m length of the plots was based on the fact that the maximum tracer movement was less than 1.5 m in all test runs and, therefore, 3 m should be enough to capture the full range of soil translocation. The centre of the plot was designated as the channel area (20 cm wide). For C0, the channel area was left untouched. For C10 and C20, channels 10-cm-wide-by-10-cm-deep and 20-cm-wide-by-20-cm-deep, respectively, were dug. For the rest of the plot area, the cement cube tracers were placed on both sides of the channel in a grid pattern as shown in Fig. 2.1. There were eight columns of tracers, four on each side of the channel area, and at each point, tracers were placed at two depths (5 cm and 15 cm). Tracers were placed in the plot area using two spacings. Within the first 1 m along the tillage

direction (from the long edge of the channel area), the interval was 10 cm, whereas beyond 1 m, the interval was 20 cm. In this study, only data for the first 10 rows (i.e., 10 cm interval) of tracers were used whereas data for the next 10 rows (i.e., 20 cm interval) were dropped (see section 2.5.4 for detailed explanations). For the CT treatment, the plots were 1 m wide by 6.2 m long with the channel area (20 cm wide by 1 m long) at the centre of the plot (there were 3 m before and 3 m after the channel), long edge perpendicular to the tillage direction (Fig. 2.1). Other setups were similar to those of DT and UT.

### **2.3.3 Tillage equipment**

Tillage was conducted with a 2-m-wide, tractor-mounted cultivator equipped with sweeps (McKay 50 - 12 K) (Fig. 2.2), drawn with a John Deere® row crop tractor, both properties of the FRDC, and operated by the farm services staff. This sweep was selected given its wide use in Atlantic Canada. Also, this sweep had been used in another study, providing an opportunity for direct data comparisons (Liu et al., 2007). There were five sweeps (numbered #1 to #5 from left to right) arranged in three rows on the mounting frame (Fig. 2.2). Since there was a metal bar across the centre of the mounting frame, the centre sweep had to be shifted to one side (the right-hand side in this study). As a result, there was an overlap between the centre sweep (#3) and the second right sweep (#4) and a large gap between the centre sweep (#3) and the second left sweep (#2). Consequently, there was more disturbance of soil on the right-hand side than left-hand side of tillage equipment. The asymmetric arrangement of sweeps obviously adds uncertainty in the translocation measurements, as detailed in the discussion section below.

However, such irregular spacing is common in the real world; it is often necessary to mount tillage tools to the frame around wheels, hydraulics and other accessories. Although not desirable, it was viewed as an opportunity to explore the influence of sweep arrangement on tillage translocation.

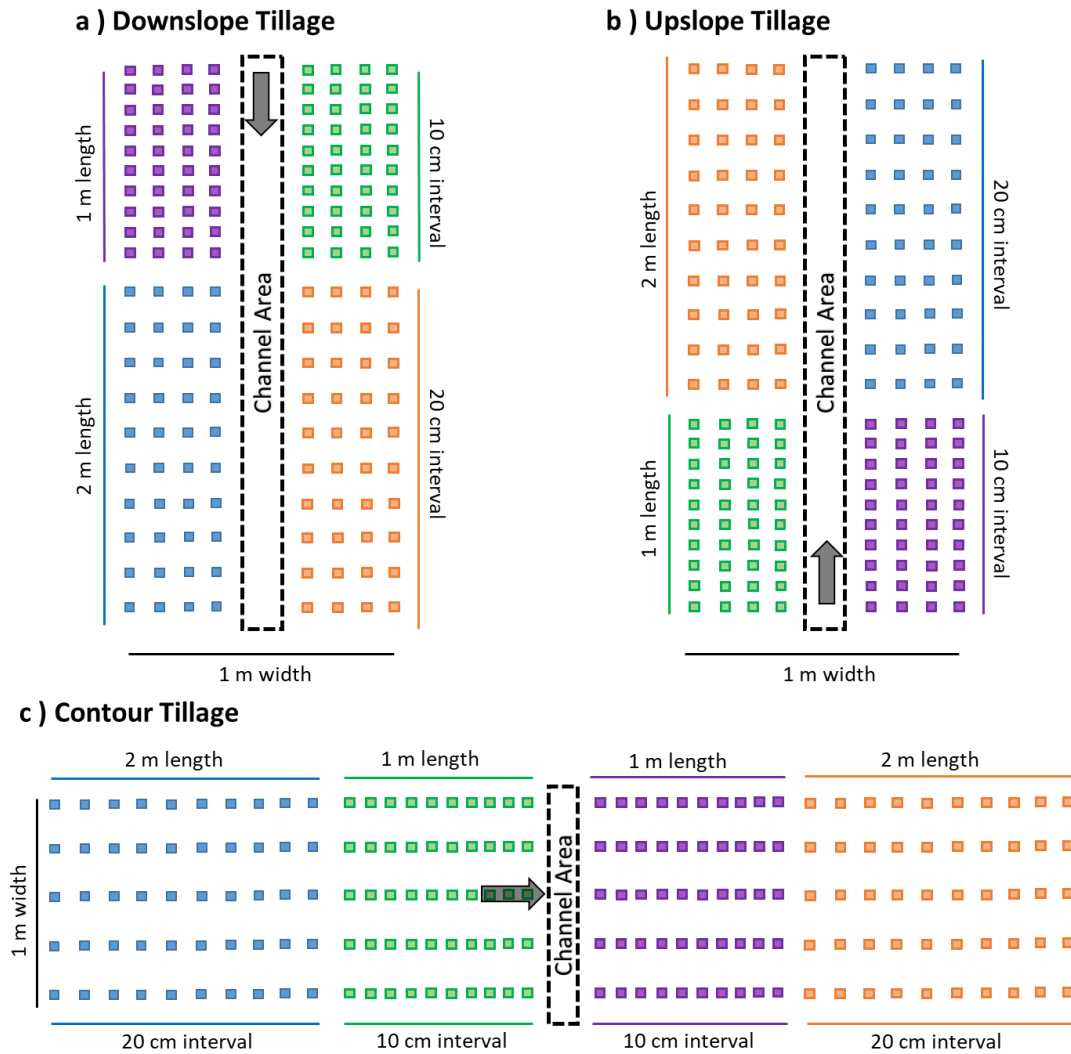


**Figure 2.1.** The layout of point tracers dyed with four different colours in: a) downslope tillage, b) upslope tillage, and c) contour tillage plots. Squares indicate point tracers.

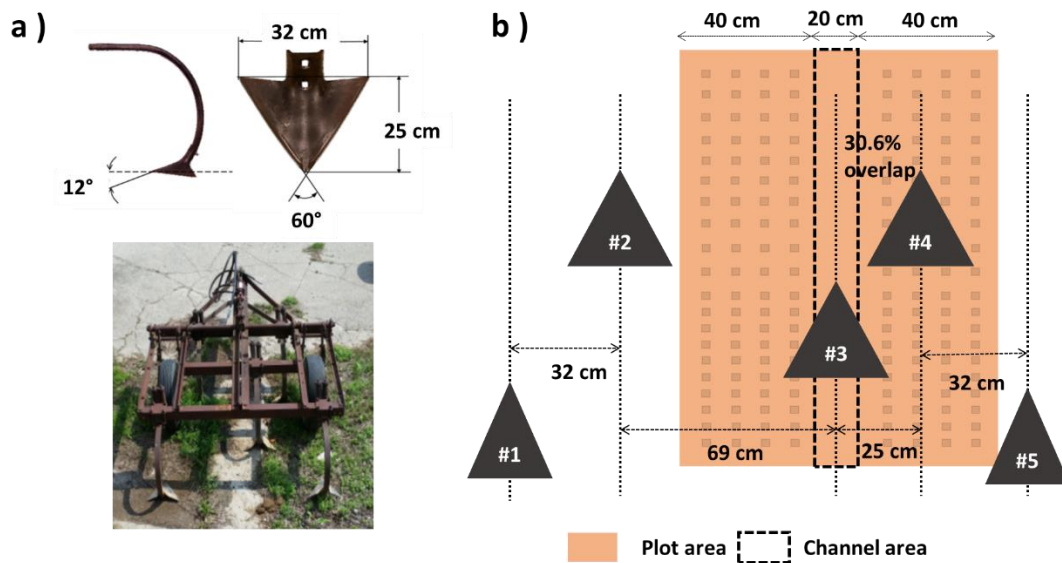


**Figure 2.2.** a) The tillage equipment with sweeps (McKay 50 - 12 K) installed, and b) the targeted layout of the sweep arrangement with the downslope tillage and upslope tillage plots.

### 2.3.4 Tillage operation and tracer sampling

To maintain similar soil moisture content for different runs, the fields were required to have a weather forecast three to four days without rainfall before each run. The field was harrowed first. The point tracers were buried at two depths in the soil after harrowing according to the grid pattern outlined above. Two plastic sticks were inserted into the soil 1 m away from the sides of the plot to mark the starting edge of the plot, creating a reference line for sampling. After the preparation of plots (tracers installed), tillage was conducted. Tillage direction was determined according to the tillage treatment (DT, UT or CT). The operator of the tillage equipment aligned the centre sweep (#3) with the centre line of the plot (also the centre line of the channel under DT and UT). Great efforts were made by the operator to keep the same tillage speed ( $\approx 3.6 \text{ km hr}^{-1}$ ) and tillage depth ( $\approx 20 \text{ cm}$ ) within each run and for all runs. Tillage speed was recorded for each run with a stopwatch.

A coordinate system was established for each plot to sample tracers. The x-axis was perpendicular to the tillage direction with the zero point at the centre line of the plot whereas the y-axis was along the tillage direction with the zero point at the start line of the plot. Coordinates of each tracer were recorded before the tillage operation. After tillage, a 2-m-by-2-m wooden frame was used as a reference for tracer sampling, similar to the method used by Li et al. (2007a) and Tiessen et al. (2007b). On the x-axis, the centre line of the frame was lined up with the centre line of the plot. On the y-axis, the frame was lined up with the plot based on the starting line marked by the two plastic sticks on the two sides of the plots. For DT and UT, tracer sampling started from 20 cm before the plot to capture any backward movement of tracers, particularly during UT. For CT, tracer sampling started from the starting line of the plot. The sampling was conducted by excavating soil and recovering tracers from 10-cm-by-10-cm cells. For each cell, all recovered tracers were recorded and bagged. It progressed cell by cell along the x-axis in rows and then row by row along the y-axis (tillage direction) until the end of the frame was reached. The frame was then moved along the y-axis and a new set of rows was sampled. The frame may be moved several times to cover the full range of tracer redistribution. Since each tracer had its unique ID and its coordinates before and after tillage were recorded, its movement can be calculated by subtracting the coordinates after tillage by those before tillage. Difference in y-axis values determined forward translocation, whereas difference in x-axis determined lateral translocation. It should be noted that because each cell was excavated as a whole, the resolution of the translocation measurement was only 10 cm.

## 2.3.5 Data Analysis

### 2.3.5.1 Factors affecting tillage translocation

Not all tracers were recovered. Tracer recovery rate was calculated and was used as an indicator for the overall accuracy for each experiment run. Differences among treatments were examined using analysis of variance (ANOVA). Tukey's test was used to compare the treatment means. Also, it has been well-documented that tillage speed and depth can affect tillage translocation (Lobb et al., 1999; Van Muysen et al., 2000). Therefore, correlation analysis was conducted between the tillage speed and the tillage translocation to check whether tillage speed affects tillage translocation significantly in this study. Tillage depth was not measured in the experiments. However, at each tracer position, tracers were buried at both 5 cm and 15 cm depths. If for most tracer positions, only tracers buried at 5 cm were moved but not those buried at 15 cm, tillage depth was likely less than 15 cm. Therefore, we calculated the percentage of positions where only the tracer at 5 cm was moved ( $P_{5\text{cm}}$ ) as follows:

$$P_{5\text{cm}} = \frac{\text{Number of tracer positions with only 5 cm tracer being moved}}{\text{Number of tracer positions with both tracers being moved}} * 100\% \quad [1]$$

$P_{5\text{cm}}$  was used as an indicator for whether or not the tillage depth was below 15 cm.

### 2.3.5.2 Tillage translocation analysis

As described above, forward and lateral translocation for a tracer were calculated by its movements along the y-axis and x-axis, respectively. These two measures are vectors. For forward translation, positive values mean that tracers have advanced along the path of tillage, whereas negative values mean that tracers have been moved backwards. For lateral

translocation, positive values were defined as tracers being moved to the right relative to the path of tillage, whereas negative values were defined as tracers being moved to the left. Since the tillage equipment used in this study was a two-way tillage tool, a sweep, it moves soil in both left and right directions. Lateral translocation for individual tracers in a plot will cancel each other so that the overall average lateral translocation is not a good indication for lateral soil movement. Therefore, the absolute lateral translocation (i.e., absolute value of lateral translocation) was calculated and used in our analysis. The total translocation represented the resultant tillage translocations from both directions and was calculated as follows:

$$\text{Total Translocation} = \sqrt{\text{Forward Translocation}^2 + \text{Lateral Translocation}^2} \quad [2]$$

The translocation data were highly skewed, so prior to statistical analysis, we first did an outlier test on the data for each column of tracers. It was found that measurements lower than the 10th percentile and greater than the 90th percentile were mostly outliers. To avoid bias due to removing outliers on one side, we removed measurements lower than the 10th percentile and greater than the 90th percentile from all datasets (see detailed discussion on experimental errors and uncertainties in section 2.5.3). The cleaned datasets were then log-transformed as follows to ensure normality prior to statistical analyses:

$$\text{Transformed data} = \log_{10}(\text{raw data} + 20) \quad [3]$$

#### **2.3.5.2.1 Downslope and upslope tillage (DT and UT)**

For DT and UT, the treatment effects of tillage direction and channel size on plot-averaged total, forward and absolute lateral translocation were analyzed using analysis of variance

(ANOVA). Also, linear regressions between the three translocation measures of individual tracers were conducted separately for the two tillage directions and the three channel sizes. Under each tillage direction, the slopes of the regression lines for different channel sizes were compared using the analysis of covariance (ANCOVA), which was used as another way to evaluate the impact of tillage direction and channel size on tillage translocation.

To better understand the impact of channels on individual tracer movement, tracers moved into the channel area (the 20-cm-wide-by-3-m-long area in the centre of the plot) were categorized based on their source areas. Horizontally, the 10 cm areas adjacent to the channel area on both sides (each marked by one column of tracers) were defined as the Near Channel Area (NCA), whereas the rest of the plot areas (marked by three columns of tracers on each side) were defined as the Outside Channel Area (OCA). Vertically, the channel area was divided into the surface layer (0 cm - 10 cm, marked by the 5 cm depth tracers) and the subsurface layer (10 cm - 20 cm, marked by the 15 cm depth tracers). Thus, there were four source areas: The Near Channel surface layer Area (NCA5), the Near Channel subsurface layer Area (NCA15), the Outside Channel surface layer Area (OCA5), and the Outside Channel subsurface layer Area (OCA15). Three parameters were calculated as follows:

$$P_{\text{all}}^i = \frac{n^i}{N^{\text{pl}}} \times 100\% \quad [4]$$

$$P_{\text{loc}}^i = \frac{n^i}{N^i} \times 100\% \quad [5]$$

$$P_{\text{con}}^i = \frac{n^i}{N^{\text{ch}}} \times 100\% \quad [6]$$

Where  $n^i$  is the number of tracers moved into the channel area from source area  $i$ ,  $N^{\text{pl}}$  is the total number of tracers originally in the whole plot,  $N^i$  is the number of tracers originally in

source area  $i$ , and  $N^{ch}$  is the total number of tracers found in the channel area after tillage. The value of  $P_{all}$  is an indication of the number of tracers (the amount of soil) moved into the channel area (versus to outside of the channel area). The value of  $P_{loc}$  is the percentage of tracers in each source area that has been moved into the channel area. It indicates the tendency of soil moving from the local source area to the channel area versus to outside the channel area. The value of  $P_{con}$  indicates the contribution of different source areas to the tracer moved into the channel area.

#### **2.3.5.2.2 Contour tillage (CT)**

For CT, the treatment effects of channel size on the averaged total, forward and absolute lateral translocation of the plot were analyzed using ANOVA, similar to that for DT and UT. Individual tracer movement relative to the channel was also analyzed based on columns of tracers parallel to the channel. Whereas the tracer columns for DT and UT were along the tillage direction, the columns for CT were perpendicular to the tillage direction. The maximum tracer movement distance for C0 was used as the limit to delineate the near versus outside channel areas. Areas within this distance before and after the channel were defined as the Near Channel Areas (NCAs) and the areas beyond this distance were defined as the Outside Channel Areas (OCAs). Consequently, oriented along the tillage direction, the columns were grouped into four areas, two Before the Channel (BC-OCA and BC-NCA) and two After the Channel (AC-NCA and AC-OCA). ANOVA was used to examine the differences among the four areas as well as the effects of channel size on translocation measures.

## 2.4 Results

### 2.4.1 Tracer recovery, tillage speed and depth

Tracer recovery ratio (RR) was an average of 96.6 % for all plots, ranging from 92.5 % to 98.3 %, and between different treatments, there was no significant difference. The less than complete recovery of tracers ( $< 100$  % RR) suggests that some tracers were missed during sampling. It is assumed that these un-sampled tracers travelled beyond the extent of sampling, and, as such, it is likely that tillage translocation has been underestimated in this study. However, the RR values were still quite high compared to other similar studies (Li et al., 2007b; Tiessen et al., 2007b). Therefore, the effect of missing tracers on the overall accuracy of the translocation measurements was considered to be acceptable. Tillage speed varied substantially between plots, ranging from 2.2 to 6.8 km hr<sup>-1</sup> with a standard deviation (SD) of 1.53 km hr<sup>-1</sup>. Average tillage speeds were 4.7 km hr<sup>-1</sup>, 4.2 km hr<sup>-1</sup> and 4.2 km hr<sup>-1</sup> for DT, UT and CT, respectively. The differences between treatments were non-significant. The SD of replicates for DT, UT and CT ranged from 1.5 to 1.7 km hr<sup>-1</sup>, 1.8 to 2.3 km hr<sup>-1</sup> and 0.5 to 0.6 km hr<sup>-1</sup>, respectively. The average speed was lower than that of the Vibrashank cultivator (6.4 km hr<sup>-1</sup>) examined by Tiessen et al. (2007b), and the variance among replicates was greater. The low speed and high variation observed in this study were likely due to the nature of speed control in a small plot study. The travelling speed over the experiment plot was affected by many factors such as tillage direction, soil condition, and the lead distance before the tractor reached the plot. The operator used gear ratio and throttle control to manage speed based on his

experience, which might not be enough to overcome local differences between plots. The fact that the variance in speed for UT and DT were much greater than that for CT indicates that the operator has made an effort to adjust gear ratio and throttle according to tillage direction in order to maintain consistent tillage speed for all plots. Nevertheless, the correlations between tillage speed and tillage translocation for the four replicates of individual treatments were all non-significant, suggesting that tillage speed did not affect tillage translocation measurements significantly in this study. For tillage depth, the  $P_{5\text{cm}}$  ranged from 0 % to 20 %, indicating that tillage depth for all runs was deeper than 15 cm.

## **2.4.2 Tillage translocation for DT and UT**

### **2.4.2.1 The total, forward and absolute lateral tillage translocation**

For DT, total translocation decreased with channel size, averaging 24 cm, 23 cm and 21 cm with SDs of 2 cm, 7 cm and 5 cm for C0, C10 and C20, respectively (Fig. 2.3). For UT, total translocation showed an opposite trend, averaging 14 cm, 16 cm and 19 cm with SDs of 7 cm, 8 cm and 8 cm for C0, C10 and C20, respectively. For both DT and UT, the differences between channel sizes were non-significant, probably due to the high variability among replicates. For C0, the total translocation of 24 cm for DT was significantly greater than that of 14 cm for UT, indicating greater translocation with downslope tillage than upslope tillage, as observed in many previous studies (Lobb et al., 1999; Montgomery et al., 1999; Novak and Hůla, 2017a, b; Xu et al., 2019; Zhao et al., 2018). For C10 and C20, the differences between DT and UT were not significant, suggesting that the presence of a channel diminishes the effect

of DT and UT on total translocation. Overall, the average total translocation for DT was 21 cm, which was significantly greater ( $P = 0.03$ ) than that for UT (16 cm).

As a component of total translocation, forward translocation decreased with channel size for DT and increased with channel size for UT, which were similar to the respective trends of DT and UT for total translocation (Fig. 2.3). For DT, forward translocation averaged 18 cm, 15 cm and 10 cm for C0, C10 and C20, respectively, compared to 7 cm, 8 cm and 11 cm for UT. The SDs for DT were similar to those of the total translocation, whereas for UT, the SDs were much lower. For DT, the differences in forward translocation between channel sizes were non-significant, but for UT, measures of forward translocation for C0 and C10 were significantly lower than that for C20 ( $P = 0.09$ ), suggesting that the presence of the larger channel significantly increased forward translocation under UT. For the comparison of DT versus UT, the patterns of forward translocation were also similar to those of total translocation. For C0, DT was significantly greater than UT, whereas for C10 and C20, no significant

differences were observed between DT and UT. The overall average forward translocation of DT was significantly greater than that of UT.

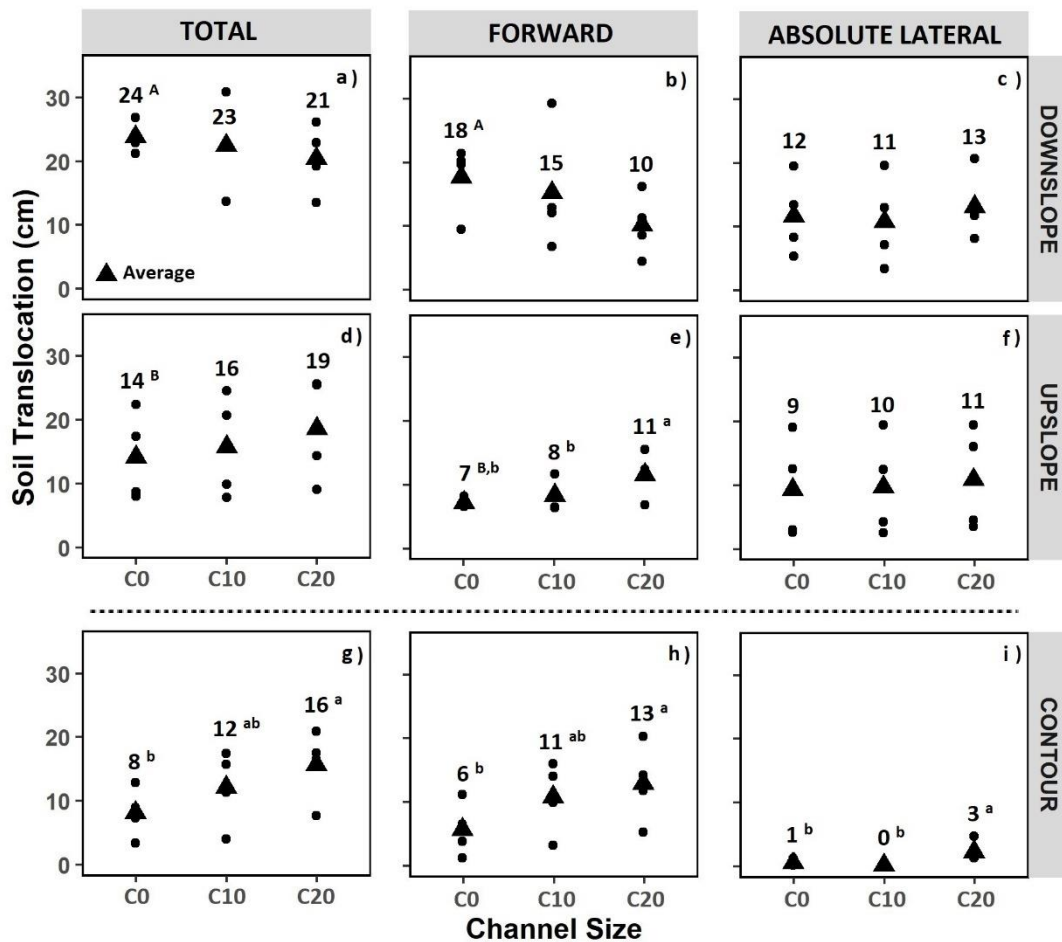


**Figure 2.3.** Tillage translocation measurements for all three channel sizes under all three tillage direction treatments. a) DT, total translocation; b) DT, forward translocation; c) DT, absolute lateral translocation; d) UT, total translocation; e) UT, forward translocation; f) UT, absolute lateral translocation; g) CT, total translocation; h) CT, forward translocation; and i) CT, absolute lateral translocation. Capital letters indicate the comparisons between downslope and upslope tillage treatments, and lower-case letters indicate the comparisons between channel sizes within each chart. Mean values with different letters are significantly different from each other at  $P < 0.10$  based on the Tukey test.

Absolute lateral translocation for DT showed no obvious trend with channel size and was 12 cm, 11 cm and 13 cm for C0, C10 and C20, respectively (Fig. 2.3). For UT, absolute lateral

translocation increased with channel size, which was similar to that of total translocation and forward translocation. The SDs for both DT and UT were similar to that of the total translocation. For both DT and UT, the differences in absolute lateral translocation between channel sizes were non-significant. The comparisons of DT versus UT for absolute lateral translocation were different from those for total and forward translocation. There was no significant difference between DT and UT in absolute lateral translocation for any individual channel size, nor for the overall average. The net lateral translocations were close to 0 for all individual channel sizes for both DT and UT, but the variation increased with increasing channel size for both tillage directions (data not shown).

With the regression analysis of individual tracer movement data, for DT, the regression coefficients between forward translocation (x) and absolute lateral translocation (y) were 0.33, 0.11 and -0.04 for C0, C10 and C20, respectively (Table 2.1). These regression coefficients were significantly different from each other ( $P < 0.05$ ). For C0, there was a significant positive correlation between forward and absolute lateral translocation ( $P < 0.001$ ). This is expected because when the tracer is moved by a tillage implement, the energy will be exerted on both forward and lateral directions. With C20, the correlation between forward and absolute lateral translocation was non-significant ( $P = 0.24$ ), indicating the strong impact of the 20-cm-by-20-cm channel on the correlation. This was likely due to the impact of the large channel on the allocation of energy in different directions. This impact is also reflected in the regression analysis of total versus forward and absolute lateral translocation (data not shown). For C0, the regression coefficients for total versus forward (0.87) and total versus absolute lateral

translocation (0.97) were high. For C20, the regression coefficient for total versus forward translocation (0.35) was significantly lower than that for C0 whereas the regression coefficient for total versus absolute lateral translocation (0.75) was slightly, but not significantly, lower than that for C0. The impact was also observed with C10 as the regression coefficient between forward and absolute lateral translocation for C10 was significantly lower than that of C0 ( $P = 0.03$ ). The mechanisms of tracer movement as affected by the channels will be discussed in detail in section 2.5.1.

For UT, the regression coefficients between forward translocation and absolute lateral translocation were 0.25, 0.23 and 0.34 for C0, C10 and C20, respectively. Although the regression coefficient for C20 was slightly greater than those for C0 and C10, the differences were non-significant (Table 2.1), indicating that the presence of the channels had no significant impact on the correlation between forward and absolute lateral translocation for UT. This result is again reflected in the regression analysis of total versus forward and absolute lateral translocation as there were no significant differences between C0 and C20 for both regression coefficients (data not shown). However, this was different from DT where channels were found to have a significant impact on the correlation between forward and absolute lateral translocation. This is related to the mechanisms of tracer movement with the presence of a channel under different tillage directions, which will be discussed in detail in section 2.5.1. Overall, results for all three tillage translocation measures suggest that the presence of channels had a strong impact on forward translocation, but not on absolute lateral translocation.

**Table 2.1** Results of the linear regression analyses between absolute lateral translocation (y) and forward translocation (x).

Tillage Direction	Channel Size	Linear regression	N
DT	C0	$y = 1.1 + 0.25^c x$	494
	C10	$y = 1.3 + 0.11^b x$	491
	C20	$y = 1.5 - 0.04^a x$	499
UT	C0	$y = 1.1 + 0.25^a x$	494
	C10	$y = 1.1 + 0.23^a x$	496
	C20	$y = 1.0 + 0.34^a x$	417

Note: translocation values were log transformed based on Eq. [2]. N is the number of data points used in the linear regression analysis. Regression coefficient denoted with different letters are significantly different from each other at  $P < 0.10$  based on ANCOVA.

#### 2.4.2.2 Individual tracer movement relative to the channel

For DT,  $P_{all}$  increased with channel size in most cases, suggesting that with increased channel size, more soil tended to be moved into the channel area (Fig. 2.4). This effect of channel size was statistically significant for the OCA5 source area, although it was non-significant for other source areas. Among all four source areas, OCA5 had the highest  $P_{all}$  values for all three channel sizes, probably due to the fact that the size for OCA was three times of that for NCA. For the same reason,  $P_{all}$  values for OCA15 were greater than those for NCA15, except for C20. With respect to the soil layers,  $P_{all}$  values for the surface layer (represented by tracers at 5 cm) were consistently greater than those for the subsurface layer (represented by tracers at 15 cm), indicating the stronger movement of the surface layer soil. For UT,  $P_{all}$  values for C0 were consistently lower than the corresponding values for DT, indicating the greater movement of soil with DT than UT, which agrees with the plot translocation measurement

results shown in the previous section. Similar to that for DT, a consistent trend of  $P_{all}$  increasing with channel size was observed for all four source areas (Fig. 2.4). For the two surface layer source areas (NCA5 and OCA5), the effect of channel size on  $P_{all}$  was significant, whereas for the two subsurface layer source areas, it was non-significant. This suggests that the presence of a channel had a stronger impact on the surface layer than the subsurface layer. In fact, this was likely the case for DT as well because the channel size effect was significant for OCA5 (a

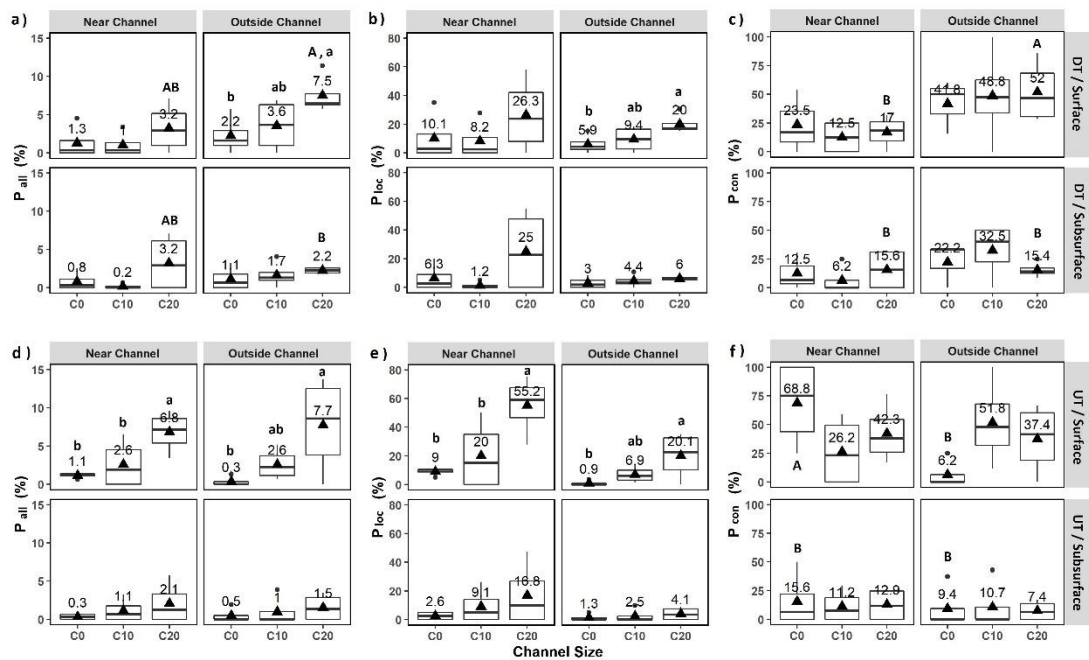


**Figure 2.4.** The three parameters ( $P_{all}$ : the percentage of soil being moved into the channel area as opposed to outside of the channel area,  $P_{loc}$ : the percentage of soil in each source area being moved into the channel area, and  $P_{con}$ : the contribution of different source area to soil being moved into the channel area) calculated to indicate individual tracer movement relative to the channel. a)  $P_{all}$  for DT; b)  $P_{loc}$  for DT; c)  $P_{con}$  for DT; d)  $P_{all}$  for UT; e)  $P_{loc}$  for UT and f)  $P_{con}$  for UT. Capital letters indicate the comparisons between source areas and lower-case letters indicate the comparisons between channel sizes. Mean values with different letters are significantly different from each other at  $P < 0.10$  based on the Tukey test. Only significant comparisons are denoted.

surface layer), but not for OCA15 (a subsurface layer). With respect to the comparison of the two soil layers, similar to the pattern of DT,  $P_{all}$  values for the surface layer were consistently greater than those for the subsurface layer except for C0 in OCA.

Similar to the trend for  $P_{all}$ ,  $P_{loc}$  also increased with channel size for DT in most cases (Fig. 2.4). Again, the difference in  $P_{loc}$  between channel sizes was significant for OCA5 only. Unlike that for  $P_{all}$ , for the four different source areas, under C0, NCA5 had the highest  $P_{loc}$  values whereas OCA15 had the lowest  $P_{loc}$  values with OCA5 and NCA15 in between. The same pattern was observed under C20, suggesting that the effect of the channels on increasing  $P_{loc}$  was similar for all four source areas. With respect to the comparison between NCA and OCA,  $P_{loc}$  values for NCA were greater than those for OCA except for C10. This was opposite to that for  $P_{all}$ , indicating that although there was more soil moving into the channel area from OCA than from NCA, from the perspective of local source area, NCA had proportionally more soil moving into the channel area than OCA had. For the two soil layers, the pattern of  $P_{loc}$  was similar to that of  $P_{all}$ : the values for the surface layer were consistently greater than those for the subsurface layer. For UT,  $P_{loc}$  again increased with channel size. Also, the effect of channel size was significant for the two surface layer source areas but not for the two subsurface layer source areas. For the comparison between different source areas, the pattern was similar to that of DT, with the highest  $P_{loc}$  value for NCA5, the lowest for OC15 and those for OCA5 and NCA15 in between for all three channel sizes with the only exception of C0. Similar to those of DT, the  $P_{loc}$  values also showed the pattern of NCA > OCA and surface layer > subsurface layer.

No consistent trend with channel size was observed for  $P_{con}$  under DT (Fig. 2.4). For the four different source areas, OCA5 had the highest  $P_{con}$  value whereas NCA15 had the lowest  $P_{con}$  value and NCA5 and OCA15 were in between, with only one exception under C20 in NCA15 versus OCA15. This further suggests that the channels did not have a strong impact on  $P_{con}$ . With respect to the two soil layers, the  $P_{con}$  values for the surface layer (NCA5 and OCA5) were consistently greater than those for the subsurface layer (NCA15 and OCA15). Also, the overall  $P_{con}$  values for the surface layer were greater than 60 % for all three channel sizes. Both suggest that more tracers in the channel area came from the surface layer than from the subsurface layer. With respect to the comparison between NCA and OCA, the  $P_{con}$  values for NCA (NCA5 and NCA15) were lower than those for OCA (OCA5 and OCA15) except for C20 in the subsurface layer, suggesting that more tracers in the channel area came from OCA than from NCA. This was probably due to the fact that OCA was three times that of NCA in size. For UT, no consistent trend with channel size was observed either. For all four source areas, unlike that for DT, NCA5 had the largest  $P_{con}$  except for C10. With respect to the two soil layers, similar to the pattern for DT, the  $P_{con}$  values for the surface layer were greater than those for the subsurface layers except for C0 in OCA. Interestingly, for UT, the  $P_{con}$  values for NCA were greater than those for OCA except for C10 in the surface layer, suggesting that more tracers in the channels came from NCA than from OCA. This pattern was different from that for DT. This can be explained by the fact that the absolute lateral translocation for DT was greater than that for UT, therefore, tracers from OCA had a relatively greater chance to reach the channel area under DT than under UT. For UT, the lateral translocation was not high so

that only a few tracers from OCA could reach the channel. As a result, the contribution of NCA was greater than that of OCA.

### **2.4.3 Tillage translocation for CT**

#### **2.4.3.1 The total, forward and absolute lateral tillage translocation**

For CT, average total translocation was 8 cm, 12 cm and 16 cm with the SDs of 4 cm, 6 cm, 6 cm for C0, C10 and C20, respectively (Fig. 2.3). The total translocation of C20 was significantly greater than that of C0. The two components of total translocation, forward translocation and absolute lateral translocation, showed similar trends to that of total translocation. Forward translocation increased with increasing channel size and had average values of 6 cm, 11 cm and 13 cm with SDs of 4 cm, 6 cm and 6 cm for C0, C10, and C20, respectively. Absolute lateral translocation had average values of 1 cm, 0 cm and 3 cm with SDs of 0 cm, 0 cm and 2 cm for C0, C10 and C20, respectively. The values of absolute lateral translocation were one order of magnitude lower than those of forward translocation, which were at the same level of total translocation, suggesting that the energy exerted by the tillage tools was mostly allocated to forward translocation. Similar to total translocation, for both forward and absolute lateral translocation, significant differences were observed between C20 and C0. These results suggest that the large channel (i.e., C20) increased tillage translocation in both directions. Net lateral translocation in the context of CT indicates the net downslope translocation. The values were negative (downslope) but close to 0, and there was no significant difference between channel sizes (data not shown).

### **2.4.3.2 Individual tracer movement relative to the channel**

Where there was no channel (C0), with only a few exceptions, total translocation of individual tracers was lower than 40 cm (Fig. 2.5). This indicates that if the channel is within 40 cm distance of a tracer, it will have a direct impact on total translocation whereas if the channel is beyond 40 cm distance of a tracer, its impact will be much lower. Therefore, we used the 40 cm lines before and after the channel to define the four areas along the tillage direction as: the BC-OCA from the starting line of the plot to the 40 cm line before the channel, the BC-NCA from the 40 cm line before the channel to the front edge of the channel, the AC-NCA from the end edge of the channel to the 40 cm line after the channel, and the AC-OCA from there on. Because tracers were installed in 10 cm intervals, there were four and six columns of tracers for the NCAs and OCAs, respectively.

For C0, the average total translocation ranged from 4 cm to 11 cm and the differences between the four areas were non-significant as expected, except that AC-OCA was significantly lower than AC-NCA. This was likely due to experimental error but can also be a result of human error on controlling tillage speed. Under C10, the average total translocation ranged from 8 cm to 18 cm. For each column, values for C10 were consistently greater than those for C0. For both NCAs and OCAs, total translocations for C10 were significantly greater than those for C0, suggesting that the impact of the channel was significant around the channel area and extended to the outside channel area. Similar to that for C0, the differences between the four area were mostly non-significant for C10 except that AC-OCA was significantly lower than BC-NCA. Under C20, the average total translocations ranged from 9 cm to 28 cm, and for

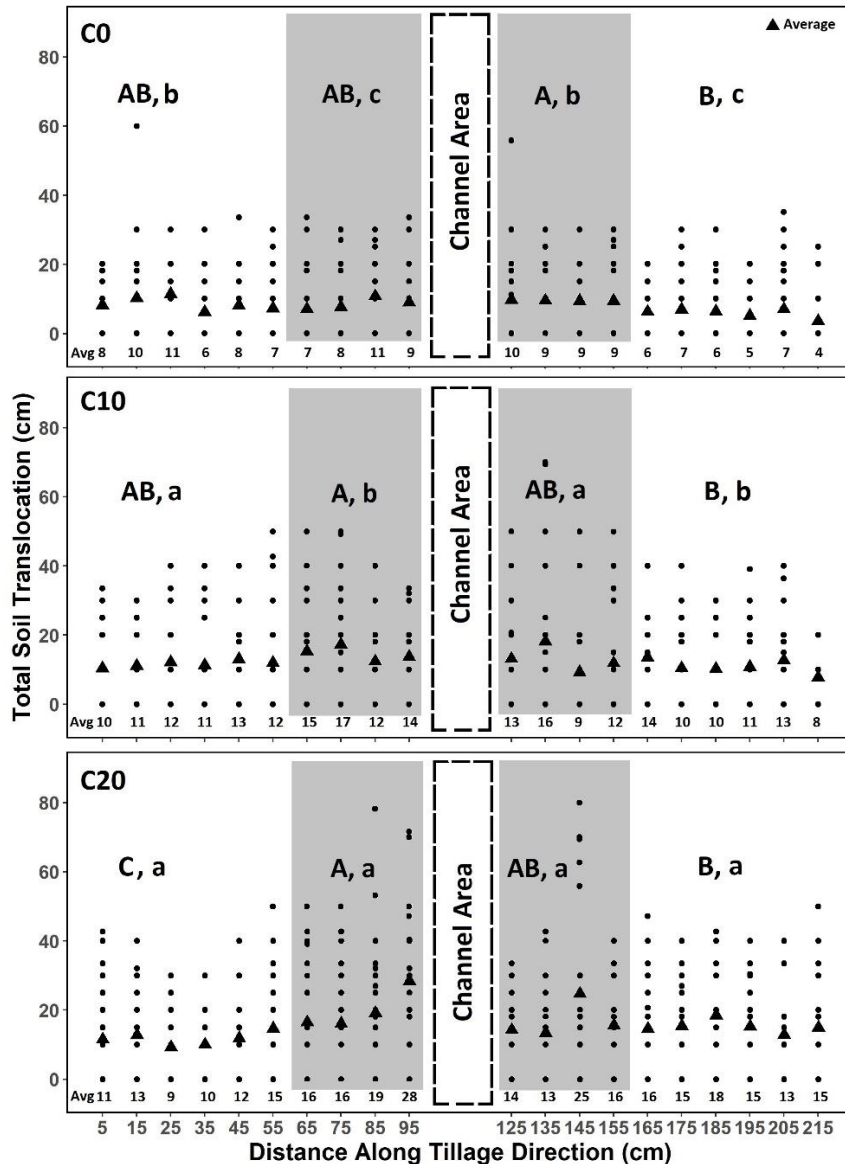


**Figure 2.5.** The total soil translocation of individual tracers under Contour Tillage treatment (CT) with channels in three different sizes (C0, C10 and C20). The shaded areas are NCAs before and after the channel area. Capital letters indicate the comparisons between different areas (within a chart) and lower-case letters indicate the comparisons between channel sizes (across different charts). Mean values with different letters are significantly different from each other at  $P < 0.10$  based on the Tukey test.

each column the values were consistently greater than those for C0 and C10. Grouped into areas, for BC-NCA,  $C20 \gg C10 \gg C0$  whereas for AC-NCA,  $C20 > C10 \gg C0$ , suggesting that the channels had a strong impact on total translocation in NCAs. Also, for BC-OCA, C20

$\approx C10 \gg C0$  whereas for AC-OCA,  $C20 \gg C10 \gg C0$ , suggesting that the impact of a channel on total translocation extended to the outside channel area. Regarding the comparisons between the four areas, the total translocation for C20 followed the order of BC-NCA > AC-NCA > AC-OCA  $\gg$  BC-OCA. The fact that total translocations for both NCAs were significantly greater than those for OCA suggests that the impact of the channel was stronger for NCA than for OCA. As components of total translocation, both forward and absolute lateral tillage translocation showed similar trends as those for total translocation (data not shown). Overall, the results suggest that the presence of a channel increased both forward and absolute lateral translocation, particularly for soil/tracers in the NCAs, and therefore total translocation.

## **2.5 Discussion**

### **2.5.1 Mechanism of soil movement around channels**

During tillage, soil in front of the tillage tool is disturbed and moved. The area of soil being impacted by the tillage tool is termed the zone of influence (ZoI, Sharifat and Kushwaha, 2000). This ZoI can be represented as a simple circular-shaped area in front of the tillage tool with the strength of impact and, therefore, soil movement from the tillage tool decreasing with distance in both forward and lateral directions (Fig. 2.6). The size of this zone is determined by the energy exerted by the tillage tool on the soil—the greater the energy, the larger the size of ZoI, which leads to greater total soil translocation. The shape of this zone is determined by the relative magnitude of forward versus lateral soil translocation. When forward translocation is greater than lateral translocation, ZoI is an oval shape with the long axis along the tillage

direction. When lateral translocation is greater, ZoI is also an oval shape but with the long axis perpendicular to the tillage direction.

#### **2.5.1.1 Downslope and upslope tillage with a channel**

During the tillage operation, tractor forward force propels soil in the direction of tillage. Additionally, gravity plays an essential role in in facilitating macro- and micro-topographic downslope soil displacement. On a macro-topographic scale, soil moves downslope, while on a micro-topographic scale, the channel walls form steep slopes that guide soil movement. The empty space created by channel functions like a trap: on one hand, lateral soil movement is greatly increased due to bank failure; on the other hand, sliding and rolling of soil particles are greatly reduced in the channel area, thus the overall soil movement, especially forward soil movement, is reduced (referred to as the trapping effect herein). Secondly, if tillage depth remains constant, there is less soil to move in the tillage layer because of the channel, whereas the overall energy acting upon the tillage layer stays the same and, therefore, the energy intensity increases, leading to a greater potential for soil movement (referred to as the energy-intensity-increase effect herein). The shape of the ZoI is determined by the relative importance of these factors as well as the location of the channel relative to the tillage tool.

When the tillage tool is going through the middle of the channel, channel banks collapse on both sides and the soil falls into the channel (especially from the surface layer). Around the channel, the direction of soil movement is pointing towards the channel. If the trapping effect overwhelms the energy-intensity-increase effect, the overall soil movement will decrease,

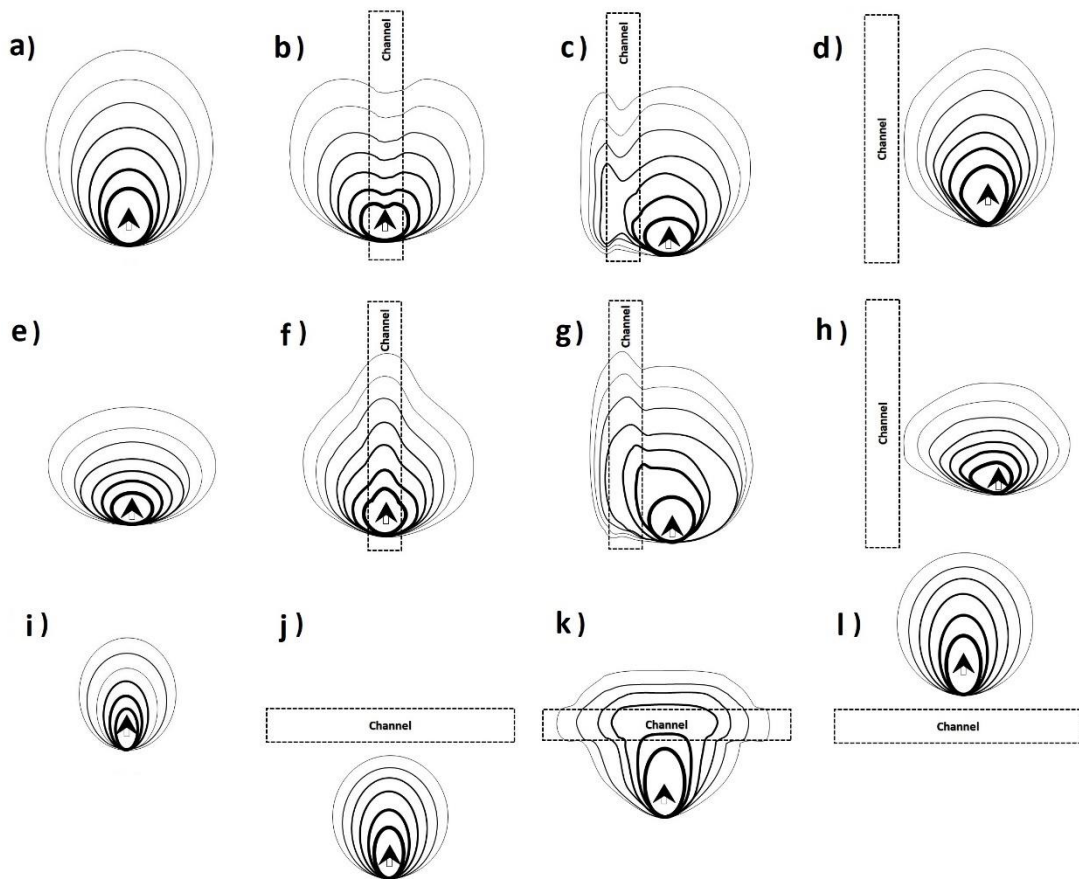


**Figure 2.6.** Illustration of Zone of Influence (ZoI) for a tillage tool under different channel conditions and tillage directions. a) to d), e) to h) and i) to l) are for downslope, upslope and contour tillage, respectively. a) no channel, forward > lateral; b) sweep going through the channel, forward > lateral; c) sweep close to the channel, forward > lateral; d) sweep within impact range of the channel, forward > lateral; e) no channel, forward < lateral; f) sweep going through the channel, forward < lateral; g) sweep close to the channel, forward < lateral; h) sweep within impact range of the channel, forward < lateral; i) no channel, forward > lateral; j) sweep before the channel; k) sweep going across the channel; and l) sweep passed the channel. Circles are iso-intensity lines. Soil particles theoretically move in directions perpendicular to the iso-intensity lines. The thickness of the line indicates the degree of influence (decreases from the centre to outside).

resulting in a flattened and widened ZoI with a dent in the middle of the circle. In contrast, if the energy-intensity-increase effect dominates, the overall soil movement will increase, resulting in a ZoI with a rise in the middle of the circle. When the channel is located close to the tillage tool (within the original ZoI of the tillage tool when there is no channel), this zone

will be deformed around the channel. In particular, because of the disruption of the channel, the influence of the tillage tool will not go as far as when there is no channel, resulting in denser iso-intensity lines running parallel and close to the channel. The shape of the iso-intensity lines in the channel, again, is determined by the relative magnitude of the energy-intensity-effect versus the trapping effect. When the trapping effect dominates, there is a dent in the middle of ZoI and when the energy-intensity-effect dominates, there is a rise in the middle of ZoI. When the channel is located outside but close to the original ZoI of the tillage tool, it may still have an effect if the zones of tillage tools overlap. Liu et al. (2007) estimated that the ZoI of a tillage tool they tested extends to approximately 30 cm from the edge of the tillage tool. Normally, for primary tillage equipment, there is no gap between tillage tools so that ZoIs of adjacent tillage tools overlap. Consequently, the channel not only can affect ZoI of the tillage tool going through it but also those of the adjacent tillage tools. The iso-intensity-lines of the ZoI for the adjacent tillage tool will be drawn toward the channel. When the channel is located far enough from a tillage tool so that the ZoI of this tillage tool does not overlap with the tillage tool going through the channel, the impact of the channel on the ZoI of this tillage tool is likely small and can be considered the same as that for the no channel condition.

The mechanism of soil movement described above can be used to explain the results on soil translocation and individual tracer movement observed in this study. The tillage equipment used in this study has five tillage tools (sweeps), numbered 1 to 5 from left to right. The centre sweep (#3) was lined up with the channel so that the ZoI of this sweep is like the scenario of tillage tool going through the middle of the channel as shown in Fig. 2.6.b and 2.6.f. For the

adjacent sweep to the right (#4), it overlapped with sweep #3 and the edge of this sweep was only about 5 cm away from the boundary of the channel. Using the 30 cm range of the ZoI estimated by Liu et al. (2007), the entire channel should be within the ZoI of sweep #4 as shown in Fig. 2.6.c or 2.6.g. For the adjacent sweep to the left (#2), there was a gap, and the edge of this sweep was about 37 cm away from the edge of the centre sweep. Using the 30 cm range of the ZoI as the reference, there will be an overlap between the ZoIs of sweeps #2 and #3 so that the ZoI of sweep #2 is impacted by the channel and will be like the ones shown in Fig. 2.6.d or 2.6.h. The far-left sweep (#1) will have a ZoI like that shown in Fig. 2.6.a or 2.6.e since the ZoI of this sweep will not be impacted by the channel whereas the far-right sweep (#5) will have a ZoI like that shown in Fig. 2.6.d or 2.6.h. It should be noted that the alignment of the centre sweep to the centre line of the channel was not precise in the experiment and the 30 cm range of the ZoI is a very rough estimate. Should the sweep be shifted to the right for a short distance or the range of the ZoI change (almost definitely will be the case, Lobb et al., 2001), the ZoIs for all the sweeps, especially those for sweep #2 and #3 will change. These variations are important but it is not possible to explore all the possibilities. Therefore, the following discussion is based on the assumption of a 30 cm ZoI from the edge of the sweep and the precise alignment of the centre sweep with the centre line of the channel. However, the variable nature of soil movement during tillage is taken into consideration when needed.

Under DT, when there was no channel (C0), forward translocation was slightly greater than lateral translocation so the ZoIs for all sweeps would be in an oval shape with the long axis along the tillage direction (Fig. 2.6). When there was a channel (C10 and C20), the ZoIs

for sweeps #1 through #5 would be like those shown in Fig. 2.6.a, 2.6.d, 2.6.b, 2.6.d, 2.6.d, respectively. For sweep #1, the ZoI would remain the same while those for sweeps #2, #3, #4 and #5 would have changed their size and shape. Relating to the results we observed for DT, when there was a channel, sweeps #2, #3, #4 and #5 were likely under the impacts of both the energy-intensity-increase effect and the trapping effect. For forward translocation, trapping effects overwhelmed the energy-intensity-increase effect so that it decreased, whereas for lateral translocation, the energy-intensity-increase effect was slightly stronger so that it increased slightly, leading to an overall slight decrease in total translocation. The decrease in forward translocation was reflected in the flattened top and the dent around the channel areas for sweep #3 and #4. The slight increase in lateral translocation was reflected in the denser parallel iso-intensity lines drawn towards the channel. The slight decrease in total translocation should be reflected in the sizes of the ZoI being smaller, but this was difficult to visualize from the figures. From the perspective of individual tracer movement, comparing with-channel to no-channel conditions, greater  $P_{all}$  and  $P_{loc}$  values indicate the strong energy-intensity-increase effect (more soil movement) and the trapping effect (more soil in the channel areas) whereas similar  $P_{con}$  values indicate that the energy-intensity-increase effect and the trapping effect cancelled each other to some degree so that the lateral translocation from different source areas were equally affected.

Under UT, when there was no channel (C0), forward translocation was slightly lower than lateral translocation, the ZoIs for all sweeps would be in an oval shape with the long axis perpendicular to the tillage direction (Fig. 2.6). The overall size of the ZoI would be smaller

than those under DT given that the values of the respective translocation measures were lower. When there was a channel (C10 and C20), the ZoIs for sweep #2, #3, #4 and #5 changed their size and shape. Relating to the results we observed for UT, when there was a channel, sweep #2, #3, #4 and #5 were likely dominated by the energy-intensity-increase effect, leading to increases in forward, lateral and total soil translocation. The increase in forward translocation was reflected in the extensions around the channel areas for sweep #3 and #4 (Fig. 2.6.f and 2.6.g versus 2.6.e). The increase in lateral translocation was reflected in the denser parallel iso-intensity lines drawn towards the channel whereas the increase in total translocation was reflected in the greater sizes of ZoI (Fig. 2.6.f, 2.6.g and 2.6.h versus 2.6.e). Also, greater  $P_{all}$  and  $P_{loc}$  values for the with-channel than for the no-channel condition again indicate the strong impact of both the energy-intensity-increase effect and the trapping effect. However, the  $P_{con}$  value was lower for NCA5 but greater for OCA5. This can be explained by the dominance of the energy-intensity-increase effect, which increased lateral translocation so that more tracers from OCA5 were able to reach the channel area.

### **2.5.1.2 Contour tillage with a channel**

When there is a channel orientated perpendicular to the tillage direction, the empty space created by the channel can also have the energy-intensity-increase effect and the trapping effect. Similar to that under DT and UT, the shape of the ZoI is determined by the location of the channel relative to the tillage tool. As the tillage tool moves towards the channel, the energy-intensity-increase effect may exist at a substantial distance from the channel but should be

minimal. When the tillage tool gets close to the channel, it will breach the channel bank, causing it to collapse and soil to fall into the channel. If this trapping effect overwhelms the energy-intensity-increase effect, the overall soil movement, especially forward soil movement, will decrease, resulting in a truncated ZoI. However, if the energy-intensity-increase effect dominates, the overall soil movement will increase, resulting in a widened ZoI going across the channel with dense iso-intensity lines parallel to the channel (Fig. 2.6.k). After the tillage tool passes the channel, the energy-intensity-increase effect still exists but there will be no trapping effect, resulting in a larger ZoI compared to no-channel condition (Fig. 2.6.l).

In this study, for CT, the channel position was the same for all sweeps except that the sweeps in the front row reached the channel before the sweeps in the back row. However, the effect of this time difference on the sweeps' ZoIs was expected to be low. Therefore, the ZoIs for all five sweeps were assumed to be the same. For the no-channel condition (C0), forward translocation was significantly greater than lateral translocation ( $P < 0.10$ , based on a two-sample t-test) so that the ZoI would be in an oval shape with the long axis along the tillage direction, similar to that for DT but smaller in size (Fig. 2.6.i). When there is a channel, the energy-intensity-increase effect seems to dominate because forward, lateral and total translocation all increased. Evidence of this was observed in that: the forward and lateral translocation increased for individual tracers across the length of the plot, especially in the area right before and after the channel (Fig. 2.5). Along the tillage path, the ZoI of a tillage tool will be the same as that of the no channel condition, initially (Fig. 2.6.i). As it moves closer to the channel, the size of the ZoI may increase due to the energy-intensity-increase effect (Fig. 2.6.j).

Once the front end of ZoI reaches the channel, ZoI will also be affected by the trapping effect, with a shape affected strongly by the channel (Fig. 2.6.k). When the tillage equipment passes the channel, ZoI will again only be affected by the energy-intensity-increase effect (Fig. 2.6.l) and the size of it will decrease along the path until it becomes the same as that of the no channel condition.

### **2.5.2 Implication for conservation tillage practices**

Contour tillage is one of the widely used conservation tillage practices to reduce runoff, control water erosion and improve soil sustainability (Bogunovic et al., 2018; Stevens et al., 2009). However, is contour tillage the most efficient way to eliminate channels such as rills and ephemeral gullies created by water erosion? The efficiency of infilling a channel with tillage can be assessed with the tillage translocation measures as follows: the magnitude of tillage translocation is an indicator of the ability of tillage to smooth the soil surface; the difference in translocation between with and without channels is an indicator of the additional soil movement due to the existence of channel. For DT and UT, tillage was conducted along the channel so that channel infilling is mainly determined by lateral translocation, whereas for CT, tillage was conducted perpendicular to the channel so that the channel infilling is mainly determined by forward translocation. Our results show that lateral translocation for DT was slightly greater than that for UT, indicating that DT can create a smoother surface than UT. However, there was a slightly stronger increase with channel size in lateral translocation for UT than DT, indicating that UT may be able to fill the channel slightly better. Evidence of this

was also observed in the sums of  $P_{all}$  values from the four source areas, which were 5.5 %, 6.5 % and 16.1 % under DT and 2.2 %, 7.3 % and 18.1 % under UT for C0, C10 and C20, respectively. Greater  $P_{all}$  values for C0 with DT than UT indicate greater soil movement with DT, whereas greater  $P_{all}$  values for C10 and C20 with UT than DT indicate more soil being moved to the channels for UT than DT. For CT, the forward translocation where there was a channel (especially C20) was greater than the respective lateral translocation for DT and UT. The increase of translocation with channel size was also greater for CT than those for DT and UT. These observations suggest that CT can create a smoother surface and fill the channel better than DT and UT.

Based on these assessments, we recommend CT when one of the objectives for primary tillage (using a tillage equipment similar to the one used in this study) is filling channels. However, channels are normally oriented along the slope. If smoothing the channel is the only purpose of the tillage pass (e.g., when ephemeral gullies occur after primary tillage), CT is not very efficient as the equipment needs to be turned back and forth. Under such circumstances, DT and UT may be a better choice. However, even with DT and UT, keeping the tillage direction at an angle towards the channel may help smoothing the surface and filling the channel better.

It should be noted that the sweep used in this study is a two-way tillage tool commonly used for conservation tillage from the perspective of water erosion control because it does not invert the soil thus exerts less soil disturbance and leaves more crop residues on the soil surface than typical one-way tillage equipment does (e.g., a mouldboard plough). For the same reason

of less soil disturbance, a two-way tillage tool is also generally believed to cause less tillage erosion. However, Tiessen et al. (2007a) examined a similar two-way tillage tool and found that it was as erosive as a one-way tillage tool. From the perspective of smoothing channels, the greater soil disturbance with a one-way tillage equipment may lead to greater efficiency for channel filling. However, the process of soil movement by a one-way tillage tool is very different from that of a two-way tillage tool and requires further examination.

### **2.5.3 Experimental errors and uncertainties**

The data of this study were highly variable, not only for the replicates of the same treatments but also for different columns of tracers in the same plot and even for individual tracers in the same column. Part of this high variability was due to the erratic nature of soil movement during tillage but high experimental errors and uncertainties due to limitations in experiment setup and control certainly contributed substantially to the high variability as well. First, operational parameters such as tillage speed and depth have not been strictly controlled. For example, tillage speed in this study ranged from 2.2 km h<sup>-1</sup> to 6.8 km h<sup>-1</sup>. Although statistical analysis show that tillage translocation measures were not significantly correlated with tillage speed, large variation in tillage speed certainly can cause variations in these measures among replicates for the same treatment. Using a lower gear ratio and greater engine speed to have more control on the tractor speed may help to keep the tillage speed the same for different runs. Second, the arrangement of sweeps was asymmetrical and the alignment of the equipment with the channel was not precise. As described above, there was a metal bar across

the centre of the mounting frame so that the centre sweep was shifted toward the right-hand side, leaving a large gap between sweeps #2 and #3 and an overlap between sweep #3 and #4. Also, although extreme caution has been taken by the operator to align the tillage equipment along the centre line of the channel, a 5 - 10 cm error was possible. Together, these two factors created large uncertainties for the same columns of tracers under different replicates (as an extreme example, imagine in one run the channel was between sweeps #2 and #3 whereas in another run the channel was between sweeps #3 and #4). Third, field conditions vary from plot to plot and from time to time. Although all plots were on the same slope (less than 1 ha in area), differences in micro-topography and soil are inevitable. Soil conditions (especially moisture) also change depending on weather. Although efforts were made to conduct the experiment runs in similar soil conditions, they were certainly not exactly the same. Last, the sampling was based on a grid of 10 cm by 10 cm, which limits the resolution of translocation measurement to 10 cm. This low resolution resulted in the rounding of tillage translocation measures and likely contributed substantially to the high uncertainties of the translocation data.

The high variability and uncertainties of the data posed great challenges in the statistical analysis. As described in section 2.3.5.2, in this study, extreme values were removed prior to statistical analyses. It should be noted that extreme values should not be treated blindly as unreal. In fact, tillage translocation experiments with bulk tracers have demonstrated that the amount of tracers moved to the tail of the tracer distribution curve, although small, often dominates the shape of the curve and, therefore, is very important for determining the amount of tillage erosion (Li et al., 2007a; Tiessen et al., 2007a). In the case of this study, the point

tracer method used had a much lower tracer density than the bulk tracer method and, therefore, likely has much greater errors towards the tail of the tracer distribution curve (with extremely high tillage translocation values). Since this study was designed to compare differences between treatments, the focus was on the central tendency of the datasets. Removal of extreme values with high errors should increase the accuracy of the central tendency estimates and, therefore, was considered justified.

#### **2.5.4 Future studies**

Using the tracer method, there are two ways to calculate tillage translocation. One way is to calculate it from the tracer distribution as conducted in this study, and the other way is to use a summation curve with convolution (Lobb et al., 2001). Theoretically, the two methods should produce the exact same value for tillage translocation. However, the distribution method is easier to apply whereas the summation curve method is able to provide more information regarding the dispersion of the translocated soil. In this study, tracers were buried in rows beyond the range of expected tillage translocation. The design was to enable the use of the summation curve method. However, this was beyond the scope of this paper, so only the first 10 rows of the tracers' data were used. An additional study is underway to use the full range of the tracer data to examine the dispersion of tracers along the tillage path as well as the errors and uncertainties associated with both the distribution method and the summation curve method.

Another direction for future study is to incorporate knowledge gained from this experiment into tillage erosion models. Current tillage erosion models such as the Directional Tillage Erosion Model (DirTilLEM, Li et al., 2009) and the Water and Tillage Erosion Model (WaTEM, Van Oost et al., 2000) compute tillage erosion rate for each grid cell in a Digital Elevation Model (DEM). None of these models take into account the effect of channels on tillage erosion. The knowledge obtained from this study can be used to fill this gap. For example, the DEM used in the model can be prepared to label cells where channels are located. Tillage translocation from these channel cells can be calculated differently based on the differences observed in translocation with and without channels in this study. This would enable the model to simulate tillage erosion for field with channels. This not only provides a more accurate estimation for tillage erosion but also establishes a link between tillage erosion and water erosion via channels, facilitating a comprehensive modeling of water and tillage erosion as well as their interactions.

## **2.6 Conclusion**

In this study, the role of channels and tillage direction on tillage translocation was examined. The presence of channels reduced tillage translocation during DT but increased tillage translocation during UT. For both DT and UT, substantial channel infilling with translocated soil occurred. The soil falling into the channels was mainly from the surface layer for both DT and UT but for DT, it was mainly from the area away from the channel whereas for UT, it was mainly from the area adjacent to the channel. For CT, the presence of channels

increased tillage translocation but unlike DT and UT, the channel was oriented perpendicular to the tillage direction so that tillage was more effective in filling the channel. For the mechanisms involved in tillage translocation with the presence of a channel, we conclude that the relative importance of the trapping effect (channel functions like a trap) versus the energy-intensity-increase effect (greater energy intensity due to less soil being moved with the presence of a channel) is likely responsible for the different patterns of tillage translocation under different treatments. If the trapping effect dominates, the overall soil movement, especially forward soil movement, tends to decrease, whereas if the energy-intensity-increase effect dominates, the overall soil movement tends to increase. The relative importance of the trapping effect and the energy-intensity-increase effect is determined by the shape and size of the tillage tool's ZoI. The presence of a channel, its location and orientation relative to the tillage tool, and the tillage direction can all affect the shape and size of the ZoI. With respect to sustainable soil management, the best practice is to reduce the formation of channels by water erosion. If channels are formed by water erosion, CT is recommended because it will induce lower tillage translocation and fill in the channel more effectively than DT and UT. Moreover, the knowledge gained from this study on the effects of existing channels on tillage translocation can be used to enhance the tillage erosion model so that it can be connected to water erosion models, providing more realistic and accurate predictions of tillage erosion and the overall soil erosion on agricultural lands.

## 2.7 Acknowledgements

This study was funded by the Agriculture and Agri-food Canada project “Characterizing and modeling the interactions between water and tillage erosion under potato and cereal production systems” [project number J-000994] (PI: Li) and project “Sustainability measures to monitor and analyze the environmental impact of Canadian agriculture” [project number J-002316] (PI: McConkey and McDonald) as well as a Canadian Natural Science and Engineering Research Council Discovery Grant (PI: Lobb). The authors would like to thank Dr. Zhisheng Xing and Mr. Alyre Godin for their insightful suggestions for the experiment, and Meagan Betts, Tegan Smith, Joyce Wang and Samantha Soubasis for helping with the field work. We are also grateful to Mr. Jacques Williams and the rest of the crew in the farm services unit of the Fredericton Research and Development Centre for managing the field and conducting the tillage operations.

## 2.8 References

- Bogunovic, I., Pereira, P., Kistic, I., Sajko, K., Sraka, M., 2018. Tillage management impacts on soil compaction, erosion and crop yield in Stagnosols (Croatia). *CATENA* 160, 376–384. <https://doi.org/10.1016/j.catena.2017.10.009>.
- Chen, H., Cai, Q., 2006. Impact of hillslope vegetation restoration on gully erosion induced sediment yield. *Sci. China Series D* 49, 176–192. <https://doi.org/10.1007/s11430-005-0177-4>.

- Dai, J., Zhang, J., Zhang, Z., Jia, L., Xu, H., Wang, Y., 2020. Effects of water discharge rate and slope gradient on runoff and sediment yield related to tillage erosion. *Arch. Agron. Soil Sci.* 1–13. <https://doi.org/10.1080/03650340.2020.1766676>.
- Foster, G.R., 1986. Chapter 4. Understanding ephemeral gully erosion. In: *Soil Conservation: An Assessment of the National Resources Inventory, Vol. 2*. The National Academies Press, Washington, DC, pp. 90–125. <https://doi.org/10.17226/648>.
- Govers, G., Lobb, D.A., Quine, T.A., 1999. Tillage erosion and translocation: emergence of a new paradigm in soil erosion research. *Soil Tillage Res.* 51, 167–174. [https://doi.org/10.1016/S0167-1987\(99\)00035-5](https://doi.org/10.1016/S0167-1987(99)00035-5).
- Lal, R., 2001. Soil degradation by erosion. *Land Degrad. Dev.* 12, 519–539. <https://doi.org/10.1002/ldr.472>.
- Li, S., Lobb, D.A., Lindstrom, M.J., 2007a. Tillage translocation and tillage erosion in cereal-based production in Manitoba, Canada. *Soil Tillage Res.* 94, 164–182. <https://doi.org/10.1016/j.still.2006.07.019>.
- Li, S., Lobb, D.A., Lindstrom, M.J., Farenhorst, A., 2007b. Tillage and water erosion on different landscapes in the northern North American Great Plains evaluated using <sup>137</sup>Cs technique and soil erosion models. *CATENA* 70, 493–505. <https://doi.org/10.1016/j.catena.2006.12.003>.
- Li, S., Lobb, D.A., Tiessen, K.H.D., 2009. Modeling tillage-induced morphological features in cultivated landscapes. *Soil Tillage Res.* 103, 33–45. <https://doi.org/10.1016/j.still.2008.09.005>.

- Li, S., Lobb, D.A., Tiessen, K.H.D., 2013. Soil erosion and conservation based in part on the article “Soil erosion and conservation” by W. S. Fyfe, which appeared in the encyclopedia of environmetrics. In: El-Shaarawi, A.H., Piegorisch, W.W., Chebana, F., Ouarda, T.B. (Eds.), Encyclopedia of Environmetrics. <https://doi.org/10.1002/9780470057339.vas031.pub2>.
- Liu, J., Chen, Y., Lobb, D.A., Kushwaha, R.L., 2007. Soil-straw-tillage tool interaction: field and soil bin study. *Can. Biosys. Eng.* 49, 2.
- Lobb, D.A., Kachanoski, R.G., 1999. Modeling tillage erosion in the topographically complex landscapes of southwestern Ontario, Canada. *Soil Tillage Res.* 51, 261–277. [https://doi.org/10.1016/S0167-1987\(99\)00042-2](https://doi.org/10.1016/S0167-1987(99)00042-2).
- Lobb, D.A., Kachanoski, R.G., Miller, M.H., 1995. Tillage translocation and tillage erosion on shoulder slope landscape positions measured using <sup>137</sup>Cs as a tracer. *Can. J. Soil Sci.* 75, 211–218. <https://doi.org/10.4141/cjss95-029>.
- Lobb, D.A., Kachanoski, R.G., Miller, M.H., 1999. Tillage translocation and tillage erosion in the complex upland landscapes of southwestern Ontario, Canada. *Soil Tillage Res.* 51, 189–209. [https://doi.org/10.1016/S0167-1987\(99\)00037-9](https://doi.org/10.1016/S0167-1987(99)00037-9).
- Lobb, D.A., Quine, T.A., Govers, G., Heckrath, G.J., 2001. Comparison of methods used to calculate tillage translocation using plot-tracers. *J. Soil Water Conserv.* 56, 321–328.
- Lobb, D.A., Lindstrom, M.J., Schumacher, T.E., 2003. soil erosion processes and their interactions: implications for environmental indicators, agricultural impacts on soil erosion

- and soil biodiversity: developing indicators for policy analysis. In: Proceedings from an OECD Expert Meeting—Rome. Italy, March, pp. 325–336.
- Montgomery, J.A., McCool, D.K., Busacca, A.J., Frazier, B.E., 1999. Quantifying tillage translocation and deposition rates due to moldboard plowing in the Palouse region of the Pacific Northwest, USA. *Soil Tillage Res.* 51, 175–187. [https://doi.org/10.1016/S0167-1987\(99\)00036-7](https://doi.org/10.1016/S0167-1987(99)00036-7).
- Morgan, R.P.C., 2009. *Soil Erosion and Conservation*, 3rd ed. John Wiley & Sons.
- Nachtergaele, J., Poesen, J., 1999. Assessment of soil losses by ephemeral gully erosion using high-altitude (stereo) aerial photographs. *Earth Surf. Proces. Landforms: J. Br. Geomorphol. Res. Group* 24, 693–706. [https://doi.org/10.1002/\(SICI\)1096-9837\(199908\)24:8%3C693::AID-ESP992%3E3.0.CO;2-7](https://doi.org/10.1002/(SICI)1096-9837(199908)24:8%3C693::AID-ESP992%3E3.0.CO;2-7).
- Novak, P., Hůla, J., 2017a. The influence of sloping land on soil particle translocation during secondary tillage. *Agron. Res.* 15, 799–805.
- Novak, P., Hůla, J., 2017b. Translocation of the upper soil layer in multiple operations of seedbed preparation. *Res. Agric. Eng.* 63, S46–S52. <https://doi.org/10.17221/40/2017-RAE>.
- Poesen, J., 1996. Contribution of gully erosion to sediment production. In: *Erosion and Sediment Yield: Global and Regional Perspectives: Proceedings of an International Symposium Held at Exeter, UK, from 15 to 19 July 1996*. IAHS, p. 251.

- Poesen, J., Nachtergaele, J., Verstraeten, G., Valentin, C., 2003. Gully erosion and environmental change: importance and research needs. *CATENA* 50, 91–133. [https://doi.org/10.1016/S0341-8162\(02\)00143-1](https://doi.org/10.1016/S0341-8162(02)00143-1).
- Poesen, J., Torri, D.B., Vanwalleghem, T., 2011. Gully erosion: procedures to adopt when modeling soil erosion in landscapes affected by gullyng. *Handbook of Erosion Modeling*, pp. 360–386. <https://doi.org/10.1002/9781444328455.ch19>.
- Rees, H.W., Fahmy, S.H., 1984. *Soils of the Agriculture Canada Research Station*. LRRI, Research Branch, Agriculture Canada, Fredericton, NB.
- Sharifat, K., Kushwaha, R.L., 2000. Modeling soil movement by tillage tools. *Canadian Agric. Eng.* 42, 165–172.
- Stevens, C.J., Quinton, J.N., Bailey, A.P., Deasy, C., Silgram, M., Jackson, D.R., 2009. The effects of minimal tillage, contour cultivation and in-field vegetative barriers on soil erosion and phosphorus loss. *Soil Tillage Res.* 106, 145–151. <https://doi.org/10.1016/j.still.2009.04.009>.
- Tiessen, K.H.D., Lobb, D.A., Mehuys, G.R., Rees, H.W., 2007a. Tillage erosion within potato production in Atlantic Canada: II Erosivity of primary and secondary tillage operations. *Soil Tillage Res.* 95, 320–331. <https://doi.org/10.1016/j.still.2007.02.009>.
- Tiessen, K.H.D., Mehuys, G.R., Lobb, D.A., Rees, H.W., 2007b. Tillage erosion within potato production systems in Atlantic Canada: I. Measurement of tillage translocation by implements used in seedbed preparation. *Soil Tillage Res.* 95, 308–319. <https://doi.org/10.1016/j.still.2007.02.003>.

- Van Muysen, W., Govers, G., Van Oost, K., Van Rompaey, A., 2000. The effect of tillage depth, tillage speed, and soil condition on chisel tillage erosivity. *J. Soil Water Conserv.* 55, 355–364.
- Van Oost, K., Govers, G., Desmet, P., 2000. Evaluating the effects of changes in landscape structure on soil erosion by water and tillage. *Landscape Ecol.* 15, 577–589. <https://doi.org/10.1023/A:1008198215674>.
- Van Oost, K., Van Muysen, W., Govers, G., Deckers, J., Quine, T.A., 2005. From water to tillage erosion dominated landform evolution. *Geomorphology* 72, 193–203. <https://doi.org/10.1016/j.geomorph.2005.05.010>.
- Van Oost, K., Govers, G., De Alba, S., Quine, T.A., 2006. Tillage erosion: a review of controlling factors and implications for soil quality. *Progress Phys. Geography Earth Environ.* 30, 443–466. <https://doi.org/10.1191/0309133306pp487ra>.
- Wang, Y., Zhang, J.H., Zhang, Z.H., Jia, L.Z., 2016. Impact of tillage erosion on water erosion in a hilly landscape. *Sci. Total Environ.* 551-552, 522–532. <https://doi.org/10.1016/j.scitotenv.2016.02.045>.
- Xu, H.C., Jia, L.Z., Zhang, J.H., Zhang, Z.H., Wei, Y.H., 2019. Combined effects of tillage direction and slope gradient on soil translocation by hoeing. *CATENA* 175, 421–429. <https://doi.org/10.1016/j.catena.2018.12.039>.
- Zhang, J.H., Wang, Y., Zhang, Z.H., 2014. Effect of terrace forms on water and tillage erosion on a hilly landscape in the Yangtze River Basin, China. *Geomorphology* 216, 114–124. <https://doi.org/10.1016/j.geomorph.2014.03.030>.

Zhang, J., Yang, M., Deng, X., Liu, Z., Zhang, F., 2019. The effects of tillage on sheet erosion on sloping fields in the wind-water erosion crisscross region of the Chinese Loess Plateau.

Soil Tillage Res. 187, 235–245. <https://doi.org/10.1016/j.still.2018.12.014>.

Zhao, P., Li, S., Wang, E., Chen, X., Deng, J., Zhao, Y., 2018. Tillage erosion and its effect on spatial variations of soil organic carbon in the black soil region of China. Soil Tillage Res.

178, 72–81. <https://doi.org/10.1016/j.still.2017.12.022>.

## 2.9 Nomenclature

AC-NCA	the near channel area after the channel for plot under contour tillage
AC-OCA	the outside channel area after the channel for plot under contour tillage
ANCOVA	analysis of covariance
ANOVA	analysis of variance
BC-NCA	the near channel area before the channel for plot under contour tillage
BC-OCA	the outside channel area before the channel for plot under contour tillage
C0	no channel treatment
C10	treatment with a 10 cm by 10 cm channel
C20	treatment with a 20 cm by 20 cm channel
CT	contour tillage
DT	downslope tillage
FRDC	Fredericton Research and Development Centre
i	denotes the source area
NCA	the near channel areas
NCA15	subsurface (10 cm - 20 cm) layer of the near channel area for plot under downslope and upslope tillage

NCA5	surface (0 cm - 10 cm) layer of the near channel area for plot under downslope and upslope tillage
N <sup>ch</sup>	the total number of tracers found in the channel area after tillage
n	the number of tracers moved into the channel area from source area i
N	the number of tracers originally in source area i
N <sup>pl</sup>	the total number of tracers originally in the whole plot
OCA	the outside channel areas
OCA15	subsurface (10 cm - 20 cm) layer of the outside channel area for plot under downslope and upslope tillage
OCA5	surface (0 cm - 10 cm) layer of the outside channel area for plot under downslope and upslope tillage
P <sub>5cm</sub>	the percentage of positions where only the tracer at 5 cm was moved, used as an indicator for whether or not the tillage depth was below 15 cm
P <sub>all</sub>	the number of tracers moved into the channel area (versus to outside of the channel area)
P <sub>con</sub>	the contribution of different source areas to the tracer moved in the channel area
P <sub>loc</sub>	the proportion of soil in each source area moved into the channel area
RR	the tracer recovery ratio
SD	standard deviation
UT	upslope tillage
ZofI	the zone of influence

### **3. SHORT-TERM EFFECTS OF AN EXISTING CHANNEL, A SINGLE PASS OF TILLAGE AND THEIR INTERACTION ON THE GENGARATION OF RUNOFF AND SEDIMENT**

Zheng, F., Lobb, D.A. and Li, S., 2023. The short-term effects of an existing channel, a single pass of tillage and their interaction on the generation of runoff and sediment. *Soil Tillage Res.*, 226, p.105575.

Received 12 April 2022; Received in revised form 14 October 2022; Accepted 29 October 2022; Available online 7 November 2022.

#### **Contributions of authors**

The authors confirm contribution to the paper as follows: 1. study conception and design: Zheng, F, Lobb, D.A. and Li, S.; 2. resources provided: Lobb, D.A. and Li, S.; 3. data collection: Zheng, F.; 4. data analysis: Zheng, F.; 5. data visualization: Zheng, F.; 6. data interpretation: Zheng, F., Lobb, D.A. and Li, S., 7. writing—original draft preparation: Zheng, F.; 8. writing—review and editing: Lobb, D.A. and Li, S.; 9. funding: Lobb, D.A. and Li, S.. The author confirms sole responsibility for the following: study conception and design, data collection, analysis, and paper preparation.

#### **3.1 Abstract**

A critical time for both water and tillage erosion is the period between growing seasons when the field is tilled and thus bare or nearly bare. During this period, there is a high risk for water erosion, leading to water eroded channels. The existing channels, tillage operations and the combination of these two may strongly affect runoff and sediment generations in the

following water erosion events. However, knowledge on this is limited. In this study, plot experiments were conducted to quantify the short-term effects of an existing channel, a single pass of tillage and their interactions on the generations of runoff and sediment. Four treatments: no channel, no tillage (NN, as the control); with a channel, no tillage (CN); no channel, with tillage (NT); and with a channel, with tillage (CT) were examined. Plots under the four treatments were placed under simulated rainfall for at least one hour. Runoff and sediment samples were collected every 5-minutes after runoff initiation. The effects of treatments on the amounts of runoff and sediment were analyzed with ANOVA and ANCOVA. We found that with an existing channel, runoff initiation has accelerated and runoff discharge and sediment export have increased whereas with a single pass of tillage, runoff initiation was delayed and runoff discharge and sediment export have decreased. When an existing channel was tilled, the effects of tillage dominated while the existing channel only demonstrated some minor impacts. Applying this knowledge to a cereal-potato crop rotation common in Atlantic Canada, we recommend spring primary tillage after cereal harvesting and late fall primary tillage after potato harvesting to reduce the overall soil erosion.

### **3.2 Introduction**

Soil erosion is a global environmental issue, leading to degraded soil quality and reduced crop productivity (Lal, 2001). In general, cultivated fields are subject to water, wind and tillage erosion, although one erosion process normally dominates (Li et al., 2012). These soil erosion processes may interact with each other, increasing or decreasing the total amount of soil erosion.

Therefore, the total soil erosion observed in cultivated fields is a combined result of wind, water and tillage erosion, and their interactions (Lobb et al., 2003). In humid and subhumid climate regions, wind erosion is often low but tillage and water erosion and their interactions can all be high (e.g., Li et al., 2007). As a result, in order to accurately quantify the total soil erosion, both the individual erosion processes and their interactions need to be quantified.

Water erosion can take the forms of sheet, rill and gully erosion (Brady and Weil, 2016). Rill and gully erosion are both channelized erosions. In a rainfall event, water erosion starts in the form of splash and sheet erosion. As rainfall progresses, runoff starts to concentrate, incising the soil surface and forming small channels termed rills. Rills can develop into large channels or gullies over several consecutive rainfall events (Kinnell, 2005; Morgan, 2009). Gullies can be ephemeral or permanent. Ephemeral gullies are defined as “small channels eroded by concentrated overland flow that can be easily filled by normal tillage, only to reform again in the same location by additional runoff events” (SSSA, 2020). When the channels are too big to be erased by normal tillage operations, they become permanent topographic features and are referred to as classic gullies (Bennett and Wells, 2019).

Channels contribute to erosion in two ways: source of sediment and pathway for sediment transport. First, concentrated water flow in the channel can detach a lot of sediments by head cutting (Hosseinalizadeh et al., 2019a, b), channel bed incision (Qin et al., 2019), channel widening (Wells et al., 2013) and channel wall collapsing (Zegeye et al., 2018). The USDA-NRCS (1997) reported that channels or ephemeral gullies contribute on average 38 % of total erosion in 17 states in the USA. Poesen et al. (2003) reported that based on data collected in

different parts of the world, sediment contribution from channels to total sediment yield caused by water erosion at various scales (from plot to watershed scale) ranged from 10% to 94%. Second, channels converge flows from interrill areas and provide pathways for rapid discharge of sediment produced by interrill and rill erosion, increasing the efficiency of sediment delivery (Souchère et al., 2003).

Tillage is often used to clean crop residue, prepare the field for seeding, control weeds and enhance soil conditions for crop growth (e.g., reducing soil compaction and increase water surface retention and infiltration) (Lobb et al., 2007). All these tillage operations will cause soil redistribution, thus, tillage erosion (Li et al., 2012). Tillage also changes the soil physical properties thus can affect water erosion in subsequent rainfall events. Many studies reported that tillage increases soil roughness and surface retention thus can effectively reduce surface runoff and sediment yield (Cogo et al., 1984; da Rocha Junior et al., 2016; Gómez and Nearing, 2005; Johnson et al., 1979; Römkens et al., 2002). Tillage practices can contribute to the creation of a rough soil surface at the micro-topographic scale through several mechanisms. These include the disruption of soil aggregates, uneven incorporation of organic residues, variations in tillage depth, and the displacement of soil during tillage operations. Additionally, the choice of tillage implements, and the uneven distribution of residue cover can further contribute to surface roughness. The extent to which tillage creates a rough soil surface depends on factors such as soil type, equipment used, and the specific goals of tillage.

Another important but less noted function of tillage is to fill in and eliminate rills and ephemeral gullies. Tillage practices play a vital role in smoothing the land surface at the meso-

topographic scale, specifically in the context of filling channels or depressions within the landscape. Through the movement of soil during tillage operations, areas of lower elevation can be strategically filled with soil from higher ground, effectively leveling out the terrain and minimizing the visibility of channels. This process not only helps reduce erosion risks by compacting soil particles and preventing deeper channel formation but also prepares a uniform seedbed for planting while enhancing water management and machinery accessibility. Process wise, tillage filling channels is a form of tillage erosion (soil is redistributed by tillage from surrounding areas to fill the channel). The result of this special form of tillage erosion, however, can affect the water erosion in a subsequent rainfall event. On one hand, this may lead to reduced runoff and water erosion as it eliminates the pathways for sediment delivery and the source of channelized erosion. On the other hand, newly deposited soil in the channels is loose and not well structured. As a result, during the next water erosion event, when runoff re-converge, the newly deposited soil is easily erodible. So, there is a potential for increased erosion due to tillage filling existing channels. Clearly, further investigation is required to determine the overall resultant effects of tillage filling existing channels.

Given this knowledge gap, this study was designed to characterize and quantify the effects of: a) an existing channel; b) a single pass of tillage; and c) a single pass of tillage filling an existing channel on the generation of runoff and sediment on fields that are bare. The goal was to better understand the underlying mechanisms leading to these effects and to develop strategies to minimize the overall runoff and sediment losses from cultivated fields during the critical period of soil erosion.

Between growing seasons, for fields that are bare, channelized erosion and tillage often occur in an alternating but consecutive sequence, so that there may be linkages and interactions between these two processes (Lobb et al., 2003). Linkages refer to the simple additive effects between the two processes, whereas interactions occur when one process changes the erodibility of the landscape for another process or when one process works as a delivery mechanism for another process (Li et al., 2007; Li et al., 2008b; Lobb et al., 1995; Van Oost et al., 2009). Wang et al. (2016) reported that tillage erosion increases soil erodibility and delivers the soil for water erosion in sloping fields, accelerating water erosion. Dai et al. (2020) reported that tillage erosion can change hillslope hydrological processes and increase sediment yield by water erosion. However, in these studies, the effects of existing channels and tillage have not been individually quantified, leaving a knowledge gap on how existing channels and tillage individually affect water erosion and how an existing channel can link and interact with tillage in a water erosion event.

### **3.3 Materials and Methods**

#### **3.3.1 Study area and plot layout**

The study was conducted in field plots in the Experimental Farm of the Fredericton Research and Development Centre (FRDC) in New Brunswick, Canada. The major cash crop in this province is potato, mostly grown under rain-fed agriculture production systems (AAFC-CHD, 2019). This area features a cold and humid continental climate with an average daily temperature of 5.6 °C and an average annual precipitation of 1077.7 mm (ECCC, 2022). Soil

at the study site is an Orthic Humo-Ferric Podzol developed on a coarse loamy fluvial deposit over coarse loamy morainal lodgement till (Rees and Fahmy, 1984). The topsoil is friable, yellowish brown (10 YR) sandy loam with 10 - 25 % angular cobbles and gravels, while the subsoil is firm, dark brown (7.5 YR) sandy loam with 10 - 20 % angular gravels and some cobbles. Overall, the soil is well-drained (Rees and Fahmy, 1984).

The experiment was conducted following a Latin Square design, with time being the row block, field being the column block and four treatments allocated to the cells (i.e., specific time-field combination) according to a randomly selected Latin Square (Table 3.1, Fig. A.1). The four treatments were no channel, no tillage (NN), with a channel, no tillage (CN), no channel, with tillage (NT), and with a channel, with tillage (CT). Treatment NN was used as the control. The four fields (10-m-wide-by-80-m-long) were used to reflect spatial variations such as soil properties and micro-topography variations. They were established on an east-north facing slope with a slope gradient of ~10 % in the farm. The four times of the experiments were used to reflect temporal variations of soil properties, such as soil moisture changes at different soil layers due to precipitation. Ideally, we would like to finish the experiment in a very short window to keep the field conditions the same for all plot experiments. This was not possible because each plot experiment took half a day to one day to finish and rainfall is frequent in the summer. Therefore, the plot experiments were conducted at four times in the summer of 2016 and each time, only four plot experiments were done (Table 3.1). The time selection was based on rainfall. At each time, the experiment was started two days after a rainfall event with at least three days without rainfall in the weather forecast. The Latin Square

design was used because after accounting for the two block factors (field and time), variabilities in soil parameters that could not be measured without altering outcomes (e.g., subsoil compaction, porosity, antecedent water content, temperature, etc.) would be included in any statistically significant findings.

**Table 3.1** The Latin Square experimental design used in this study. Time and field were used as row and column factor to block temporal and spatial variations on experimental conditions, respectively. The treatments (i.e., NN, CN, NT, CT) were allocated to specific time and field based on a random selected Latin square

	Field 1	Field 2	Field 3	Field 4
2016 Jul 5 - 7	NT	CT	NN	CN
2016 Jul 21 - 24	NN	CN	NT	CT
2016 Aug 10 - 11	CT	NT	CN	NN
2016 Sep 5 - 6	CN	NN	CT	NT

### 3.3.2 Plot setup

Before each run, each field was disc harrowed to mimic a bare soil surface after harvesting. In each field, a 2-m-by-2-m plot area was marked. The plot surface was further smoothed using a rake drawn in the direction perpendicular to the slope. For treatments CN and CT, a 30-cm-wide and 30-cm-deep channel was manually excavated along the slope in the centre of the plot, mimicking a water erosion channel (Fig. 3.1.a). The channel size of 30-cm-wide and 30-cm-deep was used because it is the size often used to differentiate ephemeral gully and classic gully (Poesen et al., 2003). For treatments NT and CT, tillage operation was conducted with a cultivator (Fig. 3.1.b). The sweep (McKay 50 - 12K) mounted on the cultivator was about 30 cm wide and 25 cm long. In each tillage operation, the centre sweep was lined up with the centre-line of the plot (also center-line of the channel in CN and CT). The tillage was always

conducted downslope along the slope direction. Tillage speed was targeted at  $\sim 3.6 \text{ km hr}^{-1}$  and tillage depth was controlled at  $\sim 20 \text{ cm}$ .



**Figure 3.1.** a) a CN treatment plot before tillage (the red line delineates the boundary of the plot); b) the tractor hooked with a chisel plow used in this study; c) an NT treatment plot during the rainfall simulation experiment; and d) an NT treatment plot after rainfall simulation.

After the plot was prepared according to the treatment (i.e., with or without channel and with or without tillage operation), along the edges of the 2-m-by-2-m plot area, galvanized iron sheets were punched into the soil to at least 10 cm deep (Fig. 3.1.d). About 10 cm of the galvanized iron sheet was left above the soil surface to create a wall, which worked as a physical boundary to prevent water and soil from moving in or out the plot area. A tube of 10 cm in diameter and  $\sim 70 \text{ cm}$  long was installed in the middle of the wall on the downslope edge. The tube was installed at a level flush to the base of the channel or the soil surface (depending on the treatment), working as the outlet for runoff water and sediment.

### 3.3.3 Rainfall simulation and data collection

Rainfall events were simulated with a medium sized, movable rainfall simulator (Chow and Rees, 1994). The rainfall simulator was equipped with continuous, downward-flow, wide-angle full-jet stainless steel nozzles (Fig. 3.1.c). Two aluminum support frames were designed with upright holders on the top to hang two nozzles assembled on a horizontal boom. On the boom, the middle position between the two nozzles was adjusted to approximately 2-m right above the centre of the plot. At this height, the two nozzles can cover about a 4.0-m-by-2.5-m area on the ground. The boom on the frame was connected to a Honda® water pump by a hose. A pressure gauge and a valve were connected between the water pump and the rainfall simulator.

The rainfall simulator was calibrated and factors affecting the rainfall intensity and uniformity (such as nozzle type, slope and water pressure) have been rigorously tested (see details in Chow and Rees, 1994). The effects of water pressure and slope were found nonsignificant. The nozzle type did not show large impact either. Nevertheless, the same nozzle and water pressure were used throughout the experiment. Because the ground coverages of the nozzles overlap each other, the rainfall intensity and uniformity depend on the target area on the ground are different. With a 2-m-by-2-m area target area in the middle as in this study, the rainfall intensity and uniformity were estimated to be approximately  $70 \text{ mm hr}^{-1}$  and 75 %, respectively (Chow, personal communication). These values were confirmed with Measurements of precipitation volume with five one-litre cups placed in each plot. The surface

area of these five cups only occupied about 1 % of the entire plot surface area. Nevertheless, the amount of precipitation intercepted by these cups was subtracted from the total amount of precipitation the plot received. Two tarps were used to wrapped around the frames of the rainfall simulator to block the wind, reducing its impact on the simulated rainfall.

A stopwatch was used to record the runoff initiation and sampling times. The stopwatch was started when the rainfall simulation started. When runoff started to flow at the outlet tube, the time was recorded and the first runoff sample was collected with a one-litre cup. When the cup was filled, another cup was used until it reached the 5 min after runoff initiation. Then, runoff water samples were taken as the sum volume of cups collected in each 5-min interval. For all plots, simulated rainfall continued for one hour after runoff initiation. Therefore, in total, there were 13 runoff water samples collected for each plot.

All samples were sent to the Soil Hydrology Laboratory in FRDC for analysis. Volume and weight of all water samples were measured with a graduated cylinder and a scale, respectively. Sediment amount in each sample was determined gravimetrically by weighing samples before and after they were dried at 120 °C for 24 hours.

### **3.3.4 Data analysis**

Seven runoff and sediment measures: runoff initiation time (min), runoff flow rate (mm hr<sup>-1</sup>), runoff discharge (mm), runoff coefficient (%), sediment yield (kg m<sup>-2</sup> hr<sup>-1</sup>), total sediment export (kg), and sediment concentration (g L<sup>-1</sup>) were recorded or calculated. The runoff initiation time was recorded when runoff started to flow at the tube outlet. The runoff flow rate

and sediment yield were calculated for each 5-min sample as the runoff (mm) and sediment export (kg), respectively, divided by the sample collection time (min). The runoff discharge and total sediment export were calculated as the cumulative total runoff depth and sediment export, respectively. The runoff coefficient was defined as the runoff discharge divided by the corresponding total precipitation. The sediment concentration was calculated as the sediment export divided by the runoff volume. If there was no runoff generated, the concentration data was considered as null in the following statistical analysis.

The runoff initiation was different for each experimental run. In order to compare the results between different treatments, except for the runoff initiation time, the data of all other six parameters were linearly aligned to 5-min time interval points after rainfall simulation started. Further analyses were all based on these aligned data. The runoff and sediment data were highly skewed. To ensure normality prior to statistical analysis, the data were log-transformed as follows:

$$\text{Transformed data} = \log_{10}(\text{raw data} + 1) \quad [1]$$

After the log-transformation, the General Linear Model of Latin Square was constructed:

$$y_{ij(k)} = \mu + \text{time}_i + \text{field}_j + \text{treatment}_{(k)} + e_{ij(k)} \quad [2]$$

Where:  $y$  represents one of the parameters examined.  $\text{Time}_i$  and  $\text{field}_j$  are the row and column effects of the Latin Square design, respectively. All row and column effects and  $\text{treatment}_{(k)}$  were considered as fixed effects. For paired treatment comparisons, the Fisher Least Significant Difference method was used.

To better characterize the changes of runoff and sediment parameters over time and the differences between treatments, The rainfall event was divided into four stages, each 15-min long (i.e., stage-1: 0 - 15 min; stage-2: 20 - 30 min; stage-3: 35 - 45 min; and stage-4: 50 - 60 min). For each stage, liner regressions between the runoff and sediment measures and rainfall simulation time were conducted:

$$y = a + bx \quad [3]$$

Where: y represents the parameter being tested. x represents the time after rainfall initiation. a and b represent the intercept and slope, respectively. For each parameter, the slopes and intercepts of the regression lines for different treatments were compared using the analysis of covariance (ANCOVA).

The runoff discharge and total sediment export values were also used to examine the effects of rainfall events of different magnitudes. For example, at 15 min, total precipitation was 17.5 mm. Assuming rainfall stopped at 15 min, the runoff discharge is then the total runoff for an event with a total rainfall of 17.5 mm. Following this logic, the runoff discharge values at 15, 30, 45 and 60 min can be considered to represent events with total rainfall of 17.5, 35, 52.5 and 70.0 mm, which were referred to as small, medium, large and extremely large events, respectively. It should be noted that the events separated by time were not independent events and, therefore, the discussion will be focused on the periods of transition to reflect the shifts of different controlling processes.

## 3.4 Results

### 3.4.1 Runoff

The runoff initiation time was highly variable for all treatments (Fig. 3.2). It ranged from 15.0 to 30.3 min, 6.0 to 18.5 min, 16.2 to 28.5 min, and 9.8 to 28.1 min, with a mean of 22.4, 11.5, 24.9 and 22.3 min and a CV of 35 %, 46 %, 23 % and 38 % for NN, CN, NT and CT, respectively (Fig. 3.2). The mean runoff initiation time followed an order of NT > NN > CT > CN. However, only the difference between NT and CN was statistically significant ( $P < 0.10$ ).

After runoff initiation, the average runoff flow rates (RFR) increased throughout the entire experimental periods for all treatments with only one exception (for CN, the RFR dropped from 40 to 45 min) (Fig. 3.3.a). The RFR curves for NN, NT and CT appear to follow a similar pattern with time: in the beginning, there was a period of slight increase of RFR (15 - 30 min for NN, 15 - 25 min for both NT and CT); then, there was a period of steep RFR increase (30 - 50 min for NN, 25 - 55 min for both NT and CT); and in the end, the RFR leveled off (50 - 60 min for NN, and 55 - 60 min for both NT and CT). For CN, the RFR increased rapidly in 10 - 25 min; then, the increase of the RFR reduced, and there was a period of steady RFR increase from 25 - 40 min; and in the end, the RFR leveled off in 40 - 60 min.

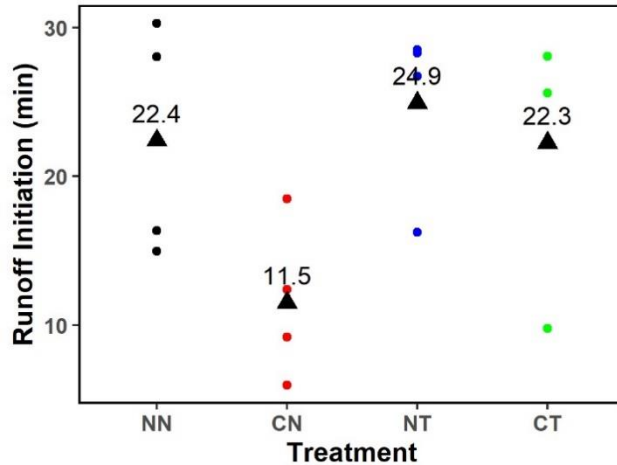


**Figure 3.2.** The runoff initiation time (minute) for different treatments (NN, CN, NT and CT). For each treatment, the four dots represent the four repeats and the triangle represents average values of the four repeats.

Comparing the four treatments, the RFR values followed a consistent order of  $CN > NN > CT > NT$  with the exceptions for the first 15 min (when the RFRs for NN, NT and CT were all close to zero) and the period from 45 min to 60 min when the RFR values for NN were greater than those for CN and those for CT and NT were similar (Fig. 3.3.a). The differences in RFR between the treatments at 15 and 30 min were overall significant ( $P < 0.10$  for CN vs. NN at 15 min, CN vs. CT at 15 min and CN vs. NT at both 15 and 30 min, Table 3.2). With the ANCOVA analyses of the four stages, there were more significant differences between the treatments, especially for stage-3 where the intercepts for CN and NN were found to be significantly greater than those for NT and CT (Table A.1). Overall, these comparisons indicate that the presence of a channel facilitated a quicker runoff initiation and resulted in greater RFR values until when it started to level off. On the other hand, tillage led to slower runoff initiation and lower RFRs and when tillage was conducted with an existing channel, the effect of tillage

overwhelmed that of the channel so that the RFR curves for NT and CT were very close to each other.

The runoff discharge (RD) for all treatments increased exponentially after runoff initiation (Fig. 3.3.b). There was a consistent order of  $CN > NN > CT > NT$  throughout the whole period of rainfall simulation. This order was similar to that for the RFR except that the differences between treatments were more pronounced with the RD curves than with the RFR curves (Table S1) and the difference between CN and NN did not reverse during stage-4 as did with the RFR curves. The runoff coefficient (RC) followed a similar pattern to that of the RD: RC increased exponentially after runoff initiation with a consistent order of  $CN > NN > CT > NT$  (Fig. 3.3.c).

### **3.4.2 Sediment**

For NN, after runoff initiation, the average sediment yield (SY) kept at a low level until 30 min when it started to increase slowly but steadily to reach  $0.37 \text{ kg m}^{-2} \text{ hr}^{-1}$  at 45 min (Fig. 3.3.d). There appeared to be a big jump from 45 min to 50 min and then the SY values maintained between  $0.58$  and  $0.65 \text{ kg m}^{-2} \text{ hr}^{-1}$ . For CN, after runoff initiation, the mean SY increased steadily to  $0.59 \text{ kg m}^{-2} \text{ hr}^{-1}$  at 30 min. Then, the slope of the SY curve increased dramatically and the SY value reached  $1.41 \text{ kg m}^{-2} \text{ hr}^{-1}$  at 40 min. However, there was a decrease of SY from 40 to 45 min and at 45 min, the SY dropped to  $1.22 \text{ kg m}^{-2} \text{ hr}^{-1}$ . After 45 min, the SY increased again and reached  $1.71 \text{ kg m}^{-2} \text{ hr}^{-1}$  at 60 min. For NT, after runoff

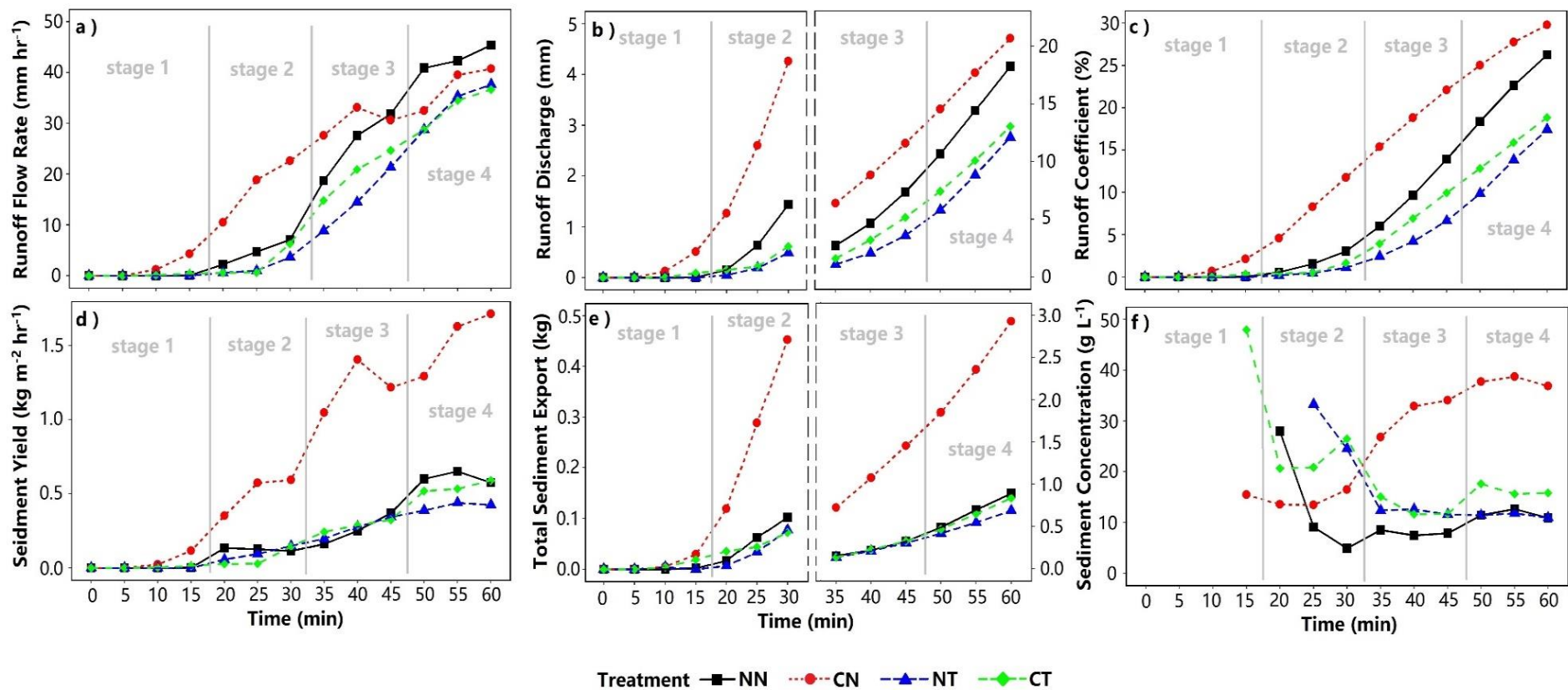


**Figure 3.3.** Changes of: a) runoff flow rate (mm hr<sup>-1</sup>); b) runoff discharge (mm); c) runoff coefficient (%); d) sediment yield (kg m<sup>-2</sup> hr<sup>-1</sup>); e) total sediment export (kg); and f) sediment concentration (g L<sup>-1</sup>) with time for the four treatments.

**Table 3.2** The mean and coefficient of variation for runoff flow rate (RFR), runoff discharge (RD), runoff coefficient (RC), sediment yield (SY), total sediment export (TSE), and sediment concentration (SC) at 15, 30, 45 and 60 min after rainfall simulation started

Time min	Treatment	RFR		RD		RC		SY		TSE		SC	
		Mean mm hr <sup>-1</sup>	CV %	Mean mm	CV %	Mean %	CV %	Mean kg m <sup>-2</sup> hr <sup>-1</sup>	CV %	Mean kg	CV %	Mean g L <sup>-1</sup>	CV %
15	NN	0.0 b	200	0.0 b	200	0.0 b	200	0.00 b	200	0.00 a	200	N/A	N/A
15	CN	4.3 a	81	0.5 a	114	2.1 a	93	0.12 a	118	0.03 a	136	15.5	5.5
15	NT	0.0 b	N/A	0.0 b	N/A	0.0 b	N/A	0.00 b	N/A	0.00 a	N/A	N/A	N/A
15	CT	0.4 b	200	0.1 b	200	0.3 b	200	0.01 b	200	0.02 a	200	47.9	N/A
30	NN	7.1 ab	89	1.4 ab	114	3.1 ab	107	0.11 a	107	0.10 a	135	4.9	15.4
30	CN	22.6 a	30	4.3 a	53	11.8 a	39	0.59 a	79	0.45 a	131	16.5	17.5
30	NT	3.6 b	77	0.5 b	142	1.1 b	121	0.15 a	137	0.08 a	175	24.5	N/A
30	CT	6.3 ab	14	0.6 ab	75	1.6 ab	60	0.14 a	44	0.07 a	136	26.5	N/A
45	NN	31.9 a	14	7.4 ab	38	13.9 ab	32	0.37 b	78	0.32 b	71	7.9 b	42.8
45	CN	30.6 a	18	11.6 a	33	22.1 a	27	1.22 a	45	1.45 a	93	34.0 a	7.0
45	NT	21.3 a	30	3.6 b	53	6.6 b	45	0.34 b	68	0.30 b	102	11.6 b	10.7
45	CT	24.7 a	8	5.2 ab	7	9.9 ab	6	0.32 b	41	0.32 b	54	11.7 b	20.6
60	NN	45.4 a	9	18.2 a	19	26.3 a	18	0.58 b	46	0.89 b	59	10.9 b	23.4
60	CN	40.8 a	14	20.7 a	20	29.8 a	18	1.71 a	34	2.93 a	53	36.9 a	11.3
60	NT	37.7 a	9	12.1 a	19	17.4 a	18	0.42 b	23	0.69 b	64	10.9 b	10.2
60	CT	36.7 a	5	13.1 a	5	18.8 a	5	0.59 b	18	0.83 b	20	15.8 b	10.0

Mean values with different letters are significantly different from each other at  $P < 0.10$  based on the Fisher LSD test.

initiation, the SY was at a very low level, slightly lower than those of the NN. After 20 min, the slope of the SY curve started to increase. The increase in the SY was steady and the SY reached its peak ( $0.44 \text{ kg m}^{-2} \text{ hr}^{-1}$ ) at 55 min, and then decreased slightly at 60 min. For CT, similar to NT, the SY was low before 25 min. Then, the SY curve started to rise and reached  $0.32 \text{ kg m}^{-2} \text{ hr}^{-1}$  at 45 min, very close to those of NN and NT. There was a jump from 45 to 50 min to reach  $0.52 \text{ kg m}^{-2} \text{ hr}^{-1}$  and then increased slightly to  $0.59 \text{ kg m}^{-2} \text{ hr}^{-1}$  at 60 min.

Comparing the four treatments, the SY curves followed a consistent order of  $\text{CN} > \text{NN} \approx \text{NT} \approx \text{CT}$ , with the exception of the period from 45 to 60 min when the SY value for NT was lower than those for NN and CT. For the four times examined, the SY for CN was significantly greater than that for NN, NT and CT, except for that at 30 min ( $P < 0.10$ , Table 3.2). In contrast, the differences between NN, NT and CT were all non-significant at any given time. With the ANCOVA analyses of the four stages, the differences between CN and the other treatments were more pronounced: the intercepts for CN were significantly greater than those for NN, NT and CT for all four stages (Table A.1). Again, the differences between NN, NT and CT were non-significant for all stages except for that between NT and CT at stage-4 ( $P < 0.10$ , Table A.1). The SY curves for NT and CT were almost identical to that for NN. This was different for the RFR curves, for which NT and CT were consistently lower than NN. Overall, these results suggest that the presence of a channel accelerated the erosion. On the other hand, tillage did not significantly accelerate or reduce SYs and when tillage was conducted with an existing channel, the effect of tillage overwhelmed that of the channel.

The total sediment export (TSE) for all treatments increased exponentially after runoff initiation (Fig. 3.3.e). This was similar to that of RD. There was a consistent pattern of  $CN > CT \approx NN > NT$  throughout the whole period of the rainfall simulation except for the first 25 min which was similar to that for the SY.

For NN and NT, the Sediment Concentration (SC) had a similar decreasing trend with time (Fig. 3.3.f). Since both RFR and SY increased with time, the decreasing trend of SC suggests that the increase of RFR was relatively greater than the increase of SY, an effect likely caused by changes in the erosion process (e.g., surface sealing). Such effect was stronger prior to 30 min than after as the slopes of the SC curves were greater (in terms of the absolute values) before 30 min than after. The SC followed a consistent order of  $NT > NN$  except for the stage-4, indicating that the soil erodibility of NT and NN followed the same order. For CN, the SC trend with time was different: it increased continuously with time except for the beginning and the end of the event, indicating a continuous increase of soil erodibility with time under CN. For CT, the SC was greater than that for CN at 15 min, indicating greater erodibility for CT, probably due to the loose soil surface with CT. From 20 to 30 min, the SC values for CT were greater than that for CN but the SC curves were in parallel, indicating that increase of soil erodibility during this period were similar. Then, from 30 to 45 min, the SC value for CT decreased dramatically and became similar to that for NT. After 45 min, the SC value for CT increased again, and became greater than those for NT and NN but still much lower than that for CN.

## 3.5 Discussion

### 3.5.1 Runoff and sediment generations on a bare soil surface

For the NN treatment (representing an undisturbed bare soil surface), during a rainfall event, water is firstly infiltrated into the soil profile or detained in the small depressions on the soil surface. Small event (e.g., an event lasts less than 15 minutes in our experiment) may not generate runoff. Only when the rainfall intensity exceeds the infiltration rate and the surface retention capacity, surface runoff will occur. Surface runoff begins as sheet flow, which is slow, so that its ability to detach and transport soil particles is limited. As rainfall progresses, infiltration decreases, mainly due to surface sealing, thus runoff increases (Fig. 3.3.a). At 60 min, the final runoff flow rate for NN was  $45.4 \text{ mm hr}^{-1}$ , which translates to an infiltration rate of  $24.6 \text{ mm hr}^{-1}$  (based on an estimated rainfall intensity of  $70 \text{ mm hr}^{-1}$ ), similar to that of a typical sandy loam soil with bare soil surface (Huffman et al., 2013).

With increased runoff, the sheet flow becomes faster, having more erosive power and higher transport capacity. As a result, sediment yield also increases (Fig. 3.3.d). However, the sheet flow also becomes thicker, creating a barrier for rainfall splash, resulting in less soil detachment. This explains why sediment concentration for NN decreased from 20 to 45 minute (Fig. 3.3.f). As runoff continuous to increase, water converges thus has more erosive power and can incise into the soil surface to form small channels (rills), resulting in increased erosion. The NN plots did not have well defined rills but there were clear signs of rill development (Fig. A.2.b). The development of rills for NN likely started at around 45 min as the sediment yield

had a jump at 45 min and the sediment concentration also started to increase slightly from 45 min (Fig. 3.3.d, 3.3.f).

### **3.5.2 Effects of an existing channel**

The presence of a channel provides an existing path for runoff water to converge. This reduces the retention capacity of the soil surface and shortens the pathway for the surface runoff to reach the plot outlet. As a result, the runoff initiation time for CN was much shorter than that for NN (Fig. 3.2). As rainfall progresses, infiltration also decreased with CN as it did with NN, thus runoff flow rate increased. The runoff flow rate for CN was slightly lower than that for NN at the last stage (stage-4), indicating a greater infiltration with CN (Table A.1). This can be explained by water depth in the channel: when it is high, on top of moving downward, water can also move into the soil profile through the side walls, increasing the effective surface area for infiltration. However, concentrated flow in the channel can cut into the channel walls, causing channel wall erosion and, therefore, sediment yield for CN was much greater than that for NN (Fig. 3.3.d). As the runoff increased, channel wall erosion also increased so that the sediment concentration for CN increased continuously with time (Fig. 3.3.f).

Erosion of the channel walls can also cause channel wall failure. In the case of a small channel wall failure, the channel maintains its shape and size so runoff is not significantly impacted. However, sediment yield will increase due to ample supply of loose channel wall materials falling into the channel after the channel wall fails. For the CN plots in this study, between approximately 25 and 40 min, the sediment yield increased three times during this period, whereas the increase in the runoff flow rate was only 1.8 times (Fig. 3.3.d). This likely

was related to small channel wall failures as field records show that visible channel wall deformation started to occur at around the same time. When a major channel wall failure happens, the channel may be partially blocked so that both runoff and sediment yield can be reduced, as shown with the CN plots between approximately 40 and 45 min (Fig. 3.3.a, 3.3.d). Towards the end of the experiment, major channel wall failure occurred to all CN plots and the channel were mostly filled (Fig. A.2.d). During this period, the increase in the sediment yield was 44%, whereas the increase in the runoff flow rate was only about 33%. This might indicate a substantial erratic increase in the erodibility of the soil, caused by the major channel wall failure.

Overall, the existing channel not only serves as a rapid pathway for water flowing to the edge of the plot but also provides a significant sediment source due to erosion of channel walls and channel wall failure. This finding agrees with the results reported in many previous studies (Wu et al., 2019; Xu et al., 2019) and confirms that water erosion will be increased when there is an existing channel.

### **3.5.3 Effects of tillage**

Tillage changes several soil physical properties thus affecting water erosion. First, tillage creates a rough soil surface, leading to increased soil surface retention at the micro—topographic scale (Fig. A.2.e). Second, tillage loosens the tillage layer soil thus increases its porosity and hydraulic conductivity. This will lead to greater water storage capacity and improved infiltration (Bescansa et al., 2006; Lipiec et al., 2006). Third, tillage breaks up existing soil structure and can lead to greater soil erodibility. The effects of tillage on runoff

and water erosion are well reflected when comparing the results of NT to NN. A delayed runoff initiation with NT can be explained by the increased surface retention and tillage layer water storage capacities with NT (Fig. 3.2). Similar results have been reported in many previous studies (Álvarez-Mozos et al., 2011; Burwell and Kramer, 1983; da Rocha Junior et al., 2016; Onstad et al., 1984; Zhao et al., 2018). The consistently lower runoff flow rates with NT was likely due to the greater infiltration with NT. Although NT consistently had lower runoff flow rate, sediment yield values for NT were mostly similar to those of NN, which can be explained by the greater soil erodibility with NT (Fig. 3.3.d). This is also evidenced in that the sediment concentration for NT was consistently greater than that for NN except for the stage-4 (Fig. 3.3.f).

It should be noted that the results from this study appear to contradict the conclusion of reducing tillage leading to reduced water erosion reported in many studies (Lindstrom et al., 1981; Rockström et al., 2009). The reason for the difference lies in that this study was focused on the short-term effects of a single tillage pass on a bare soil surface whereas those above-mentioned studies were comparing tillage with no-tillage conditions in the long term. First, the references of the comparisons were completely different (tilled bare soil surface for this study and no-till surface for the other studies). Second, the current study focused on the instant or short-term effects but those above-mentioned studies focused on the long-term effects for which instant or short-term effects of field operations were eliminated by keeping the timings and field conditions the same (e.g., Lindstrom et al., 1981; Rockström et al., 2009). Therefore, there is no real contradiction between this study and those long-term studies. In fact, previous

studies on the short-term effects of tillage showed similar results to this study (Bahmani, 2019; Mosaddeghi et al., 2009).

#### **3.5.4 Effects of tilling an existing channel**

Tillage smooths the soil surface. Small topographic features can be eliminated completely by tillage. When a topographic feature is larger or similar in size to the tillage depth or the size of the cutting tools of the tillage implement (e.g., sweeps of a field cultivator), it cannot be eliminated. However, it still will be deformed and reshaped. A channel is a topographic feature, so the effect of tillage on a channel is dependent on the size of the channel relative to the depth of tillage and the size of the cutting tool.

In this study, the channel was 30 cm by 30 cm in size whereas the tillage tool was 30 cm wide and the tillage depth was about 20 cm. For the CT plots, the channels had not been eliminated by tillage but they had been mostly filled and substantially reshaped, leaving a soil surface very similar to that of the NT, except that there was still a remnant shallow channel in the middle of the plot (Fig. A.2.g). Runoff and sediment data also showed the dominant effects of tillage as the runoff flow rate and sediment yield curves for CT were very close to those for NT and very different from those for CN (Fig. 3.3). However, there was some evidence signalling the impact of the remnant shallow channel. For example, curves for runoff, sediment and sediment concentration for CT were mostly between those for NT and CN, although much closer to NT than CN. These results suggest that the removal of a channel by tillage may reduce the runoff flow rate and sediment yield induced by the channel. However, it should be noted that many factors can affect the outcome of the experiments. The confluence of these factors

not controlled in this experiment will be the reality in field situations, so these results may not apply to all scenarios.

### **3.5.5 Implications for soil and water conservation in Atlantic Canada**

Taking into account both crop management and climate conditions, we use the cereal-potato rotation in Atlantic Canada as an example to discuss possible management adjustment for reducing the risk of erosion. In the province of New Brunswick and much of Atlantic Canada, agriculture is dominated by rainfed potato production systems, in which cash crop potato is in rotation with other crops such as cereals. Crops are usually planted in early spring (e.g., late May to early June for potato) and harvested in mid-fall (e.g., late September to early October for potato). The period after fall harvesting to snow cover (normally October to November, referred to as the fall critical period) and the period after snowmelt to seed germination (normally April to May, referred to as the spring critical period) are the times when there is no soil surface cover and the field is most susceptible to water and wind erosion.

Many tillage operations can be conducted during the two critical periods, including primary tillage, secondary tillage (to smooth the field, prepare the seedbed or make the potato hills) and seeding or planting operations. Primary tillage is most effective in eliminating channels. It is traditionally conducted in the fall, mostly to save time for the busy spring season when the time window for tillage is narrow. However, fall primary tillage buries crop residue and leaves the field bare so that the field is more vulnerable to water and wind erosion. Therefore, spring tillage has been promoted as a Beneficial Management Practice (BMP) to reduce erosion (De Baets et al., 2011).

With respect to climate in Atlantic Canada, precipitation is evenly distributed across the year (Vasseur and Catton, 2008). Precipitation amount and intensity in the two critical periods are similar and large events are rare. The biggest difference between the two critical periods is probably snowmelt. In early spring, snow accumulated in the winter is melted in a short period, often resulting in some biggest runoff events in the year. Although snowmelt does not detach sediment, the convergence of flow as well as channel creation and development are similar to rainfall events. Therefore, early spring is the time when channelization is the most severe. In addition, soil is often saturated after snowmelt so that rainfall events immediately after snowmelt often have the highest runoff coefficient. Moreover, this period often coincides with seedbed preparation and planting so soil cover is limited.

Taking into consideration of all factors described above, to minimize erosion, we recommend spring primary tillage over fall primary tillage after the cereal crop. The reason is that there is usually plenty of crop residue left in the field after harvesting cereal crops. Decay of the cereal crop residue is slow so that it provides good ground protection. If the field is not tilled, the protection can last until the primary tillage in the next spring. With the ground well protected, channelized erosion in the fall rarely happens. While channelized erosion may become severe after snowmelt, the period is short and the channels are soon erased by spring primary tillage. However, the crop following cereal is potato and farmers are often reluctant to leave primary tillage to the spring in a potato year because it may cause delay in potato planting, a risk most farmers will not take. Therefore, primary tillage is usually conducted in the fall. If primary tillage has to be conducted in the fall, doing it as late as possible will prolong the period

of residue cover. Alternatively, broadcasting some cover crop seeds along with fall tillage may also provide some cover in the fall and in the following spring.

After the potato crop, we recommend primary tillage late in the fall over in the spring. Residue cover after potato harvesting is poor and potato residue is much easier to decompose so that the field is not well protected even without tillage. In such case, there is great chances for channels to be created in the fall. If not erased, these channels will continue to develop in the spring after snowmelt and channelized erosion will be accelerated as shown with the CN treatment. While spring primary tillage can erase those channels, the most critical time immediately after snowmelt is missed as tillage can only be conducted when the soil is dry, usually weeks after snowmelt. By conducting primary tillage late in the fall, early development of channels in the fall can be terminated. Although channels may re-develop during snowmelt period, the severity of channelized erosion should be much lower as demonstrated with the CT treatment.

### **3.5.6 Future studies**

Variation among replicates in this study often exceeded the differences between treatments, so that most of the comparisons were non-significant. The high variation was likely rooted from differences in experimental conditions such as wind, soil texture, structure and moisture, micro-topography and tillage speed and depth. Although efforts had been made to reduce these errors (e.g., a tarp was used to block the wind for the rainfall simulator, experiment timing was selected so that surface soil moisture was similar), controlling these factors in the field was difficult. Therefore, one direction in the future is in-house soil bin study for which most

experimental conditions can be strictly controlled. Moreover, this study examined only one channel size and one tillage condition. Further studies on different channel sizes and tillage conditions (different types of tillage equipment, tillage speed and depth) are needed in order to better understand the variations under real-world conditions.

This study is a plot-scale study and the plot was only 2-m-by-2-m in size, which was too small for processes occurring at the field scale. With a longer slope, concentrated flow certainly will be more developed. As a result, water erosion might be underestimated in this study. A field-scale rainfall simulation experiment may allow better examination of erosion with concentrated flow, showing more distinct results between different treatments. However, such experiment would be very costly and very challenging in terms of its logistics and error control. An alternative method is probably a watershed scale study, which can be used to quantify the overall effects of water erosion and the interactions between water and tillage erosion at the watershed scale.

### **3.6. Conclusion**

In the context of examining the short-term effects of an existing channel and a single pass of tillage on subsequent water erosion events in fields that are bare, this study showed that with an existing channel, runoff initiation is accelerated and runoff discharge and sediment export are increased whereas with a single pass of tillage, runoff initiation is delayed and runoff discharge and sediment export are decreased. When an existing channel is tilled, the effects of tillage dominate so that runoff initiation may be delayed and runoff discharge and sediment export are decreased. Applying this knowledge to guide crop management practices, for a

cereal-potato crop rotation common in Atlantic Canada, we recommend spring primary tillage after cereal harvesting and late fall primary tillage after potato harvesting.

### **3.7. Acknowledgements**

This study was funded by the Agriculture and Agri-food Canada project “Characterizing and modeling the interactions between water and tillage erosion under potato and cereal production systems” [project number J-000994] (PI: Li) and project “Sustainability measures to monitor and analyze the environmental impact of Canadian agriculture” [project number J-002316] (PI: McConkey and McDonald) as well as a Natural Science and Engineering Research Council of Canada Discovery Grant (PI: Lobb). The authors would like to thank Zhisheng Xing and Yulia Kupriyanovich for their insightful suggestions for the experiment, and Meagan Betts, Tegan Smith and Michael Colford for helping with the field work. We are also grateful to Jacques Williams and the rest of the crew in the farm services unit of the Fredericton Research and Development Centre for managing the field and conducting the tillage operations.

### **3.8 References**

Agriculture and Agri-Food Canada - Crops and Horticulture Division (AAFC-CHD), 2019.

Potato Market Information Review 2018–2019. ISSN: 1929–7165. AAFC No. 13006E.

Alvarez-Mozos, J., Campo, M.A., Giménez, R., Casalí, J., Leibar, U., 2011. Implications of scale, slope, tillage operation and direction in the estimation of surface depression storage.

Soil Tillage Res. 111, 142–153. <https://doi.org/10.1016/j.still.2010.09.004>.

- Bahmani, O., 2019. Evaluation of the short-term effect of tillage practices on soil hydro-physical properties. *Pol. J. Soil Sci.* 52, 43. <https://doi.org/10.17951/pjss.2019.52.1.43>.
- Bennett, S.J., Wells, R.R., 2019. Gully erosion processes, disciplinary fragmentation, and technological innovation. *Earth Surf. Process. Landf.* 44, 46–53. <https://doi.org/10.1002/esp.4522>.
- Bescansa, P., Imaz, M.J., Virto, I., Enrique, A., Hoogmoed, W.B., 2006. Soil water retention as affected by tillage and residue management in semiarid Spain. *Soil Tillage Res.* 87, 19–27. <https://doi.org/10.1016/j.still.2005.02.028>.
- Brady, N.C., Weil, R.R., 2016. *The Nature and Properties of Soils*, 15 ed. Pearson. Burwell, R., Kramer, L., 1983. Long-term annual runoff and soil loss from conventional and conservation tillage of corn. *J. Soil Water Conserv.* 38, 315–319.
- Chow, T.L., Rees, H.W., 1994. Effects of potato hilling on water runoff and soil erosion under simulated rainfall. *Can. J. Soil Sci.* 74, 453–460. <https://doi.org/10.4141/cjss94-059>.
- Cogo, N.P., Moldenhauer, W.C., Foster, G.R., 1984. Soil loss reductions from conservation tillage practices. *Soil Sci. Soc. Am. J.* 48, 368–373. <https://doi.org/10.2136/sssaj1984.03615995004800020029x>.
- da Rocha Junior, P.R., Bhattarai, R., Alves Fernandes, R.B., Kalita, P.K., Vaz Andrade, F., 2016. Soil surface roughness under tillage practices and its consequences for water and sediment losses. *J. Soil Sci. Plant Nutr.* 16, 1065–1074. <https://doi.org/10.4067/S0718-95162016005000078>.

- Dai, J., Zhang, J., Zhang, Z., Jia, L., Xu, H., Wang, Y., 2020. Effects of water discharge rate and slope gradient on runoff and sediment yield related to tillage erosion. *Arch. Agron. Soil Sci.* 1–13. <https://doi.org/10.1080/03650340.2020.1766676>.
- De Baets, S., Poesen, J., Meersmans, J., Serlet, L., 2011. Cover crops and their erosion-reducing effects during concentrated flow erosion. *CATENA* 85, 237–244. <https://doi.org/10.1016/j.catena.2011.01.009>.
- Environment and Climate Change Canada (ECCC), 2022. Canadian Climate Normals 1981–2010 Station Data. Available online at: [https://climate.weather.gc.ca/climate\\_normals/results\\_1981\\_2010\\_e.html?stnID=6157&autofwd=1](https://climate.weather.gc.ca/climate_normals/results_1981_2010_e.html?stnID=6157&autofwd=1). Accessed on July, 2022.
- Gómez, J.A., Nearing, M.A., 2005. Runoff and sediment losses from rough and smooth soil surfaces in a laboratory experiment. *CATENA* 59, 253–266. <https://doi.org/10.1016/j.catena.2004.09.008>.
- Hosseinalizadeh, M., Kariminejad, N., Chen, W., Pourghasemi, H.R., Alinejad, M., Mohammadian Behbahani, A., Tiefenbacher, J.P., 2019a. Gully headcut susceptibility modeling using functional trees, naïve Bayes tree, and random forest models. *Geoderma* 342, 1–11. <https://doi.org/10.1016/j.geoderma.2019.01.050>.
- Hosseinalizadeh, M., Kariminejad, N., Chen, W., Pourghasemi, H.R., Alinejad, M., Mohammadian Behbahani, A., Tiefenbacher, J.P., 2019b. Spatial modeling of gully headcuts using UAV data and four best-first decision classifier ensembles (BFTree, Bag-

- BFTree, RS-BFTree, and RF-BFTree). *Geomorphology* 329, 184–193. <https://doi.org/10.1016/j.geomorph.2019.01.006>.
- Huffman, R.L., Fangmeier, D.D., Elliot, W.J., Workman, S.R., 2013. Chapter 5: Infiltration and Runoff. ASABE, St. Joseph, MI.
- Johnson, C., Mannering, J., Moldenhauer, W., 1979. Influence of Surface Roughness and Clod Size and Stability on Soil and Water Losses. *Soil Sci. Soc. Am. J.* 43, 772–777. <https://doi.org/10.2136/sssaj1979.03615995004300040031x>.
- Kinnell, P.I.A., 2005. Raindrop-impact-induced erosion processes and prediction: a review. *Hydrological Processes: Int. J.* 19, 2815–2844. <https://doi.org/10.1002/hyp.5788>.
- Lal, R., 2001. Soil degradation by erosion. *Land Degrad. Dev.* 12, 519–539. <https://doi.org/10.1002/ldr.472>.
- Li, S., Lobb, D.A., Lindstrom, M.J., Fahrenhorst, A., 2007. Tillage and water erosion on different landscapes in the northern North American Great Plains evaluated using <sup>137</sup>Cs technique and soil erosion models. *CATENA* 70, 493–505. <https://doi.org/10.1016/j.catena.2006.12.003>.
- Li, S., Lobb, D.A., Lindstrom, M.J., Fahrenhorst, A., 2008. Patterns of water and tillage erosion on topographically complex landscapes in the North American Great Plains. *J. Soil Water Conserv.* 63, 37–46. <https://doi.org/10.2489/jswc.63.1.37>.
- Li, S., Lobb, D.A., Tiessen, K.H.D., 2012. Soil erosion and conservation. In: El-Shaarawi, A.H., Piegorsch, W.W., Chebana, F., Ouarda, T.B. (Eds.), *Encyclopedia of Environmetrics*, second ed. John Wiley & Sons Ltd., Chichester, UK, pp. 2505–2512.

- Lindstrom, M.J., Voorhees, W.B., Randall, G.W., 1981. Long-term tillage effects on interrow runoff and infiltration. *Soil Sci. Soc. Am. J.* 45, 945–948. <https://doi.org/10.2136/sssaj1981.03615995004500050025x>.
- Lipiec, J., Ku's, J., Słowińska-Jurkiewicz, A., Nosalewicz, A., 2006. Soil porosity and water infiltration as influenced by tillage methods. *Soil Tillage Res.* 89, 210–220. <https://doi.org/10.1016/j.still.2005.07.012>.
- Lobb, D.A., Kachanoski, R.G., Miller, M.H., 1995. Tillage translocation and tillage erosion on shoulder slope landscape positions measured using <sup>137</sup>Cs as a tracer. *Can. J. Soil Sci.* 75, 211–218. <https://doi.org/10.4141/cjss95-029>.
- Lobb, D.A., Lindstrom, M.J., Schumacher, T.E., 2003. Soil erosion processes and their interactions: implications for environmental indicators, *Agricultural Impacts on Soil Erosion and Soil Biodiversity: Developing Indicators for Policy Analysis. Proceedings from an OECD Expert Meeting—Rome, Italy, March*, pp. 325–336.
- Lobb, D.A., Huffman, E., Reicosky, D.C., 2007. Importance of information on tillage practices in the modeling of environmental processes and in the use of environmental indicators. *J. Environ. Manag.* 82, 377–387.
- Morgan, R.P.C., 2009. *Soil Erosion and Conservation*, 3rd ed. John Wiley & Sons.
- Mosaddeghi, M.R., Mahboubi, A.A., Safadoust, A., 2009. Short-term effects of tillage and manure on some soil physical properties and maize root growth in a sandy loam soil in western Iran. *Soil Tillage Res.* 104, 173–179. <https://doi.org/10.1016/j.still.2008.10.011>.

- Onstad, D.W., Shoemaker, C.A., Hansen, B.C., 1984. Management of potato leafhopper, *Empoasca fabae* (Homoptera: Cicadellidae), on alfalfa with the aid of systems analysis. *Environ. Entomol.* 13, 1046–1058. <https://doi.org/10.1093/ee/13.4.1046>.
- Poesen, J., Nachtergaele, J., Verstraeten, G., Valentin, C., 2003. Gully erosion and environmental change: importance and research needs. *CATENA* 50, 91–133. [https://doi.org/10.1016/S0341-8162\(02\)00143-1](https://doi.org/10.1016/S0341-8162(02)00143-1).
- Qin, C., Zheng, F., Wilson, G.V., Zhang, X.J., Xu, X., 2019. Apportioning contributions of individual rill erosion processes and their interactions on loessial hillslopes. *CATENA* 181, 104099. <https://doi.org/10.1016/j.catena.2019.104099>.
- Rees, H.W., Fahmy, S.H., 1984. Soils of the Agriculture Canada Research Station, Fredericton, NB. LRRI, Research Branch, Agriculture Canada.
- Rockström, J., Kaumbutho, P., Mwalley, J., Nzabi, A.W., Temesgen, M., Mawenya, L., Barron, J., Mutua, J., Damgaard-Larsen, S., 2009. Conservation farming strategies in East and Southern Africa: yields and rain water productivity from on-farm action research. *Soil Tillage Res.* 103, 23–32. <https://doi.org/10.1016/j.still.2008.09.013>.
- Römkens, M.J.M., Helming, K., Prasad, S.N., 2002. Soil erosion under different rainfall intensities, surface roughness, and soil water regimes. *CATENA* 46, 103–123. [https://doi.org/10.1016/S0341-8162\(01\)00161-8](https://doi.org/10.1016/S0341-8162(01)00161-8).
- Soil Science Society of America (SSSA), 2020. Glossary of Soil Science Terms. Soil Science Society of America, Madison, WI. <https://www.soils.org/publications/soils-glossary> . accessed 14 July 2022.

- Souchère, V., Cerdan, O., Ludwig, B., Le Bissonnais, Y., Couturier, A., Papy, F., 2003. Modeling ephemeral gully erosion in small cultivated catchments. *CATENA* 50, 489–505. [https://doi.org/10.1016/S0341-8162\(02\)00124-8](https://doi.org/10.1016/S0341-8162(02)00124-8).
- USDA-NRCS, 1997. *America's Private Land, A Geography of Hope*. USDA-NRCS, Washington, DC. Van Oost, K., Cerdan, O., Quine, T.A., 2009. Accelerated sediment fluxes by water and tillage erosion on European agricultural land. *Earth Surf. Process. Landf.* 34, 1625–1634. <https://doi.org/10.1002/esp.1852>.
- Vasseur, L., Catton, N., 2008. Atlantic Canada. In: Lemmen, D.S., Warren, F.J., Lacroix, J., Bush, E. (Eds.), *From Impacts to Adaptation: Canada in a Changing Climate*. Government of Canada, Ottawa, ON, pp. 119–170.
- Wang, Y., Zhang, J.H., Zhang, Z.H., Jia, L.Z., 2016. Impact of tillage erosion on water erosion in a hilly landscape. *Sci. Total Environ.* 551–552, 522–532. <https://doi.org/10.1016/j.scitotenv.2016.02.045>.
- Wells, R.R., Momm, H.G., Rigby, J.R., Bennett, S.J., Bingner, R.L., Dabney, S.M., 2013. An empirical investigation of gully widening rates in upland concentrated flows. *CATENA* 101, 114–121. <https://doi.org/10.1016/j.catena.2012.10.004>.
- Wu, T., Pan, C., Li, C., Luo, M., Wang, X., 2019. A field investigation on ephemeral gully erosion processes under different upslope inflow and sediment conditions. *J. Hydrol.* 572, 517–527. <https://doi.org/10.1016/j.jhydrol.2019.03.037>.
- Xu, X., Zheng, F., Wilson, G.V., Zhang, X.J., Qin, C., He, X., 2019. Quantification of upslope and lateral inflow impacts on runoff discharge and soil loss in ephemeral gully systems

under laboratory conditions. *J. Hydrol.* 579, 124174

<https://doi.org/10.1016/j.jhydrol.2019.124174>.

Zegeye, A.D., Langendoen, E.J., Guzman, C.D., Dagnew, D.C., Amare, S.D., Tilahun, S.A.,

Steenhuis, T.S., 2018. Gullies, a critical link in landscape soil loss: A case study in the subhumid highlands of Ethiopia. *Land Degrad. Dev.* 29, 1222–1232.

<https://doi.org/10.1002/ldr.2875>.

Zhao, P., Li, S., Wang, E., Chen, X., Deng, J., Zhao, Y., 2018. Tillage erosion and its effect on

spatial variations of soil organic carbon in the black soil region of China. *Soil Tillage Res.*

178, 72–81. <https://doi.org/10.1016/j.still.2017.12.022>.

### 3.9 Nomenclature

ANCOVA	analysis of covariance
ANOVA	analysis of variance
CN	with a channel, no-tillage
CT	with a channel, with tillage
CV	coefficient of variation
FRDC	Fredericton Research and Development Centre
NN	no channel, no-tillage (control)
NT	no channel, with tillage
RC	runoff coefficient
RD	runoff discharge
RFR	runoff flow rate
SC	sediment concentration
SY	sediment yield
TSE	total sediment export

## **4. INTEGRATING WATER AND TILLAGE EROSION MODELS TO SIMULATE TOTAL SOIL EROSION IN CULTIVATED FIELDS**

### **Contributions of authors**

The authors confirm contribution to the paper as follows: 1. study conception and design: Zheng, F, Lobb, D.A. and Li, S.; 2. resources provided: Lobb, D.A. and Li, S.; 3. data collection: Zheng, F.; 4. data analysis: Zheng, F.; 5. data visualization: Zheng, F.; 6. data interpretation: Zheng, F., Lobb, D.A. and Li, S., 7. writing—original draft preparation: Zheng, F.; 8. writing—review and editing: Lobb, D.A. and Li, S.; 9. funding: Lobb, D.A. and Li, S.. The author confirms sole responsibility for the following: study conception and design, data collection, analysis, and paper preparation.

### **4.1 Abstract**

Cultivated lands suffer from both water and tillage erosion and their interactions. Therefore, it is necessary to consider all forms of erosion to better estimate total soil erosion. Individual models have been developed to simulate sheet and rill erosion, gully erosion and tillage erosion separately. Efforts have been made to link these models to simulate two erosion processes. However, no study has been carried out to simulate all three erosion processes, and no model has been developed to take into account the interaction between the two erosion processes. In this study, we examined two field sites in Atlantic Canada (the PEI site and the NB site). The Raster-RUSLE2 (RUSLER), Ephemeral Gully Erosion Estimator (EphGEE) and Modified Directional Tillage Erosion Model (ModDirTilLEM) were used to simulate sheet and rill

erosion, gully erosion and tillage erosion, respectively, on these two sites. In particular, the ModDirTilIEM was modified from the established tillage erosion model (DirTilIEM) to incorporate the interaction between gully and tillage erosion. The model-predicted erosion patterns and rates were validated against air photos, topographic features and their evolutions obtained using photogrammetry, manually measured gully cross sections, runoff and sediment yield monitored at the outlet of the catchment, and Cs-137 derived erosion rates. The results indicate that the individual models provide reasonable estimation for the individual erosion processes. For both the PEI site and the NB site, the pattern of total erosion was closer to that of tillage erosion. Integrating tillage and water erosion models improved the accuracy of the estimation for total soil erosion. However, errors and uncertainties around the ephemeral gully areas were very high. This could be due to the dynamic erosion processes in these areas or the low resolution and accuracy of the model input data. In either case, it indicates that the gully area is a weak point for soil erosion modeling, and there is an urgent need to integrate water and tillage erosion models at the process level to simulate the dynamic nature of soil redistribution in the gully areas.

## **4.2 Introduction**

Soil erosion is a global issue, degrading soil properties and threatening the sustainability of the agricultural industry and the environment (Lal, 2001; Morgan, 2009). Water, wind and tillage erosion have been recognized as the major forms of soil erosion (Li et al., 2007a; Lobb et al., 1995).

Historically, soil erosion studies mainly focus on the single erosion process, like water erosion, wind erosion and tillage erosion, respectively (Lal, 2001). However, it is hard to justify the separation of these erosion forms in cultivated lands. The cultivated lands usually suffer all erosion types. In Atlantic Canada, the contribution of wind erosion was considered insignificant for cropland compared to that in prairies and boreal plains in Canada, with a relatively dry climate and cultivated land with little protection from wind (McConkey et al., 2010). As a result, in Atlantic Canada, water and tillage erosion forms are considered the major contributors to soil erosion.

There are linkages and interactions between water and tillage erosion processes (Li et al., 2007b; Lobb et al., 2003). The linkage is simply the summation of the soil loss caused by both erosion processes. For example, water erosion mainly causes soil erosion on middle slope positions, whereas tillage erosion can cause soil erosion on hilltops. The summation of erosion caused by these two forms can greatly explain the soil erosion on hilltops and middle slope positions. However, the pattern of total soil erosion is more complicated with the involvement of the interactions between erosion processes (Li et al., 2007b). The interaction refers to that one erosion process affects another erosion process. In cultivated lands, the interaction process between water and tillage erosion is likely to occur around the gully area, especially the ephemeral gully area (depression or lower slope area), because the channels are commonly eliminated or smoothed by tillage. For example, the results of Chapter 2 indicated that the ephemeral gullies could trap the soil translocated by tillage to decrease tillage translocation or serve as hollow areas to increase the tillage translocation (Zheng et al., 2021).

Numerous erosion models were developed based on the results obtained from soil erosion studies. Still, most of them only focused on a single erosion process, like the water erosion process or tillage erosion process. Sheet and rill erosion are often modeled with the Universal Soil Loss Equation (USLE) and its revised version RUSLE and RUSLE2 or the Water Erosion Prediction Project (WEPP) hillslope model. RUSLE2 is based on data collected from runoff plots (22.1 m in length). Therefore, the drainage area is not large enough for channel formation (Merritt et al., 2003; Wischmeier and Smith, 1978). The hillslope version of WEPP does not account for runoff concentration, thereby, gully erosion (Flanagan and Nearing, 1995). For the simulation of ephemeral gully erosion, the Ephemeral Gully Erosion Model (EGEM) was developed for this specific process using semi-empirical formulations (Woodward, 1999). However, this model performed poorly and has some limitations (Capra et al., 2005; Nachtergaele et al., 2001). For example, the model requires the input of the location and length of gullies to obtain the results.

The linkage of sheet & rill erosion and ephemeral gully erosion can be conducted using the watershed version of WEPP (Flanagan and Nearing, 1995). In addition, the Annualized Agricultural Non-Point Pollution Watershed model (AnnAGNPS) can be used to simulate all water erosion forms as well (Bingner et al., 2003). Gordon et al. (2007) successfully modeled ephemeral gully erosion using AnnAGNPS. Besides, Chemicals, Runoff, and Erosion from Agricultural Management Systems (CREAMS) was developed to provide another approach, estimating all water erosion forms (Knisel and Foster, 1981; Knisel, 1980). Dabney et al. (2015) proposed a physical-based model called Ephemeral Gully Erosion Estimator (EphGEE), which

was integrated with the raster-based RUSLE2 (RUSLER). The locations of ephemeral gullies can be extracted from the RUSLER directly for the utilization of EphGEE. More importantly, unlike other integrated water erosion models, EphGEE considered the interaction effects – the impacts of tillage on gully: the variation of gully soil erodibility, the change of runoff curve number and the condition of gullies (tillage filling).

In addition to the water erosion, many efforts were made to simulate tillage erosion. The tillage erosion can be modeled along hillslopes using the Tillage Erosion Prediction (TEP) and the Tillage Translocation Model (TillTM) (Li et al., 2008b; Lindstrom et al., 2000). For field-scale modeling (2-dimensional), the Soil Redistribution by Tillage (SORET) model was designed to predict soil redistribution of a single tillage operation or the long-term effects of repeated operations (De Alba, 2003). The tillage Erosion Model (TilLEM) was similar to SORET in the calculation. Other than the similarities, the difference is that TilLEM considers the effect of slope curvature on tillage translocation (Li et al., 2007b). The upgraded version of the TilLEM – Directional Tillage Erosion Model (DirTilLEM) calculates the incoming and outgoing soil in four directions for each cell in the DEM. The tillage erosion rate can be determined by summing up the incoming and outgoing soil (Li et al., 2009).

Regarding the combination of water and tillage erosion models, few attempts have been made to link these two erosion forms. Water and Tillage Erosion (WaTEM) attempted to calculate both erosion rates at each grid node (Van Oost et al., 2000). The water component of WaTEM uses USLE, implicating that the water component does not account for the ephemeral gully erosion (Ahmed et al., 2013). WaTEM sums the erosion rates obtained from different

forms. Therefore, WaTEM can only estimate linkage effects between sheet, rill and tillage erosion rates.

Overall, firstly, no existing model considered all three primary erosion forms (sheet and rill, ephemeral gully, and tillage erosion) in cultivated lands. Most integrated models account for, at most, two soil erosion forms. Secondly, for these integrated models, the linkage effect was applied between different erosion processes except for RUSLER & EphGEE, considering the impact of tillage on the subsequent water erosion event. No model was developed accounting for the effect of ephemeral gullies on tillage erosion. Therefore, there was a gap between the model and reality.

To better design the conservation measures for cultivated fields, a better estimation of total erosion is necessary. Therefore, the objectives of this study are, firstly, to construct a procedure to combine all three forms of erosion (rill & sheet erosion, ephemeral gully erosion, and tillage erosion) occurred in cultivated lands together conceptually and operationally; secondly, to take one step further to account for the interaction effect between erosion forms (i.e., between ephemeral gully erosion and tillage erosion) and to model the interaction effect between these two forms; lastly, to validate the estimates obtained from models applied in cultivated fields.

## **4.3 Materials and Methods**

### **4.3.1 Study area**

Two field sites were examined in this study. The first experiment site (PEI site) was established in 2015 through 2018 at Agriculture and Agri-Food Canada's research farm

located at Harrington, Prince Edward Island (PEI), Canada (46°20'42.8"N 63°10'30.9"W). The climate of Harrington is humid-continental, with a mean annual temperature of 5.7 °C and mean monthly temperatures ranging from -7.7 °C in January to 18.7 °C in July. The mean annual precipitation is 1158.2 mm, with 25.1 % of precipitation falling as snow. Precipitation is uniformly distributed throughout the year, with each season receiving about 20 to 30 % of the annual precipitation. The climate data for Harrington was obtained from the Charlottetown Airport weather station, which is about 7.6 km southeast of the PEI site. The soil at the PEI site consists of sandy loam soil (Orthic Humo-Ferric Podzol) developed on acidic glacial till parent material. The particle distribution of the Ap horizon (0-30 cm) is 9.8 % of clay, 27.5 % of silt and 62.7 % of sand, characterized by rapid infiltration and drainage in the tillage layer.

The PEI site covers about an area of 2.3 ha, located in the north section of a watershed covering an area of 36.6 ha (Fig. 4.1). The topography of this field is rolling, with slopes ranging from 0.1 to 18.7 % (Fig. 4.2.a). The land use of the watershed is dominated by forests and crops. The southern, western and eastern side of the field is surrounded by the forest, whereas the northern side of the field faces another crop field. Prior to 2003, the PEI site field was divided into two small fields. Trees or bushes were used as a boundary to separate these two fields. These two small fields were cultivated in the direction of the north-south. After 2003, the boundary of the trees was removed, and two individual fields were combined together. Also, the tillage direction was shifted to the longer axis of the field (i.e., west-east) to accommodate the larger machinery now being used. A detailed crop or management history is

not fully available, but based on the available record, it is estimated that the field had been in grain, hay and potato rotation.

Another experiment site (NB site) was established in 2015, located near the town of Grand Falls, in the upper Saint John River Valley of New Brunswick ( $47^{\circ}05'19.2''\text{N}$   $67^{\circ}44'43.9''\text{W}$ ). Similar to that of the PEI site, the climate of Grand Falls belongs to the humid-continental region. The mean annual temperature ranges from a low of  $-12.6^{\circ}\text{C}$  in January to a high of  $18.0^{\circ}\text{C}$  in July. The precipitation varies from a low of 45.6 mm in January to a high of 179.4 mm in June, with a mean monthly value of 92 mm. About 80 % of the snowfall is contributed

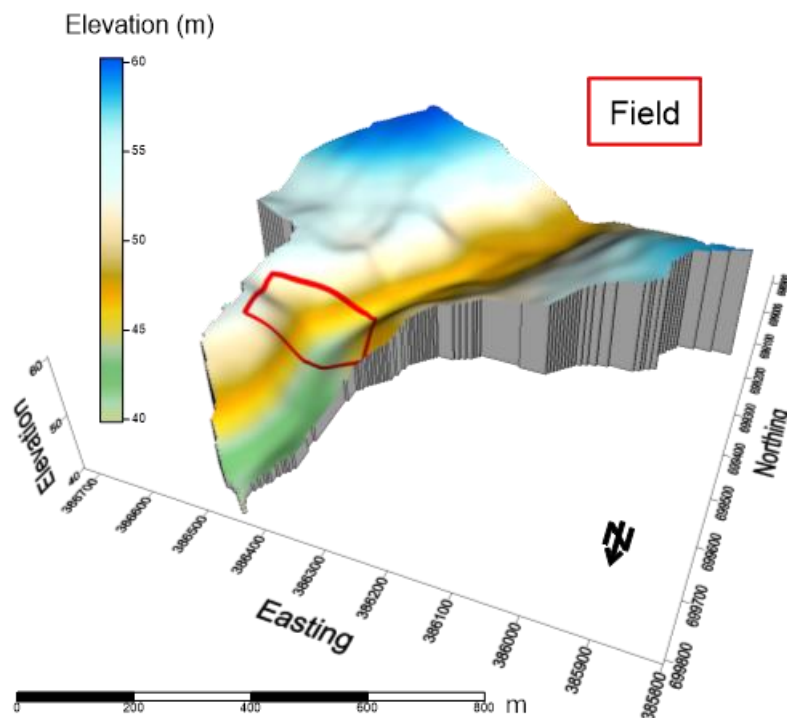


**Figure 4.1.** The location of the PEI site is within the watershed near Harrington, PEI.

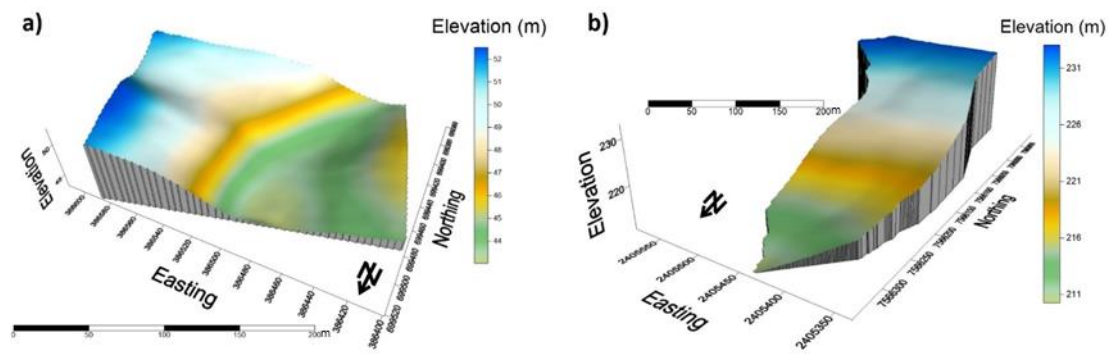


**Figure 4.2.** a) The topography of the PEI site within the watershed near Harrington, PEI; b) the topography of the NB site near Grand Falls, NB.

from December to March. All the daily weather information of this site was gathered from the St. Leonard weather station, which is 9.6 km away and is located northwest of the site. The landscapes are characterized by an undulating to the rolling surface, with average slopes of 0.1 to 9.0 %. Soils in this region develop on thin deposits (usually < 2 m over bedrock) of coarse to moderately fine textured glacial tills (gravely sandy loam to loams) and are predominantly of the Holmesville soil association (Orthic Humo–Ferric Podzols).

The total area of the catchment of the NB site is about 6.0 ha. The north-facing slope is about 450 m long with a mean of 5.7 % gradient (Fig. 4.2.b). The NB site is part of a field on a commercial potato farm and has been in agricultural production since the 1950s. Before 2007, the field was tilled along the east-west direction. Since the 1950s, the producer at this site had majorly employed the crop rotation of potato-potato-grain. After 2007, the field was cultivated along the contour lines (i.e., east-west). In addition, the contour strip rotation measure was employed. Two strips were under potato-grain and grain-potato rotation, respectively, to prevent water erosion.

### **4.3.2 Integration of erosion models**

The erosion that occurred in cultivated fields in Atlantic Canada includes water erosion (sheet and rill, ephemeral gully) and tillage erosion and their interactions. All forms of erosion mentioned can be estimated with different erosion models, including RUSLER, EphGEE, and ModDirTilLEM. The summation of all models is used to estimate the total erosion rate in cultivated fields.

#### **4.3.2.1 Water erosion - RUSLER and EphGEE**

In this study, a raster-based RUSLE2 model - RUSLER was utilized to estimate the magnitude of erosion caused by the sheet and rill flow (Dabney et al., 2015). The model's flow directions are defined using the D8 method (O'Callaghan and Mark, 1984). The flow direction codes range from 1 to 255. For example, if the direction of the steepest elevation change is to the bottom of the current centre cell, its flow direction will be coded as 4. The drainage area of the cell is determined by accumulating the weight of all cells that flow into the processing cell. Once the cell with a drainage area greater than the user-defined threshold, the cell is considered as the location of concentrated flow areas or gullies (channel cell). For cells within the defined drainage area, their flow directions of them are converted into a computational sequence using RUSLER algorithms. Based on the computed sequence, the RUSLE2 is utilized to calculate runoff, detachment, sediment delivery, and soil loss for each cell. A cell in RUSLER is equivalent to a slope segment in the RUSLE2 hillslope profile. At the bottom of the hillslope or sub-catchment, the runoff and sediment leaving the last cell continue to move into the channel cells.

The erosion caused by the ephemeral gully was estimated using EphGEE (Dabney et al., 2015). The locations of ephemeral gullies are pre-defined using RUSLER. The runoff and sediment moving into the ephemeral gully through the sheet and/or rill flows are also calculated in RUSLER. For the EphGEE simulation, the soil detachment is calculated based on the shear stress caused by flowing order; the erosion and deposition are calculated based on the sediment transport and the changes in the cross-section area of a gully. After each major tillage operation, the cross-section area of the gully is reset to zero (no erosion and no deposition). Then, the process of ephemeral gully development starts all over again. In addition, according to the algorithms in RUSLE2, runoff decreases, and sediment erodibility increases after tillage, which agrees with the results obtained from Chapter 3. A detailed description of both the RUSLER and EphGEE models can be found in the paper published by Dabney et al. (2015).

Both RUSLER and EphGEE models were used to estimate the water erosion rate in the PEI site and the NB site, respectively. The parameters used in the RUSLER and EphGEE were summarized in Table 4.1. For the PEI site, the topographic data were collected using a Light Detection and Ranging (LiDAR) system. The raw data were processed to produce a 1.5-m interval Digital Elevation Model (DEM). In order to compare and link the results of the water erosion model to those of the tillage erosion model, the cell size of 5-m was selected as a trade-off for both water and tillage erosion models. Therefore, the cell size of the DEM was converted to 5-m using ArcMap® 10.1 program. Then, the 5-m DEM was imported into the Surfer® 12 program to perform 10-pass smoothing to eliminate some artificial features, such as tillage

furrows. The catchment where the PEI site was located was clipped, and the processed catchment DEM was the input to the RUSLER and EphGEE models.

**Table 4.1** The input parameters used for RUSLER modeling

	PEI site	NB site
Field/catchment size (ha)	2.3	6.0
Cell size (m)	5	5
Drainage area threshold (cell)	250	280
Climate	Charlottetown Airport, PE	St. Leonard Airport, NB
Soil	Sandy Loam (medium to high organic matter, medium to rapid permeability)	Loam (medium to high organic matter, medium permeability)
Tillage management	Grain-hay-grain-hay-potato	Potato-potato-grain/potato-grain
Tillage depth (m)	0.22	0.26
Bulk density (kg m <sup>-3</sup> )	1342	1174

The input climate data (mean temperature, mean precipitation, and monthly rainfall erosivity) for the PEI site, which was used to determine the amount of runoff, was calculated based on the 20-year climate data obtained from the weather station of Charlottetown Airport. The soil texture of sandy loam (medium to high organic matter, medium to rapid permeability) was selected as soil input for the PEI site. The reason for choosing this texture was because of the results of the soil texture test for ten soil samples randomly collected across the field. The soil texture results showed that the percentages for clay, silt and sand were 9.8 %, 27.5 % and 62.7 %, respectively, suggesting the soil texture of sandy loam.

**Table 4.2** The crop management operations for the 5-year crop rotation (grain-hay-grain-hay-potato) used for the PEI site

Date, m/d/y	Operation	Vegetation
5/9/1	Disk, tandem heavy primary op.	
5/12/1	Harrow, coiled tine	
5/12/1	Harrow, coiled tine	
5/15/1	Drill or air seeder, double disk	Barley, spring
8/15/1	Harvest, grain, grow cover	Clover, red/timothy, spring seed
4/1/2	Begin growth	Permanent cover not harvested/Grass, cool season permanent not harvested
4/25/3	Plow, moldboard	
5/9/3	Disk, tandem light finishing	
5/12/3	Harrow, coiled tine	
5/12/3	Harrow, coiled tine	
5/15/3	Drill or air seeder, double disk	Barley, spring
8/15/3	Harvest, grain, grow cover	Clover, red/timothy, spring seed
4/1/4	Begin growth	Permanent cover not harvested/Grass, cool season permanent not harvested
5/10/5	Plow, moldboard	
5/26/5	Disk, tandem light finishing	
5/29/5	Harrow, coiled tine	
5/29/5	Harrow, coiled tine	
5/31/5	Planter, double disk on	Potato, Irish
6/20/5	Cropland/cultivators/cultivator, row	
6/20/5	Bed shaper	
6/30/5	Sprayer, fungicide	
7/15/5	Sprayer, fungicide	
7/30/5	Sprayer, fungicide	
8/15/5	Sprayer, fungicide	
8/30/5	Sprayer, fungicide	
9/15/5	Sprayer, fungicide	
9/30/5	Kill crop	
10/15/5	Harvest, dig root crops res. buried	

For the PEI site, the tillage management input for RUSLER within the catchment was not the same. The western, eastern and southern boundaries of the PEI site were surrounded by forest. For the forest area, there was no forest management built in the RUSEL2. Due to the

protection of the forest canopy, the impact of the water erosion on the forest area was minimal. Therefore, alternative graze management, which generated limited amount of runoff and sediment in the system, was selected to control the water erosion generated in this area. The fields were under crop rotation for the rest area within the catchment. Since the field land use record was not fully available, the land use for the PEI site was assumed based on the available records. The 5-year crop rotation (grain-hay-grain-hay-potato) for the PEI site was assumed as input management for RUSLER. The year and crop management operations of this 5-year rotation were summarized in Table 4.2.

The output of RUSLER was the 5-m grid-based soil loss rate ( $\text{Mg ha}^{-1} \text{ yr}^{-1}$ ). In addition, the channel network and storm events stimulated by RUSLER were the inputs for EhpGEE. The channel or ephemeral gully networks were defined with the cell contribution area threshold. The threshold set for the PEI site was 250 cells, which was equivalent to about 0.6 ha. Namely, when the cell had a contribution area greater than 250 cells, the cell was the location where ephemeral gullies went through. The changes in the cross-section area in EphGEE were used to estimate the soil erosion or deposition. Additional inputs for EphGEE were required. Firstly, the tillage depth was needed to define the non-erodible layer. In EphGEE, until an ephemeral gully reached the non-erodible layer, it was not developed horizontally. In this study, 0.22 m was set as the tillage depth for the PEI site. The tillage depth was estimated using the Cs-137 inventory and the corresponding depth migration at the crest, upslope and middle slope positions, where soil accumulation is rarely observed. Secondly, the bulk density was required to convert the cross-section area to volume for each channel cell. The input of bulk density was

**Table 4.3** The crop management operations for 3-year crop rotation (potato-potato-grain) for the NB site

Date, m/d/y	Operation	Vegetation
5/10/1	Plow, moldboard	
5/26/1	Disk, tandem heavy primary op.	
5/29/1	Harrow, coiled tine	
5/29/1	Harrow, coiled tine	
5/31/1	Planter, double disk opener	Potato, Irish
6/20/1	Cropland/cultivators/cultivator, row	
6/20/1	Bed shaper	
6/30/1	Sprayer, fungicide	
7/15/1	Sprayer, fungicide	
7/30/1	Sprayer, fungicide	
8/15/1	Sprayer, fungicide	
8/30/1	Sprayer, fungicide	
9/16/1	Sprayer, fungicide	
9/30/1	Kill crop	
10/15/1	Harvest, dig root crops res. buried	
<hr/>		
5/10/2	Plow, moldboard	
5/26/2	Disk, tandem heavy primary op.	
5/29/2	Harrow, coiled tine	
5/29/2	Harrow, coiled tine	
5/31/2	Planter, double disk opener	Potato, Irish
6/20/2	Cropland/cultivators/cultivator, row	
6/20/2	Bed shaper	
6/30/2	Sprayer, fungicide	
7/15/2	Sprayer, fungicide	
7/30/2	Sprayer, fungicide	
8/15/2	Sprayer, fungicide	
8/30/2	Sprayer, fungicide	
9/16/2	Sprayer, fungicide	
9/30/2	Kill crop	
10/15/2	Harvest, dig root crops res. buried	
<hr/>		
5/1/3	Disk, tandem heavy primary op.	
5/12/3	Harrow, coiled tine	
5/12/3	Harrow, coiled tine	
5/15/3	Drill or air seeder, double disk	Oats, spring
5/31/3	Sprayer, post emergence	
8/15/3	Harvest, killing crop 50pct standing stubble	

1342 kg m<sup>-3</sup> for the PEI site, which was obtained from soil samples across the field. The output of EphGEE was in the form of soil erosion or deposition in mass (kg) for each cell of an ephemeral gully. To obtain the erosion rate for each gully cell, the weight of soil loss or accumulation (kg) was divided by the cell area (25 m<sup>2</sup>) to calculate the rate for each cell. Then, the rate was divided by the total years of the tillage management, which was five years for the PEI site, to produce the erosion rate per year (Mg ha<sup>-1</sup> yr<sup>-1</sup>).

For the NB site, the topographic data were also collected using a LiDAR system. The raw data were processed to produce a 1-m interval DEM. Similarly, the cell size of the DEM was converted to 5-m. Then, the 5-m DEM was imported into the Surfer® 12 program to perform 30-pass smoothing to eliminate the tillage furrows across the field. The catchment of the NB site (within the crop field) was clipped, and the processed DEM was the input to the models.

The input climate data for the NB site was calculated based on the 20-year climate data obtained from the weather station of Saint-Léonard. The results of the soil texture test for ten soil samples collected in the NB site indicated the soil texture of the loam. Therefore, the loam (medium to high Organic Matter, medium permeability) was selected as soil input for the NB site. The tillage management input for RUSLER was different before and after 2008. Before 2008, the field was under a 3-year crop rotation (potato-potato-grain). After 2008, the field was divided into two sections under a 2-year strip rotation (potato-grain). The year and tillage operations of these 3-year and 2-year rotations were summarized in Table 4.3 and Table 4.4, respectively. For EphGEE modeling, the cell contribution area threshold was set as 280 cells,

which was equivalent to about 0.7 ha. The 0.26 m was set as the tillage depth for the NB site.

In addition, the input of bulk density was 1174 kg m<sup>-3</sup>.

**Table 4.4** The crop management operations for 2-year crop rotation (potato-grain) used for the NB site

Date, m/d/y	Operation	Vegetation
5/10/1	Plow, moldboard	
5/26/1	Disk, tandem heavy primary op.	
5/29/1	Harrow, coiled tine	
5/29/1	Harrow, coiled tine	
5/31/1	Planter, double disk opener	Potato, Irish
6/20/1	Cropland/cultivators/cultivator, row	
6/20/1	Bed shaper	
6/30/1	Sprayer, fungicide	
7/15/1	Sprayer, fungicide	
7/30/1	Sprayer, fungicide	
8/15/1	Sprayer, fungicide	
8/30/1	Sprayer, fungicide	
9/16/1	Sprayer, fungicide	
9/30/1	Kill crop	
10/15/1	Harvest, dig root crops res. buried	
5/1/2	Disk, tandem heavy primary op.	
5/12/2	Harrow, coiled tine	
5/12/2	Harrow, coiled tine	
5/15/2	Drill or air seeder, double disk	Oats, spring
5/31/2	Sprayer, post emergence	
8/15/2	Harvest, killing crop 50pct standing stubble	

For both the PEI and NB sites, the output soil loss rate (Mg ha<sup>-1</sup> yr<sup>-1</sup>) for each cell obtained from RUSLER was imported into Surfer® 12 program. The kriging algorithm built-in the program was utilized to generate a 5-m grid-based map. For the PEI site, the x-axis limit ranged from 386403.75 m to 386608.75 m, and the y-axis limit ranged from 699365.25 m to 699515.25 m. For the NB site, the x-axis limit ranged from 2405354.00 m to 2405579.00, and the y-axis limit ranged from 7565906.00 m to 7566341.00 m. With respect to the soil loss rate (Mg ha<sup>-1</sup>

yr<sup>-1</sup>) obtained from EphGEE, the rate in the channel cells was estimated using the method described above, and the rate in the rest cells was treated as zero erosion or deposition. Then, the full dataset was imported into Surfer® 12 program to generate a grid-based map as same size as that of RUSLER.

#### 4.3.2.2 Tillage erosion - DirTilLEM

A well-established DirTilLEM was used to model the spatial patterns of tillage erosion for both sites (Li et al., 2009). In brief, for all the tillage operations, soil materials can be translocated parallel and perpendicular to the tillage direction simultaneously (referred to as forward and lateral translocation, respectively, herein). Tillage translocation in both directions can be calculated using DirTilLEM as follows:

$$T_{Mf} = \alpha_f + \beta_f\theta_f + \gamma_f\Phi_f \quad [1]$$

$$T_{M\ell} = \alpha_\ell + \beta_\ell\theta_\ell + \gamma_\ell\Phi_\ell \quad [2]$$

Where  $f$  and  $\ell$  denoted forward and lateral translocation, respectively;  $T_M$  was tillage translocation in mass per unit width ( $\text{kg m}^{-1}$ );  $\alpha$  was tillage translocation in mass unaffected by slope gradient or slope curvature ( $\text{kg m}^{-1}$ );  $\beta$  ( $\text{kg m}^{-1} \%^{-1}$ ) and  $\gamma$  ( $\text{kg m}^{-1} (\%^{-1} \text{ m})$ ) were the additional tillage translocation due to slope gradient and slope curvature, respectively;  $\theta$  (%) was slope gradient (positive for downslope; negative for upslope), and  $\Phi$  ( $\% \text{ m}^{-1}$ ) was slope curvature (positive for convex; negative for concave).

The program was written in Visual Basic code and ran on a DEM, and numerically calculated a tillage translocation into and out of a given cell in relation to its four adjacent cardinal cells after accounting for the influence of tillage direction and field boundaries. The

net amount of soil translocated in each cell equalled to the amount of soil translocated into a given cell minus that translocated out of a given cell. The soil erosion rate was defined as the net tillage translocation divided by the cell length (5-m in this case). The positive value of the result indicated soil loss, and the negative value indicated soil accumulation ( $\text{Mg ha}^{-1} \text{ yr}^{-1}$ ). Boundary cells were considered barriers to soil movement with zero soil flux, meaning that no soil was allowed to move into a boundary cell or move out from a boundary cell.

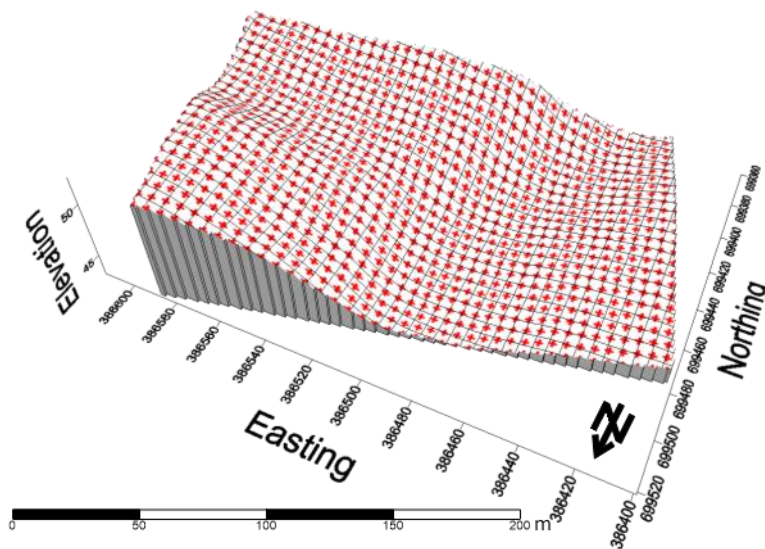


**Figure 4.3.** The grid points (red cross) along the tillage directions are generated for the tillage erosion modeling for the PEI site.

The input data for DirTilLEM included 5-m DEM, the tillage direction (i.e., 1-right, 2-bottom, 3-left, 4-up), tillage tool information (1-one-way tillage or 0-two-way tillage) and its associated tillage translocation parameters ( $\alpha$ ,  $\beta$  and  $\gamma$ ).

Firstly, for the PEI site, the input 5-m DEM data was obtained from the DEM used for RUSLER and EphGEE. The current DirTilLEM was only capable of dealing with the true north-south or east-west tillage direction. However, the PEI site was along the direction of southwest

northeast. Therefore, the DEM used for RUSLER and EphGEE was not totally suitable for DirTilLEM. Along the tillage or field direction, the 5-m grid was assigned in the PEI site (Fig. 4.3). Then, the elevations of these grids were extracted from the original DEM (used for RUSLER and EphGEE) using the Surfer® 12 program. For the NB site, input 5-m DEM was the same as that for RUSLER and EphGEE since the NB site was along the direction of the north-south.

**Table 4.5** The tillage translocation parameters ( $\alpha$ ,  $\beta$ ,  $\gamma$  and lateral throw direction) used in the ModDirTilLEM with different sites, crop rotations, and tillage tools

		One-way tillage	Two-way tillage	Channel removal tillage
PEI site 5-yr rotation (grain-hay- grain-hay- potato)	$\alpha_f$ (kg m <sup>-1</sup> )	89.4	257.2	31.1
	$\beta_f$ (kg m <sup>-1</sup> % <sup>-1</sup> )	3.2	8.5	1.3
	$\gamma_f$ (kg m <sup>-1</sup> (% <sup>-1</sup> m))	21.2	-47.3	-15.8
	Lateral throw direction	Right	Left-right	Left-right
	$\alpha_\ell$ (kg m <sup>-1</sup> )	44.7	128.6	15.6
	$\beta_\ell$ (kg m <sup>-1</sup> % <sup>-1</sup> )	1.6	4.3	0.7
	$\gamma_\ell$ (kg m <sup>-1</sup> (% <sup>-1</sup> m))	10.6	-23.7	-7.9
NB site 3-yr rotation (potato-potato- grain)	$\alpha_f$ (kg m <sup>-1</sup> )	44.7	435.3	44.7/31.1
	$\beta_f$ (kg m <sup>-1</sup> % <sup>-1</sup> )	1.6	13.4	1.6/1.3
	$\gamma_f$ (kg m <sup>-1</sup> (% <sup>-1</sup> m))	10.6	-65.6	10.6/-15.8
	Lateral throw direction	Right	Left-right	Right/Left-right
	$\alpha_\ell$ (kg m <sup>-1</sup> )	22.3	217.7	22.3/15.6
	$\beta_\ell$ (kg m <sup>-1</sup> % <sup>-1</sup> )	0.8	6.7	0.8/0.7
	$\gamma_\ell$ (kg m <sup>-1</sup> (% <sup>-1</sup> m))	5.3	-32.8	5.3/-7.9
NB site 2-yr rotation (potato-grain)	$\alpha_f$ (kg m <sup>-1</sup> )	44.7	251.5	31.1
	$\beta_f$ (kg m <sup>-1</sup> % <sup>-1</sup> )	1.6	8.2	1.3
	$\gamma_f$ (kg m <sup>-1</sup> (% <sup>-1</sup> m))	10.6	-48.2	-15.8
	Lateral throw direction	Right	Left-right	Left-right
	$\alpha_\ell$ (kg m <sup>-1</sup> )	22.3	125.8	15.6
	$\beta_\ell$ (kg m <sup>-1</sup> % <sup>-1</sup> )	0.8	4.1	0.7
	$\gamma_\ell$ (kg m <sup>-1</sup> (% <sup>-1</sup> m))	5.3	-24.1	-7.9

forward tillage is denoted as  $f$ , lateral tillage is denoted as  $\ell$ .

Secondly, for the PEI site, the model was run to simulate the tillage from 1963 to 2015 (53 years). As mentioned in 4.3.1, from 1963 to 2003, the tillage was along the direction of north-south, and the tillage was switched to the opposite direction once a year. From 2004 to 2015, the tillage was along the direction of east-west, and the tillage direction still changed once a year. For the NB site, the model estimated the tillage from 1963 to 2017 (55 years). From 1963 to 2007, the tillage was along the direction of north-south. From 2008 to 2017, the tillage direction switched to the west-east.

Lastly, for both the PEI site and the NB site, the tillage implements used in the DirTilLEM were based on the crop management operations for RUSLER. The corresponding tillage translocation parameters ( $\alpha$ ,  $\beta$  and  $\gamma$ ) were collected from field experiments conducted in Manitoba and New Brunswick and the parameters were summarized in Table 4.5 (Li et al., 2007a; Tiessen et al., 2007a; Tiessen et al., 2007b; Tiessen et al., 2007c). As mentioned in 4.3.2.1, 5-year crop rotation (grain-hay-grain-hay-potato) was assumed for the PEI site, and 3-year crop rotation (potato-potato-grain) and 2-year crop rotation (potato-grain) were utilized for the NB site. One-way tillage operation was conducted using a right-handed mouldboard plough, and two-way tillage implements were used for other tillage passes.

Similar to those of RUSLER, for both the PEI site and the NB site, the soil loss rate ( $\text{Mg ha}^{-1} \text{ yr}^{-1}$ ) for each cell obtained from DirTilLEM was imported into Surfer® 12 program. The kriging algorithm built-in the program was utilized to generate the same 5-m grid-based map as that for RUSLER.

#### 4.3.2.3 Gully effect on tillage erosion - ModDirTilLEM

On one hand, the effects of channel infilling on water erosion were not adjusted into any models since the EphGEE model had considered these effects to some extent. The EphGEE model assumes that, after each tillage operation, the channel was refilled to its original surface layer with the same tillage layer soil. Hence, the soil condition after channel infilling was same to that after tillage operation. In the Chapter 3, we found that the water erosion under the channel infilling condition was similar to that under tillage erosion. Therefore, the adjustment for EphGEE was not carried out in this thesis. On the other hand, the effects of water-eroded channels on tillage translocation were incorporated into DirTilLEM. The code of DirTilLEM was written in Visual Basic. For an easier modification, all codes were translated into the R environment. Then, a channel adjusting function was added to the DirTilLEM to account for the impact of a channel on tillage translocation. The channel location and flow direction were defined using RUSLER. The cell size of DEM was 5-m, which was wider than most of the ephemeral gullies observed in fields. The channel width of 20 cm was assumed for all ephemeral gully estimated. In Chapter 2, Zheng et al. (2021) conducted a plot experiment to quantify the impact of a channel on tillage translocation. The results indicated that, for a 20-cm-by-20-cm channel, when tillage was along with the channel, 90 % of absolute lateral soil translocation was less than 50 cm. This distance can be explained by how far the channel can influence tillage translocation. The total distance affected by the channel was equal to two distances (both sides of the channel) plus channel width ( $50\text{ cm} + 50\text{ cm} + 20\text{ cm} = 120\text{ cm}$ ). Therefore, for each 5-m cell, only 24 % area of the cell was affected by the presence of a

channel which was along the tillage direction. Namely, the influence area was 24% of the channel cell under this scenario. When tillage was perpendicular to the channel, 90 % of absolute lateral translocation was less than 120 cm. Therefore, the total influence distance was  $120 \text{ cm} + 120 \text{ cm} + 20 \text{ cm} = 260 \text{ cm}$ . When tillage was perpendicular to the channel, the influence area was 52 % of the channel cell. Since no experiment was conducted when tillage was angled with the channel, the assumption was made that the influence distance was the average of 120 cm and 260 cm (190 cm). As a result, the influence area was 38 % of the channel cell.

For the influence area within each channel cell, the product of a Distance ratio (DR) and a Mass ratio (MR) was multiplied by the original tillage translocation obtained from DirTilLEM. The DR was calculated based on the results obtained from Chapter 2:

$$\text{DR} = \text{Translocation}_{\text{C20}} / \text{Translocation}_{\text{C0}} \quad [3]$$

Where  $\text{Translocation}_{\text{C20}}$  (m) was the tillage translocation (forward or absolute lateral) with a presence of 20-cm-by-20-cm-channel;  $\text{Translocation}_{\text{C0}}$  (m) was the tillage translocation (forward or absolute lateral) with no channel. Similarly, the MR was calculated as follows:

$$\text{MR} = \text{Mass}_{\text{C20}} / \text{Mass}_{\text{C0}} \quad [4]$$

Where  $\text{Mass}_{\text{C20}}$  (kg) was the affected soil mass with the presence of a 20-cm-by-20-cm channel;  $\text{Mass}_{\text{C0}}$  (kg) was the affected soil mass with no channel.

The downslope and upslope tillage were conducted along the 10 % slope. Therefore, the DR values obtained from the experiment were only applied to the slope with a 10 % gradient. In order to extend the application of the DR for different slope gradients, the linear regression

equations were generated for the following scenarios: Tillage Parallel to Channel and Tillage Diagonal to Channel, respectively. When the tillage was perpendicular to the channel (contour tillage), it was assumed that the slope gradient was consistently 0 % along the tillage direction. Therefore, the DR forward and DR lateral for this scenario was 2.17 and 3.00, respectively.

For the tillage parallel to the channel, the DR values applied to the forward and lateral translocations were:

$$DR_f = -5.08 \times S + 1.06 \quad [5]$$

$$DR_l = -0.69 \times S + 1.15 \quad [6]$$

Where  $f$  and  $l$  denoted the forward and lateral translocation, respectively;  $S$  was the slope gradient (%). For the tillage diagonal to channel, the DC values applied to the forward and lateral translocations were:

$$DR_f = -2.54 \times S + 1.62 \quad [7]$$

$$DR_l = -0.35 \times S + 2.08 \quad [8]$$

The channel adjusting function (CAF) was the final function applied to the influence area of the channel cell, which was defined as the product of DR and MR ( $DR \times MR$ ). The detailed parameters for each scenario are summarized in Table 4.6. Overall, based on the respective direction between tillage and channel, for the channel cell, the CAFs were applied to the tillage translocations obtained from DirTilLEM.

The CAF was only applied to the channel removal tillage pass since other passes did not directly eliminate or smooth the existing channel. For example, for the PEI site, a disc tillage pass was responsible for the channel removal; therefore, the additional channel component was

added to the tillage translocation related to this pass. For the NB site, particularly for 3-year crop rotation, the channel component was applied to a mouldboard plough and a disc tillage pass. Therefore, the tillage parameters were categorized into three groups and summarized in Table 4.5, including one-way tillage, two-way tillage, and channel removal tillage. With the consideration of the CAF, DirTilLEM was named Modified DirTilLEM (hereinafter ModDirTilLEM).

**Table 4.6** The channel adjusting function applied for the channel cell in ModDirTilLEM with different tillage directions, channel directions (the distance ratio and mass ratio are obtained from the experiment described in Chapter 2, and the channel adjusting function is obtained from the calculation of distance ratio  $\times$  mass ratio)

	Distance ratio (m m <sup>-1</sup> )	Mass ratio (kg kg <sup>-1</sup> )	Channel adjusting function (m kg m <sup>-1</sup> kg <sup>-1</sup> )
Tillage parallel to channel	Forward	$-5.08 \times S + 1.06$	Forward $-4.23 \times S + 0.89$
	Lateral	$-0.69 \times S + 1.15$	Lateral $-0.58 \times S + 0.96$
Tillage perpendicular to channel	Forward	2.17	Forward 2.00
	Lateral	3.00	Lateral 2.77
Tillage diagonal to channel	Forward	$-2.54 \times S + 1.62$	Forward $-2.27 \times S + 1.45$
	Lateral	$-0.35 \times S + 2.08$	Lateral $-0.31 \times S + 1.86$

Note: 1) the distance ratio and mass ratio are calculated from the translocated soil distance and impacted soil mass with the presence of channel (20 cm deep by 20 cm wide)  $\div$  the translocated soil distance and impacted soil mass without channel, respectively; 2) the soil mass is obtained

based on the soil volume (20 cm deep) and uniform bulk density; 3) S stands for slope gradient of the cell (%).

#### **4.3.2.4 Integrated total erosion**

To assess the total erosion rate that occurred in cultivated fields, all models of different erosion forms (sheet and rill erosion, ephemeral gully erosion, tillage erosion, and interactions) were integrated together. The combination of all erosion models was simply the summation of results obtained from all models. The outputs of these three models shared the same grid line geometry (xy limits and spacing). All three models were imported into Surfer® 12 program, and the built-in function “Math” was utilized to sum up the grid map of RUSLER, EphGEE and ModDirTilLEM together. Therefore, the soil loss rate ( $\text{Mg ha}^{-1} \text{ yr}^{-1}$ ) in each grid represented the integrated rate caused by water and tillage erosion and their interactions.

Overall, the comprehensive framework for modeling total soil erosion primarily rested upon the integration of three erosion models (RUSLER, EphGEE and ModDirTilLEM), thereby encompassing a more holistic understanding. Beyond the simple summation approach, these individual erosion models were interconnected. The RUSLER model played a pivotal role in delineating channel areas based on predetermined thresholds for upslope contribution area. This identified channel area was subsequently adopted by both the EphGEE and ModDirTilLEM models. In the case of EphGEE, its input dataset was derived from RUSLER, rendering any alterations to RUSLER's input data capable of influencing EphGEE's outcomes, such as the size of channel, the sediment amount produced by erosion. Similarly, for ModDirTilLEM, changes in the channel area's location directly impacted the manifestation of interaction effects. Notably, the present model has yet to incorporate the morphological

evolution of channels within agricultural fields. However, a promising avenue exists for the coupling of EphGEE and ModDirTilLEM, facilitating an assessment of the impact of varying channel sizes on tillage erosion. This potential coupling could significantly enhance the model's comprehensiveness.

### **4.3.3 Validation**

#### **4.3.3.1 Photo visual observation data**

The photo visual observation data were used to validate the estimated pattern of water erosion using RUSLER and EphGEE. A series of drone photos was taken using a DJI phantom 4 PRO with a CMOS sensor and 20 megapixels. The photos were taken at approximately 80 m to 100 m above the ground. The camera faced the ground. Generally, one drone photo is unable to cover the entire field. Therefore, several photos were required to cover the whole area. After the photo was taken, the built-in mosaic function in ArcMap® 10.1 program was conducted to combine all photos together.

The photos were taken several times within a year, including after snow melting, after spring tillage, after harvest, and before snowfall. Also, a few more series of the photo were taken after major storm events. The sediment accumulation can be observed in the drone photo by its brighter colour and delta shape at the end of the hillslope. In addition, the locations of the channel caused by water erosion can be observed in images. The locations of the channel in images can be compared with those of the estimated channel visually.

#### 4.3.3.2 Field survey and photogrammetry data

The field survey and photogrammetry data were used to validate the estimated ephemeral gully volume using EphGEE. For both sites, the ephemeral gullies generated after every major runoff event were measured and recorded using two methods: manual measurement and drone-based photogrammetry, respectively. Regarding manual measurement, the measurements were taken at an interval ranging from 10 m to 50 m along the gully, depending on the variations of the gully size. For each measuring location, a straight ruler was placed on the top of the gully. The gully depth was measured from a vertical measuring tape resting on the bottom of the gully to the straight ruler on the top. The depth measurement was recorded starting from the left side (facing upslope) to the right side at a 10 cm interval along the transect. The cross-section area ( $\text{m}^2$ ) of each transect was calculated based on the summation of all depth measurements and width. The measuring location information was collected using DGPS. In addition, the gully length (m) was recorded by walking along the gully with DGPS. The gully volume ( $\text{m}^3$ ) was estimated using averaged cross-section area and gully length. The resolution of this method was coarse. The photogrammetry method could provide a much finer result.

Regarding drone-based photogrammetry, the DJI phantom 4 PRO was used to conduct the survey. The flight routing was planned using Pix4D installed on the mobile device to cover the entire field. The drone flew 30 m above the ground, and image overlapping rate was set at 70 %. The camera faced the ground at a slight angle ( $10^\circ$ ). Five 1-m-by-1-m ground control points were randomly placed in the field, and their positions were recorded with DGPS for further image processing. All images collected were imported into PhotoModeler® for processing to

generate a 3D model. The volume of ephemeral gullies was extracted using the built-in tool “Define Volume” in the PhotoModeler® program.

#### **4.3.3.3 Water gauging station data**

The runoff and sediment discharge measured by the water gauging station can be used to validate the estimated runoff and sediment data using RUSLER and EphGEE. The water station and 2.5-foot H flume were set for both of the PEI and NB sites. For the PEI site, since the field was located within a watershed, two water monitoring systems were installed at the inlet and outlet of the field, respectively. The stage height sensor, in conjunction with a CR10 data logger (Campbell Scientific Inc.), was used to monitor the water depth in the flume at a 5-minute scanning interval and recorded on a 1-hour basis. If the change in the stage height was greater than 1 cm compared to the previous record, the ISCO 6712 automated water sampler (Teledyne ISCO) was triggered to take samples. The data logger also recorded the sample number, time and water depth for each collected sample. The collected samples were removed from the sampler and transferred to the laboratory in Fredericton Research and Development Centre when the sampler was full. The collected samples were analyzed the next day after collection. The sediment for each water sample was measured in the lab. The measured sediment and runoff data were utilized to validate the estimated water erosion data obtained from RUSLER and EphGEE. However, due to weather limitations, the water station only collected water samples after snow melting and before snowfall.

#### 4.3.3.4 Cs-137 data

The Cs-137 data obtained from soil samples can be used to validate the estimated total erosion using the summation of RUSLER, EphGEE and ModDirTilLEM. By far, this is the most commonly used method to validate total erosion.

For the PEI site, 50 soil samples were collected in June 2015. Six transects were designed across the field. Each transect covered the different slope positions, including upslope, midslope, lowerslope and depression, which were defined using the LandMapper program (MacMillan et al., 2003). In addition, some random sampling points were designed across the field where transects did not cover. Therefore, all soil samples were able to represent the entire field (Fig. 4.4.a). The coordinate of each sample location was generated using Surfer® 12 program (Golden Software, LLC) and was imported into the Trimble Geoexplorer 6000 Differential Global Position System (DPGS). In the field, each sample location was surveyed using DPGS with an accuracy less than 10 cm. For the NB site, 67 soil samples at the NB site were collected in October 2017. Eight transects and additional random points were designed across the field (Fig. 4.4.b). Also, these points were surveyed using DGPS.

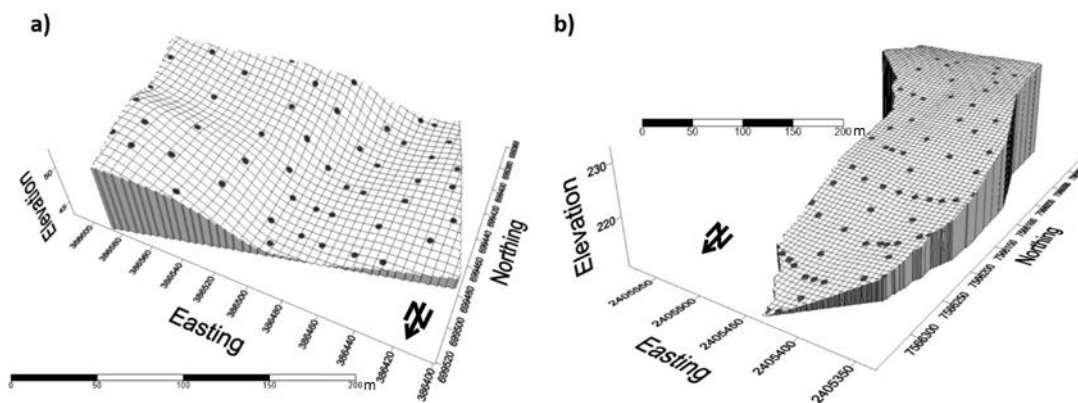


**Figure 4.4.** a) The locations (black dot) of sampling points (n=50) in the PEI site; b) the locations (black dot) of sampling points (n=67) in the NB site.

For each soil sample location, three cores were collected using a 7.6-cm diameter soil probe mounted on the Gidding System. Each soil core was taken to at least C horizon (about 1 m) and was divided into four increments (0 - 15 cm, 15 - 30 cm, 30 - 60 cm, and > 60 cm). Sampling below the tillage layer (20 to 25 cm) was to ensure that all the Cs-137 inventory could be recovered in soil samples. Based on the sample location and increment, soil samples were mixed and then collected soil samples were air-dried at room temperature (about 20°C). Dried soil samples were grounded using a grinding machine to pass through a 2-mm sieve, separating the soil solids from the rock fragments. The soil samples were analyzed for soil dry bulk density ( $\rho$ ).

A Broad Energy Germanium Detector (Canberra BEGE, Fredericton Research and Development Centre, Canada) with a detection error < 10% was utilized to detect Cs-137 radioactivity for each sample. Cs-137 inventory at each location was determined by the summation of area-based Cs-137 radioactivity of all the samples taken from different soil layers.

After the calculation of Cs-137 inventories for each sampling point, all inventories were imported into Proportional Model (PM) in the Cs-137 Erosion Calibration Models program to calculate soil erosion rates (Walling and He, 1999). The PM uses a simple linear function to convert the loss and gain of Cs-137 inventory to a loss or gain of soil mass, respectively (Walling and He, 1999). This model simulates both the water and tillage erosion process and only requires basic input data, which are the reasons for the popularity of this model in the literature. Regarding the input data for the PM, for both sites, the year of tillage commencement was set at 1963 (the year of the highest peak of Cs-137 fallout). As mentioned in section 2.2,

The tillage depth was estimated using the Cs-137 inventory and the corresponding depth migration. The tillage depth (m) was estimated at 0.22 and 0.26 m for the PEI site and the NB site, respectively. The bulk density of tillage layer was measured 1324 and 1174 kg m<sup>-3</sup> for the PEI site and the NB site, respectively.

Regarding the reference Cs-137 level used in the PM, the values for both sites were obtained from literatures (Kachanoski and Carter, 1999; Tiessen et al., 2009), which were 1572 Bq m<sup>-2</sup> and 1369 Bq m<sup>-2</sup> for sites near the PEI site and the NB site, respectively (the PEI site level was adjusted to 2015 January 1<sup>st</sup> and the NB site level was adjusted 2017 January 1<sup>st</sup>). The inventory of Cs-137 is considered a moderately variable soil property with a CV ranging from 15 % to 35 % (Sutherland, 1996). In addition, the reference sites were not designed for the field sites in this study. Therefore, the values obtained from the literature were unable to perfectly represent the reference level for both sites. For the better performance of the PM, the range of Cs-137 reference level was estimated. Then, the middle value of the lower and upper limits was calculated and applied to the PM to estimate the erosion rates. For the lower limit, it was estimated by assuming that there was no net erosion from fields. The kriging interpretation was utilized to calculate the field average of the Cs-137 inventory. The calculated field average was the lower limit of the Cs-137 reference level, which was 1789 Bq m<sup>-2</sup> and 1185 Bq m<sup>-2</sup> for the PEI site and the NB site, respectively. For the upper limit, the 25 % (the average value of the CV range) greater Cs-137 reference level (obtained from literature) was utilized. The estimated upper limit of the Cs-137 reference level was 1965 Bq m<sup>-2</sup> and 1643 Bq

$\text{m}^{-2}$  for the PEI site and the NB site, respectively. Therefore, the averaged Cs-137 reference level for the PM was  $1877 \text{ Bq m}^{-2}$  and  $1448 \text{ Bq m}^{-2}$  for the PEI site and the NB site, respectively.

Similar to those of RUSLER and ModDirTilLEM, for both the PEI site and the NB site, the estimated total erosion rate ( $\text{Mg ha}^{-1} \text{ yr}^{-1}$ ) for each point was imported into Surfer® 12 program. The kriging algorithm built-in the program was utilized to generate the same 5-m grid-based map as that for RUSLER and ModDirTilLEM.

The soil sampling points did not coincide with the grid points used for modeling. For the comparison purpose, the built-in tool “Residuals” in Surfer® was used to interpolate the erosion rate data estimated from different models onto the sampling points. The sampling points were grouped into four categories based on landform position (upslope, middle slope, lower slope, and depression).

The relationships between the estimated erosion data and Cs-137 derived total soil erosion were examined with R using the “stats” package (Team, 2013). The weighted paired t-test was used to indicate the mean difference between paired observations. Thereby, the difference of the erosion magnitude between the models could be captured. Additionally, Pearson correlation coefficients ( $r$ ) were used to indicate the correlations between the estimated water and tillage erosion rates and the total erosion rate. The discrepancy of the erosion pattern between the models could be observed.

## 4.4 Results

### 4.4.1 Modeling water erosion, tillage erosion and their interactions

#### 4.4.1.1 Sheet and rill erosion

For both sites, the pattern of RUSLER-modeled sheet and rill erosion rates ( $E_{\text{RUSLER}}$ ) was that the lowest soil losses occurred in the upslope areas (averaged 2.5 and 5.4  $\text{Mg ha}^{-1} \text{yr}^{-1}$  for PEI and the NB site, respectively), whereas the greatest soil losses occurred in the middle slope areas (averaged 2.7 and 14.5  $\text{Mg ha}^{-1} \text{yr}^{-1}$  for PEI and the NB site, respectively, Fig. 4.5, Table 4.7). For the PEI site, the soil accumulation occurred in the major part of the lower slope and depression areas. The highest soil accumulation rates (averaged  $-4.9 \text{ Mg ha}^{-1} \text{yr}^{-1}$ ) occurred in the lower slope areas, where the ground was nearly level. Whereas for the NB site, the soil accumulation (averaged 11.1  $\text{Mg ha}^{-1} \text{yr}^{-1}$ ) was not dominated in the depression areas, probably suggesting that the soil erosion was greater than soil accumulation. For the NB site, the water erosion rates were consistently greater than those for the PEI site at all landforms, probably because of the longer slope length (~400 m vs. ~100 m) and tillage management with less canopy coverage, leading to the land more vulnerable to water erosion.

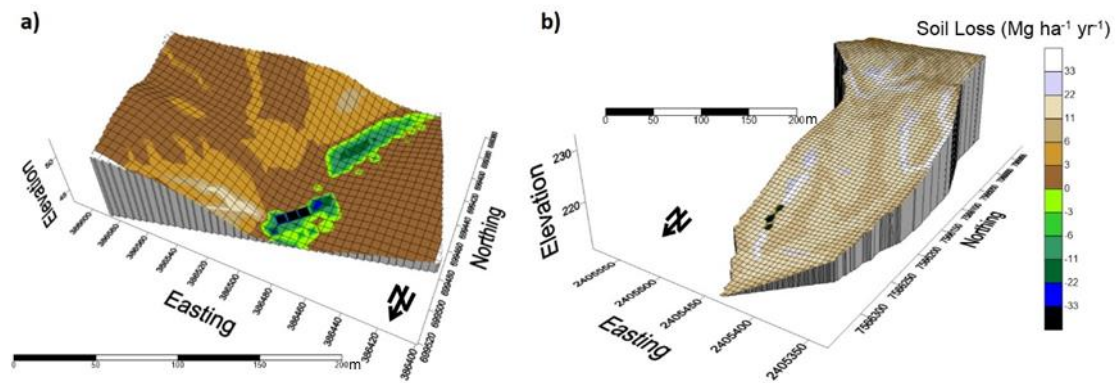


**Figure 4.5.** a) The predicted soil loss rate ( $\text{Mg ha}^{-1} \text{yr}^{-1}$ ) from RUSLER for the PEI site; b) the predicted soil loss rate ( $\text{Mg ha}^{-1} \text{yr}^{-1}$ ) from RUSLER for the NB site (the green/blue and dark colour indicate soil accumulation, whereas the brown and light colour indicate soil loss).

#### 4.4.1.2 Ephemeral gully erosion

For both sites, two gullies were simulated through modeling: one major gully (G1) and one tributary (G2) (Fig. 4.6.a). In addition, soil accumulation was not observed at the outlets of both sites. For the PEI site, most (56 %) of the gully developed in the depression area. Meanwhile, 10 % and 34 % of the gully developed in the middle and lower slope areas, respectively. For most of the cases along G1, erosion rates ( $E_{\text{EphGEE}}$ ) gradually decreased from the inlet position (south) and then slightly increased towards the outlet position. The lowest  $E_{\text{EphGEE}}$  ( $475.6 \text{ Mg ha}^{-1} \text{yr}^{-1}$ , based on the 5-m-by-5-m cell) occurred at the location of the confluence of G1 and G2, probably because the sediment delivered from G2 subdued the net soil loss in this area. Along G2,  $E_{\text{EphGEE}}$  increased steadily to the highest value ( $497.4 \text{ Mg ha}^{-1} \text{yr}^{-1}$ ) from the gully head to the middle section of G2, then  $E_{\text{EphGEE}}$  started to decrease.

**Table 4.7** The average soil erosion rate and its associated standard deviation (SD) obtained from different erosion models for overall and different landform positions for both of the PEI and NB sites

Site	Model	All landforms (Mg ha <sup>-1</sup> yr <sup>-1</sup> )	Upslope (Mg ha <sup>-1</sup> yr <sup>-1</sup> )	Midslope (Mg ha <sup>-1</sup> yr <sup>-1</sup> )	Lowerslope (Mg ha <sup>-1</sup> yr <sup>-1</sup> )	Depression (Mg ha <sup>-1</sup> yr <sup>-1</sup> )
PEI	RUSLER	1.2 (10.9)	2.5 (1.3)	2.7 (2.2)	-3.3 (21.8)	-4.9 (22.5)
	EphGEE	28.7 (160.2)	0 (0)	3.4 (57.7)	35.3 (134.9)	262.0 (444.2)
	DirTilLEM	-0.1 (8.3)	10.4 (9.8)	-0.9 (4.0)	-7.7 (2.9)	-7.8 (5.3)
	ModDirTilLEM	-0.1 (8.4)	10.4 (9.8)	-1.0 (4.0)	-7.7 (3.4)	-7.5 (5.7)
	RUSLER + ModDirTilLEM	1.1 (14.6)	12.9 (10.2)	1.7 (4.4)	-11.1 (22.5)	-12.4 (23.3)
	RUSLER+ EphGEE + ModDirTilLEM	29.8 (159.6)	12.9 (10.2)	5.2 (57.7)	24.3 (139.3)	249.6 (447.8)
NB	RUSLER	12.9 (13.5)	5.4 (3.6)	14.5 (14.9)	14.4 (13.1)	11.1 (8.8)
	EphGEE	18.8 (110.0)	0 (0)	3.2 (50.0)	53.9 (170.4)	95.7 (278.4)
	DirTilLEM	0.1 (6.0)	4.8 (5.8)	0.8 (4.2)	-3.2 (6.6)	-8.3 (5.2)
	ModDirTilLEM	0.1 (6.0)	4.8 (5.8)	0.7 (4.3)	-3.1 (6.7)	-8.1 (5.4)
	RUSLER + ModDirTilLEM	13.0 (14.0)	10.3 (6.3)	15.2 (15.1)	11.3 (14.3)	3.0 (10.4)
	RUSLER + EphGEE + ModDirTilLEM	31.8 (110.1)	10.3 (6.3)	18.4 (52.2)	65.1 (170.1)	98.7 (279.9)

For the NB site, unlike the PEI site, 84 % of the gully was in the lower slope areas. In addition, 6 % and 10 % of the gully were in the middle slope and depression areas, respectively (Fig. 4.6.b). The major gully (G1) was in the direction of south-north, flowing to the outlet of the field (north). For G1,  $E_{\text{EphGEE}}$  averaged  $606.5 \text{ Mg ha}^{-1} \text{ yr}^{-1}$ , and for the tributary (G2),  $E_{\text{EphGEE}}$  averaged  $236.2 \text{ Mg ha}^{-1} \text{ yr}^{-1}$ .

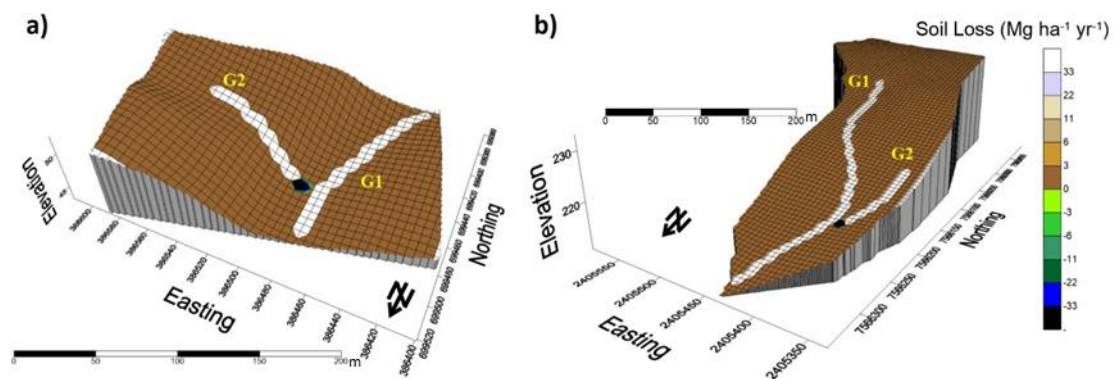


**Figure 4.6.** a) The predicted soil loss rate ( $\text{Mg ha}^{-1} \text{ yr}^{-1}$ ) from EphGEE for the PEI site, with the average soil erosion rate of  $936.0$  and  $243.4 \text{ Mg ha}^{-1} \text{ yr}^{-1}$  for the G1 and G2, respectively; b) the predicted soil loss rate ( $\text{Mg ha}^{-1} \text{ yr}^{-1}$ ) from EphGEE for the NB site, with the average soil erosion rate of  $606.5$  and  $236.2 \text{ Mg ha}^{-1} \text{ yr}^{-1}$  for the G1 and G2, respectively (the green/blue and dark colour indicate soil accumulation, whereas the brown and light colour indicate soil loss. G1 indicates the main channel and G2 indicates the tributary channel).

#### 4.4.1.3 Tillage erosion

For the PEI site, the pattern of tillage erosion rate ( $E_{\text{DirTillEM}}$ ) was varied with the local relief as expected (Table 4.7). The highest soil loss rates (averaged  $10.4 \text{ Mg ha}^{-1} \text{ yr}^{-1}$ ) occurred in the upslope area. For the middle slope area, the field average of  $E_{\text{ModDirTillEM}}$  was about  $-0.9 \text{ Mg ha}^{-1} \text{ yr}^{-1}$ , which was close to zero. For the lower slope and depression areas, as opposed to the upslope area,  $E_{\text{DirTillEM}}$  averaged  $-7.8 \text{ Mg ha}^{-1} \text{ yr}^{-1}$ , indicating the soil accumulation in these areas. The highest soil accumulation was found in the depression area near the field outlet.

Similar to the PEI site, for the NB site, the pattern of  $E_{DirTillem}$  was varied with the local relief. Except for the depression area, the magnitude of tillage erosion for the NB site was consistently less than those for the PEI site, probably because of the lower slope curvature for the NB site.

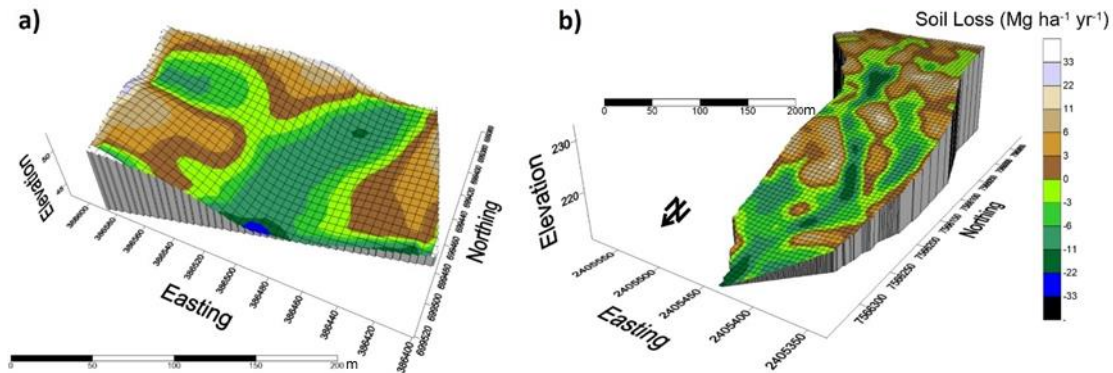


**Figure 4.7.** a) The predicted soil loss rate ( $Mg\ ha^{-1}\ yr^{-1}$ ) from DirTillem for the PEI site; b) the predicted soil loss rate ( $Mg\ ha^{-1}\ yr^{-1}$ ) from DirTillem for the NB site (the green/blue and dark colour indicate soil accumulation, whereas the brown and light colour indicate soil loss).

#### 4.4.1.4 Gully effects on tillage erosion

The basic pattern of  $E_{ModDirTillem}$  was similar to that of  $E_{DirTillem}$  (Fig. 4.7, Fig. 4.8). The gully effects only can be observed in the gully locations, which most in the lower slope and depression areas (Fig. 4.8). For both sites, there was a consistent trend that the soil accumulation rates obtained from ModDirTillem were lower those from the DirTillem (Fig. 4.8, Table 4.7). In addition, for the middle slope area, the erosion rates became less. The results suggested that, with the consideration of the effect of the gully, the soil accumulation in the gully area experienced a decrease. A greater amount of soil was translocated out of the gully and deposited in the surrounding area of the gully.

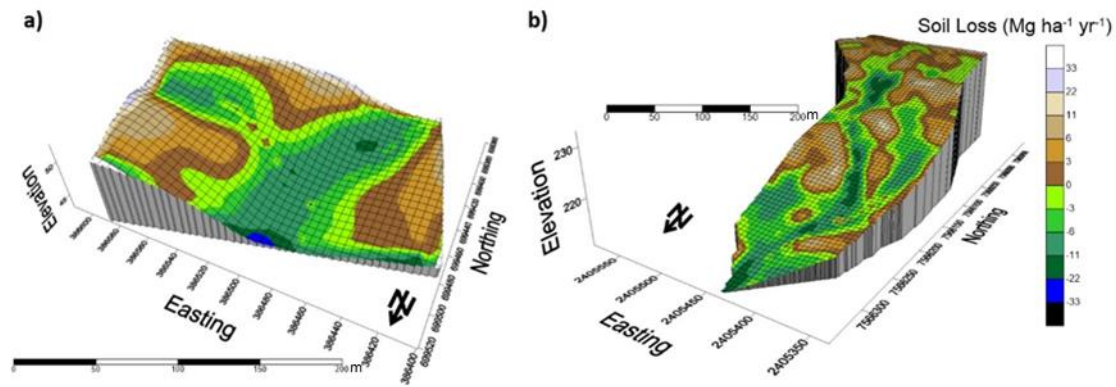


**Figure 4.8.** a) The predicted soil loss rate ( $\text{Mg ha}^{-1} \text{ yr}^{-1}$ ) from ModDirTillem for the PEI site; b) the predicted soil loss rate ( $\text{Mg ha}^{-1} \text{ yr}^{-1}$ ) from ModDirTillem for the NB site (the green/blue and dark colour indicate soil accumulation, whereas the brown and light colour indicate soil loss).

#### 4.4.1.5 Total soil erosion

For the PEI site, the total soil erosion rates ( $E_{\text{RUSLER+EphGEE+ModDirTillem}}$ ) averaged  $29.8 \text{ Mg ha}^{-1} \text{ yr}^{-1}$ , with a SD of  $159.6 \text{ Mg ha}^{-1} \text{ yr}^{-1}$  (Table 4.8.a) The majority of the land was dominated by the tillage erosion process (Fig. 4.9.a). The order of the erosion rate was followed as Depression > Lowerslope > Upslope > Midslope. The highest erosion rate,  $249.6 \text{ Mg ha}^{-1} \text{ yr}^{-1}$ , occurred in the depression area, which was about 48 times greater than the lowest erosion rate ( $5.2 \text{ Mg ha}^{-1} \text{ yr}^{-1}$ ) occurred in the midslope area. Clearly, the depression area was strongly influenced by the ephemeral gully erosion. The impact of the channel on tillage erosion was not clearly observed since the ephemeral gully erosion dominated the area where interaction effects occurred.

For the NB site,  $E_{\text{RUSLER+EphGEE+ModDirTillem}}$  averaged  $31.8 \text{ Mg ha}^{-1} \text{ yr}^{-1}$  with a SD of  $110.1 \text{ Mg ha}^{-1} \text{ yr}^{-1}$  (Table 4.7). The order of the erosion rates was slightly different from that for the PEI

site. The order was followed as Depression > Lower slope > Midslope > Upslope. Similarly, the depression area was dominated by ephemeral gully erosion.

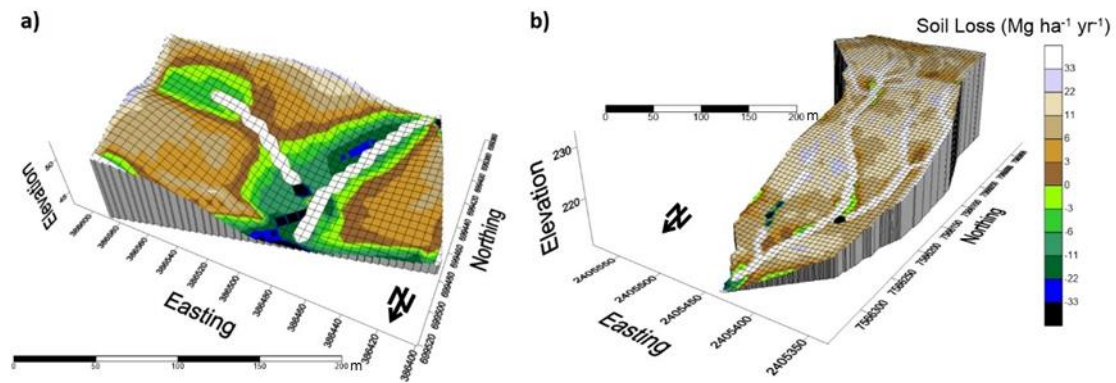


**Figure 4.9.** a) The predicted soil loss rate ( $\text{Mg ha}^{-1} \text{yr}^{-1}$ ) from the combination of RUSLER + EphGEE + ModDirTilLEM for the PEI site; b) the predicted soil loss rate ( $\text{Mg ha}^{-1} \text{yr}^{-1}$ ) from the combination of RUSLER + EphGEE + ModDirTilLEM for the NB site (the green/blue and dark colour indicate soil accumulation, whereas the brown and light colour indicate soil loss).

#### 4.4.2 Model Validation

##### 4.4.2.1 Visual observation for water erosion using photographic images

The pattern of estimated water erosion was visually compared with the observation from photographic images. For the PEI site, after snow melting in 2018, the sediment accumulation caused by the rill erosion was observed at the end of the slope (Fig. 4.10), which agreed with the results derived from RUSLER (Fig. 4.5). The predicted ephemeral gully using EphGEE was about 5 m away from the observed gully in the image. In addition, the predicted tributary gully was not clearly observed in the image. At about 20 m below the predicted tributary gully, there was a possible tributary gully observed in the image. These could be attributed to the fact that, firstly, the Lidar data was obtained about 20 years ago. Therefore, it can not reflect the evolution of the micro-topography properly. Secondly, the location of channels could be a

result of the snow topography during the winter period. Thirdly, the tillage-induced change in topography leads to the migration of concentrated flow.

For the NB site, the photo showed the sediment accumulation at the end of the slope caused by the ephemeral gully erosion (Fig. 4.11). Unlike the PEI site, the result of RUSLER showed that the soil loss near this area was probably because the soil losses were greater than soil accumulations or the EphGEE model was unable to predict the sediment accumulation properly. In addition, similar to the PEI site, the location of the predicted gully using EphGEE was not exactly the same as that of the gully observed in the image, but it is close to that of the observed gully.

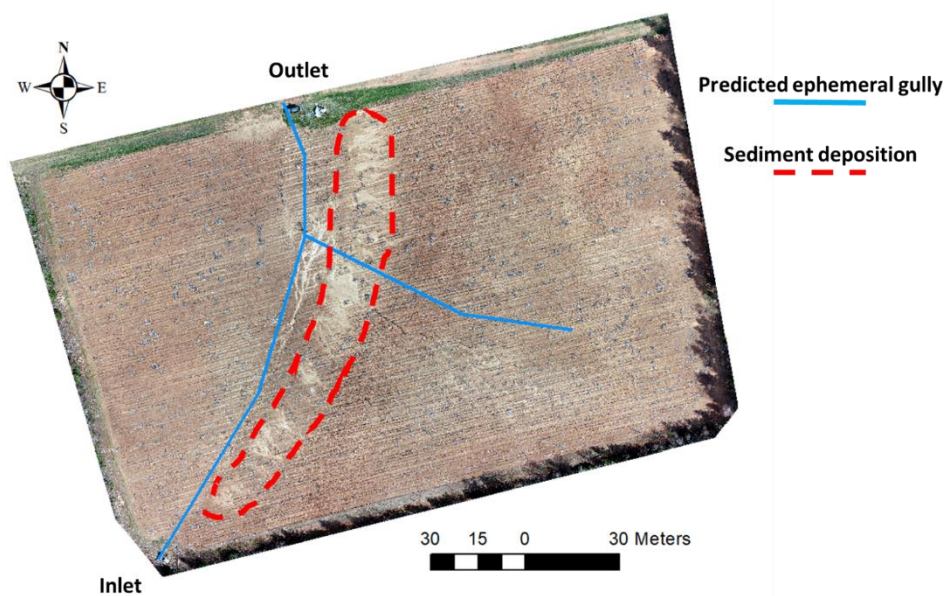


**Figure 4.10.** The drone-derived photo for the PEI site in 2018 after snow melting (the blue lines are the predicted ephemeral gully using EphGEE, and the red dash circled area is the sediment accumulation caused by rill erosion).

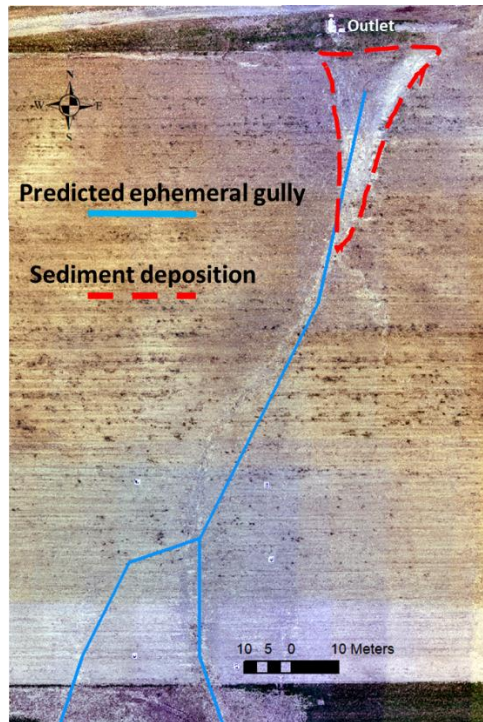


**Figure 4.11.** The drone-derived photo for the NB site in 2017 after snow melting (the blue lines are the predicted ephemeral gully using EphGEE, and the red dash circled area is the sediment accumulation caused by ephemeral gully erosion).

#### **4.4.2.2 Gully morphology observation for gully erosion using field survey and photogrammetry**

The field survey and photogrammetry method were used to validate the estimated volume using EphGEE for both the PEI site and the NB site. For the PEI site, in May 2018, after snow melting, a well-defined gully was observed at the location of G1 during the field visit (Fig. 4.10). Additionally, according to aerial imagery, this gully originally occurred in November 2017 after a major storm event. During the period from November 2017 to May 2018, no tillage operation was conducted. Therefore, the volume of the gully can reflect the soil loss by ephemeral gully erosion during this specific period. For the manual measurement, the calculated volume was approximately 15.7 m<sup>3</sup>. For the photogrammetry, the volume of the

gully extracted from PhotoModeler® software was 23.1 m<sup>3</sup>. These values were used to validate the estimated gully volume using the EphGEE model. For the same period (November 2017 to May 2018), the estimated volume of G1 was 25.0 m<sup>3</sup>, which is slightly greater than the photogrammetry-derived volume and much greater than the manual estimated volume. The difference between the estimation of the manual measurement and model prediction could be attributed to the area near the outlet, where the gully boundary was not well-defined with visual observation. Therefore, the erosion from this area was mostly neglected when the measurement was conducted. For the photogrammetry method, it is easier to define the boundary of the gully with a higher point of view.

As for the NB site, a similar validation process was conducted. The data was collected on May 10<sup>th</sup>, 2018. Two gullies were observed at the locations of G1 and G2. For these gullies, the development period was from October 2017 to May 2018. For a similar period, the manual measurement estimated volume was approximately 8.9 m<sup>3</sup>, which is lower than the model-estimated volume (11.2 m<sup>3</sup>), and the photogrammetry-derived volume was 13.8 m<sup>3</sup>, which is greater than the model-estimated volume. The locations of estimated gullies were near the observed gullies for both sites. The discrepancy in the volume between EphGEE-estimated and photogrammetry-derived was about 8% and 19% for the PEI site and the NB site, respectively, suggesting that EphGEE can produce a reasonable ephemeral gully erosion rate estimation.

#### **4.4.2.3 Total runoff and sediment discharge measured using gauging stations**

For the PEI site, during the experiment period (2015 - 2018), the change in micro-topography led to a shift in the pathway of concentrated flow. Therefore, the concentrated flow

did not flow through the flume installed at the outlet position. As a result, no sediment samples were collected from the PEI site. Thereby, no data was available for water erosion model validation. For the NB site, the runoff discharge volume was estimated using the water level measured in the flume. For example, the runoff discharge volume calculated from May 5<sup>th</sup> to Nov 2<sup>nd</sup>, 2017, was 272.3 m<sup>3</sup>. For the same period, the RUSLR-derived runoff volume from the catchment was 999.3 m<sup>3</sup>, which was 3.7 times greater than the measured data. Similarly, for the same period, the sediment was over-estimated by the model. The estimated sediment from water samples was only 866.1 kg, whereas the modeled sediment was about 20 times greater. The much greater estimated sediment yield using RUSLER and EphGEE was attributed to the greater runoff volume and sediment concentration.

#### **4.4.2.4 Estimated total soil loss and accumulation using Cs-137**

For the PEI site, based on the Cs-137 reference value of 1877 Bq m<sup>-2</sup>, the Cs-137-derived total soil erosion rates ( $E_{Cs137}$ ) averaged 2.6 Mg ha<sup>-1</sup> yr<sup>-1</sup> with a SD of 18.0 Mg ha<sup>-1</sup> yr<sup>-1</sup>. About 54 % of the area showed soil erosion, whereas approximately 46 % of the area showed soil accumulation (Fig. 4.12.a). The pattern of the results showed that the upslope area had the highest soil erosion rate (16.4 Mg ha<sup>-1</sup> yr<sup>-1</sup>), whereas the middle slope area had the lowest soil erosion rate (3.5 Mg ha<sup>-1</sup> yr<sup>-1</sup>). For both lower slope and depression areas, the soil accumulation occurred, which averaged -15.7 and -7.3 Mg ha<sup>-1</sup> yr<sup>-1</sup>, respectively.

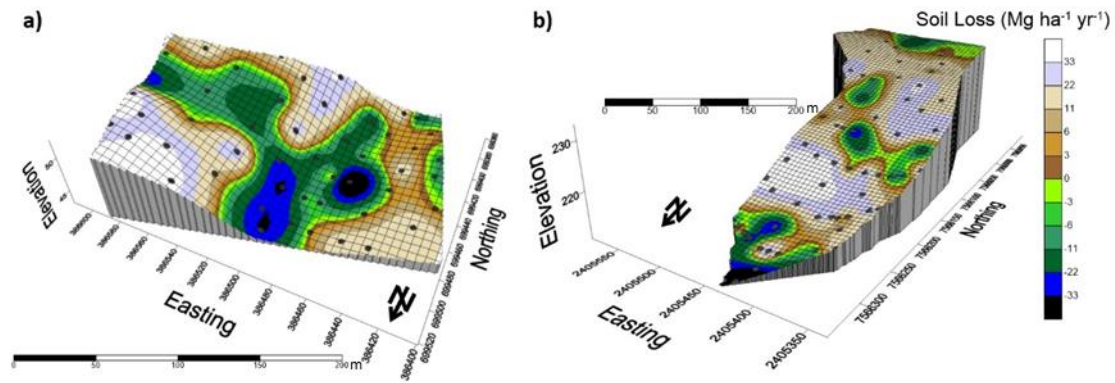


**Figure 4.12.** a) The estimated soil loss rate ( $\text{Mg ha}^{-1} \text{yr}^{-1}$ ) based on Cs-137 inventory using Proportional Model for the PEI site; b) the estimated soil loss rate ( $\text{Mg ha}^{-1} \text{yr}^{-1}$ ) based on Cs-137 inventory using Proportional Model for the NB site (the green/blue and dark colour indicate soil accumulation, whereas the brown and light colour indicate soil loss, and the black dots indicate soil sampling points. The reference Cs-137 level is  $1877 \text{ Bq m}^{-2}$  and  $1448 \text{ Bq m}^{-2}$  for PEI and NB site, respectively).

By comparing the  $E_{\text{Cs137}}$  with different modeled erosion rates at each sampling point,  $E_{\text{Cs137}}$  was significantly greater than  $E_{\text{RUSLER}}$  ( $P < 0.05$ ) and  $E_{\text{ModDirTillEM}}$  ( $P < 0.05$ ), with a difference of about  $6.1 \text{ Mg ha}^{-1} \text{yr}^{-1}$  and about  $6.8 \text{ Mg ha}^{-1} \text{yr}^{-1}$ , respectively (Table 4.8). The difference between  $E_{\text{Cs137}}$  and  $E_{\text{RUSLER+EphGEE+ModDirTillEM}}$  was  $-5.9 \text{ Mg ha}^{-1} \text{yr}^{-1}$ , which was non-significant.

The differences between  $E_{\text{Cs137}}$  and the rate of different erosion forms varied with landform positions. For the upslope area, all differences between  $E_{\text{Cs137}}$  and individual erosion rate were significant ( $P < 0.05$ ) except for the tillage erosion rate. Regarding the difference between  $E_{\text{Cs137}}$  and the sum of water and tillage erosion rates, it decreased to  $-1.1 \text{ Mg ha}^{-1} \text{yr}^{-1}$ , and the difference was non-significant, suggesting that the sum of three models might provide better performance on estimating erosion rates in the upslope area.

For the middle slope area, all differences between  $E_{\text{Cs137}}$  and other erosion rates were significant ( $P < 0.1$ ). As expected, the smallest difference occurred between  $E_{\text{Cs137}}$  and  $E_{\text{RUSLER}}$  ( $7.7 \text{ Mg ha}^{-1} \text{yr}^{-1}$ ). Regarding tillage erosion, the largest significant difference ( $10.7 \text{ Mg ha}^{-1} \text{yr}^{-1}$ )

<sup>1</sup>) was observed. For the sum of the models, the difference became smaller than  $E_{\text{ModDirTillEM}}$  and  $E_{\text{EphGEE}}$ , but greater than  $E_{\text{RUSLER}}$ , when compared with  $E_{\text{Cs137}}$ .

For the lower slope area, the pattern of consistent under-estimation was observed. All differences between  $E_{\text{Cs137}}$  and rates derived from other erosion forms were significant ( $P < 0.1$ ) except for the difference between  $E_{\text{Cs137}}$  and  $E_{\text{RUSLER+ModDirTillEM}}$ . The largest difference was observed between  $E_{\text{Cs137}}$  and  $E_{\text{EphGEE}}$  ( $-118.6 \text{ Mg ha}^{-1} \text{ yr}^{-1}$ ), whereas the smallest difference was observed between  $E_{\text{Cs137}}$  and  $E_{\text{ModDirTillEM}}$  ( $-15.2 \text{ Mg ha}^{-1} \text{ yr}^{-1}$ ). A similar pattern was observed for the depression area.

The correlation analyses for erosion estimates showed that  $E_{\text{ModDirTillEM}}$ ,  $E_{\text{RUSLER+ModDirTillEM}}$  were significantly correlated with  $E_{\text{Cs137}}$  (Table 4.9). The r-value of both  $E_{\text{RUSLER}}$  ( $r = 0.19$ ) and  $E_{\text{EphGEE}}$  ( $r = -0.15$ ) was lower than the r-values of  $E_{\text{ModDirTillEM}}$  ( $r = 0.46^{**}$ ) when correlated with  $E_{\text{Cs137}}$ . Overall, the correlations were not strong, and each model explained part of the variance of the total soil erosion. The results suggested that the pattern of tillage erosion was closer to the pattern of total erosion than that of sheet and rill erosion and ephemeral gully erosion. The r-value of  $E_{\text{RUSLER+EphGEE+ModDirTillEM}}$  ( $r = -0.10^{**}$ ), when correlated with  $E_{\text{Cs137}}$ , was less than all three erosion forms because the ephemeral gully erosion ( $r = 0.99^{**}$ ) contributed much more than other erosion forms in  $E_{\text{RUSLER+EphGEE+ModDirTillEM}}$ .

**Table 4.8** The differences ( $\text{Mg ha}^{-1} \text{ yr}^{-1}$ ) between erosion estimates obtained from sampling points for overall and different landform positions for both of the PEI and NB sites ( $H_0$ : difference = 0,  $H_a$ : difference  $\neq$  0)

Site	All landforms	Upslope	Midslope	Lowerslope	Depression
<b>PEI</b>					
n	50	14	21	7	8
$E_{\text{Cs137}} - E_{\text{RUSLER}}$	6.1*	12.5†	7.7†	-19.9*	-11.5
$E_{\text{Cs137}} - E_{\text{EphGEE}}$	-2.9	14.9*	10.1*	-118.6†	-149.1*
$E_{\text{Cs137}} - E_{\text{ModDirTillem}}$	6.8*	1.4	10.7*	-15.2*	-9
$E_{\text{Cs137}} - E_{\text{RUSLER+ModDirTillem}}$	4.9†	-1.1	8.3*	-12.4	-3.7
$E_{\text{Cs137}} - E_{\text{RUSLER+EphGEE+ModDirTillem}}$	-5.9	-1.1	8.3*	-109.6†	-135.3*
<b>NB</b>					
n	67	4	36	22	5
$E_{\text{Cs137}} - E_{\text{RUSLER}}$	2.9	-8.7	8.2**	-13.2**	-30.1
$E_{\text{Cs137}} - E_{\text{EphGEE}}$	4.0	-1.5	20.4**	-46.9†	-149.4
$E_{\text{Cs137}} - E_{\text{ModDirTillem}}$	14.9**	-4.5	18.9**	4.0	-8.3
$E_{\text{Cs137}} - E_{\text{RUSLER+ModDirTillem}}$	2.9	-11.7	6.8*	-7.9†	-20.8
$E_{\text{Cs137}} - E_{\text{RUSLER+EphGEE+ModDirTillem}}$	-8.0	-11.7	6.8*	-54.0*	-153.5

†, \*, \*\* indicate significance levels of 0.10, 0.05 and 0.01, respectively.

For the NB site, based on the  $1448 \text{ Bq m}^{-2}$  reference level, the was averaged of  $10.3 \text{ Mg ha}^{-1} \text{ yr}^{-1}$  with a SD of  $15.8 \text{ Mg ha}^{-1} \text{ yr}^{-1}$ . Overall, 78% of the field area showed soil loss, and 22 % of the area showed soil accumulation (Fig. 4.12.b). The order of soil erosion rate followed as Midslope > Lowerslope > Upslope > Depression. The soil accumulation was observed on the top and the middle section of the catchment (Fig. 4.12.b). Particularly for the middle section of the field, the locations of the soil accumulation were closely associated with the location of the ephemeral gully. The accumulation might be related to channel refilling action conducted

by the farmer. The farmer usually used the topsoil from other locations to refill channels. As a result, the Cs-137 concentration became higher than the original soil.

**Table 4.9** Correlation coefficients for different erosion estimates obtained from all sampling points for both of the PEI and NB sites

Site		$E_{Cs137}$	$E_{RUSLER}$	$E_{EphGEE}$	$E_{ModDirTillem}$
PEI	$E_{RUSLER}$	0.19			
	$E_{EphGEE}$	-0.15	-0.58**		
	$E_{ModDirTillem}$	0.46**	0.33*	-0.25†	
	$E_{RUSLER+ModDirTillem}$	0.44**	0.69**	-0.45**	0.91**
	$E_{RUSLER+EphGEE+ModDirTillem}$	-0.1	-0.51**	0.99**	-0.14
NB	$E_{RUSLER}$	0.21†			
	$E_{EphGEE}$	0.10	0.13		
	$E_{ModDirTillem}$	0.50**	-0.08	-0.19	
	$E_{RUSLER+ModDirTillem}$	0.49**	0.77**	-0.01	0.56**
	$E_{RUSLER+EphGEE+ModDirTillem}$	0.15	0.20	0.99**	-0.13

†, \*, \*\* indicate significance levels of 0.10, 0.05 and 0.01, respectively.

By comparing the  $E_{Cs137}$  with different modeled erosion rates,  $E_{Cs137}$  was not significantly different from rates from all models except for the tillage erosion model (Table 4.8).  $E_{Cs137}$  was significantly greater than  $E_{ModDirTillem}$  ( $P < 0.01$ ), with a difference of  $14.9 \text{ Mg ha}^{-1} \text{ yr}^{-1}$ .

For the upslope area, all differences between  $E_{Cs137}$  and rates derived from other erosion forms were non-significant. The largest difference was observed between  $E_{Cs137}$  and  $E_{RUSLER}$  ( $-8.7 \text{ Mg ha}^{-1} \text{ yr}^{-1}$ ), whereas the smallest difference was observed between  $E_{Cs137}$  and  $E_{EphGEE}$  ( $-1.5 \text{ Mg ha}^{-1} \text{ yr}^{-1}$ ).

For the middle slope area, all differences between  $E_{Cs137}$  and rates derived from other erosion forms were significant ( $P < 0.05$ ). The largest difference was observed between  $E_{Cs137}$  and  $E_{EphGEE}$  ( $20.4 \text{ Mg ha}^{-1} \text{ yr}^{-1}$ ), whereas the smallest difference was observed between  $E_{Cs137}$

and  $E_{\text{RUSLER}}$  ( $8.2 \text{ Mg ha}^{-1} \text{ yr}^{-1}$ ), as expected. By summing the three individual erosion forms, the difference between  $E_{\text{Cs137}}$  and  $E_{\text{RUSLER+EphGEE+ModDirTilIEM}}$  was  $6.8 \text{ Mg ha}^{-1} \text{ yr}^{-1}$ , which was less than all other erosion forms.

For the lower slope area, the largest difference was observed between  $E_{\text{Cs137}}$  and  $E_{\text{EphGEE}}$  ( $-46.9 \text{ Mg ha}^{-1} \text{ yr}^{-1}$ ), whereas the smallest difference was observed between  $E_{\text{Cs137}}$  and  $E_{\text{ModDirTilIEM}}$  ( $4.0 \text{ Mg ha}^{-1} \text{ yr}^{-1}$ ). Similarly, for the depression area, the largest difference was also observed between  $E_{\text{Cs137}}$  and  $E_{\text{EphGEE}}$  ( $-149.4 \text{ Mg ha}^{-1} \text{ yr}^{-1}$ ), whereas the smallest difference was observed between  $E_{\text{Cs137}}$  and  $E_{\text{ModDirTilIEM}}$  ( $-8.3 \text{ Mg ha}^{-1} \text{ yr}^{-1}$ ).

The correlation analyses for erosion estimates showed that  $E_{\text{RUSLER}}$ ,  $E_{\text{ModDirTilIEM}}$ , and  $E_{\text{RUSLER+ModDirTilIEM}}$  were significantly correlated with  $E_{\text{Cs137}}$  (Table 4.9). The r-value of both  $E_{\text{RUSLER}}$  ( $r = 0.21^\dagger$ ) and  $E_{\text{EphGEE}}$  ( $r = 0.10$ ) was lower than the r-values of  $E_{\text{ModDirTilIEM}}$  ( $r = 0.50^{**}$ ) when correlated with  $E_{\text{Cs137}}$ . For the combination, the r-value of  $E_{\text{RUSLER+EphGEE+ModDirTilIEM}}$  ( $r = 0.15$ ), when correlated with  $E_{\text{Cs137}}$ , was less than all three erosion forms except for the ephemeral gully erosion because the ephemeral gully erosion ( $r = 0.99^{**}$ ) contributed much more than other erosion forms in  $E_{\text{RUSLER+EphGEE+ModDirTilIEM}}$ .

## 4.5 Discussion

### 4.5.1 Erosion processes

The erosion processes in cultivated lands can be described by examining the gully area separately from the non-gully area. For the non-gully area, the linkage effect dominates the area. For the upslope, the sheet flow does not have much power to detach soil particles but is

capable of transporting sediment detached by rainfall splash. Therefore, the soil loss in the upslope is relatively low. When tillage erosion occurs on the upslope position due to the convex shape of the slope, soil loss typically occurs. Therefore, for the upslope position, the total soil loss is majorly attributed to tillage erosion. This pattern was observed for the PEI site. The average water erosion rate was about 24% of the average tillage erosion rate in this location. However, this pattern was not observed for the NB site. The water erosion rate was slightly greater than the tillage erosion rate, probably because of the landscape topography or the defects in landform classification.

For the middle slope, the runoff amount and velocity gradually increase in the upslope and reaches the peak. As the amount and velocity of water build up in the middle slope area, flow begins to channelize and cuts into the soil to form rills. The channelized flow is more erosive than the sheet flow. For both sites, the estimated water erosion rates for both sites show the trend of Midslope > Upslope. Regarding tillage erosion, the middle slope position is a transition zone, receiving and transporting a similar amount of the translocated soil. Therefore, there is usually no net soil gain or soil loss. For both sites, the results agreed with this theory that water erosion dominates the form in this area. The interaction effect might occur in this area because of the rill removal action by tillage. The additional soil erosion caused by interaction is already included in the results obtained from the USLE experiments.

In the lower slope and depression areas, where the slope gradient is reduced, the runoff amount and velocity usually reach plateaus, which do not increase. The water erosion shows a similar pattern. It gradually decreases in lower slope areas. Towards the lower end of the lower

slope or in the depression areas, soil accumulation induced by runoff usually occurs as the runoff amount and velocity reach plateaus (Li et al., 2008a). This pattern is observed in the PEI site. Regarding tillage erosion, soil accumulation occurs in the concave area (e.g., depression). Both sites showed a similar pattern as described.

For the gully area, the interaction effect dominates this section. During a large storm event, concentrated runoff occurs, thereby, the ephemeral gully erosion. Although the major tillage operation can refill the gully, preventing the gully developed into a classic gully. Meanwhile, the tillage operation continues to provide a fresh soil source for runoff water to act upon. Therefore, for both sites, ephemeral gully erosion is the largest contributor to total soil erosion. From the tillage erosion perspective, gully mostly tended to play the role of hollow space, leading to a further tillage translocation (Zheng et al., 2021). In other words, when tilling the gully, less translocated soil moved into gullies, and more soil moved to areas surrounding gullies when compared with the tillage erosion without channel effects. After tillage operation, there should be less soil for concentrated runoff to erode. In the long term, the interaction effect could facilitate the concave shape in the gully section, enhancing the generation of concentration flow.

#### **4.5.2 Model performance based on Cs-137**

The use of Cs-137 as a tracer of soil redistribution has proven to be a useful tool worldwide (Zapata, 2002). In this study, the Cs-137 method is the only way to evaluate the performance of the model on the total erosion prediction. The result indicates that, for both sites, the

difference between  $E_{Cs137}$  and  $E_{RUSLER+EphGEE+ModDirTillEM}$  was non-significant statistically, suggesting that the overall estimated total erosion rate is reasonable.

In the non-gully area, theoretically, with the assumption that Cs-137 derived total erosion rate is accurate, for the upslope area, the difference between  $E_{Cs137}$  and  $E_{RUSLER}$ ,  $E_{EphGEE}$ , and  $E_{ModDirTillEM}$  supposed to be all greater than zero, with an order of  $E_{Cs137} - E_{EphGEE} > E_{Cs137} - E_{RUSLER} > E_{Cs137} - E_{ModDirTillEM}$ . The same trend was observed for the PEI site but was not observed for the NB site. For the NB site, the difference between  $E_{Cs137}$  and  $E_{RUSLER}$ ,  $E_{EphGEE}$ , and  $E_{ModDirTillEM}$  were all less than zero, probably because the farmers dig and haul the surface topsoil from somewhere else and fill them on the upslope area. As a result, soil accumulation was observed in the upslope area. Thereby,  $E_{Cs137}$  was a negative value, which was less than the soil erosion rate (positive value).

For the middle slope area, similar to the upslope area, the difference between  $E_{Cs137}$  and  $E_{RUSLER}$ ,  $E_{EphGEE}$ , and  $E_{ModDirTillEM}$  supposes to be all greater than zero. The order follows as  $E_{Cs137} - E_{EphGEE} \approx E_{Cs137} - E_{ModDirTillEM} > E_{Cs137} - E_{RUSLER}$ . In addition,  $E_{Cs137} - E_{RUSLER}$  should be close to zero since sheet & rill erosion is the dominant erosion process in the middle slope area. For both sites, the same trend was observed. However, the  $E_{Cs137} - E_{RUSLER}$  was significantly greater than zero, probably suggesting that the water erosion was under-estimated using RUSLER at the midslope areas.

For both lower slope and depression areas, the difference should follow the order of  $E_{Cs137} - E_{EphGEE} < E_{Cs137} - E_{RUSLER} < \text{or } \approx E_{Cs137} - E_{ModDirTillEM}$ . In addition,  $E_{Cs137}$  supposes to be greater than zero. For both sites, the trend was observed. However, the differences between  $E_{Cs137}$  and

the erosion rate estimated from different models were mostly less than zero, probably suggesting that there was an underestimation of the water erosion using RUSLER.

For the gully area,  $E_{Cs137} - E_{EphGEE}$  was mostly greater than  $100 \text{ Mg ha}^{-1} \text{ yr}^{-1}$ . This could be due to the dynamic ephemeral gully erosion process. In this study, the sampling points were designed based on the landform positions. For each transect, one sampling point was assigned to each landform position. In addition, each transect is about 20 m away from the other, depending on the field size. Ephemeral gullies generally occur in the lower slope and depression areas. Thus, for each transect, only two sampling points might have a chance to capture the gully erosion process. The location of the gully is not exactly the same from event to event due to the magnitude of the storm event, micro-topography and so on (Lentz et al., 1993). The selection of the sampling points in the gully area needs to be cautious. It could be difficult to capture the long-term history of ephemeral gully erosion due to the dynamic erosion processes. Therefore, the current soil sampling plan needs to be improved. The denser layout of soil sampling points might be necessary in order to capture the long-term spatial variation of ephemeral gully erosion. The 10-m buffer zone can be established for the gully area, including all the areas that might be affected by the interactions. Within the buffer zone, ten sampling samples (about 0.5 m intervals) should be taken from the top of the buffer zone towards the centre of the gully. The density of the transect depends on the total length of the gully, but they are typically 10 to 20 m away from each other. Other than the spatial resolution, the temporal resolution could be finer as well. To better assess the ephemeral gully erosion, the timing of the soil sampling should be before the primary tillage operation to avoid disturbance.

In addition, after the tillage operation, another set of soil samples should be taken to estimate the interaction effect. With these improvements, the Cs-137 data might be able to provide a more reasonable estimation for ephemeral gully erosion. However, the cost of this soil sampling strategy is noticeable, which could be extremely high. On the other hand, the large difference of  $E_{Cs137} - E_{EphGEE}$  could be attributed to the low resolution and accuracy of the model input data. In this study, the resolution of the input DEM was 5 m, which is much wider than most of the ephemeral gully observed in fields. Therefore, a denser resolution could facilitate the accuracy of the model.

There is another possibility that the selection of the Cs-137 reference level can disturb the final total erosion estimation, thereby, the validation process. However, this is not the case for this study. For the PEI site, the possible reference level ranged from 1789 Bq m<sup>-2</sup> to 1965 Bq m<sup>-2</sup>. With these two extreme levels, the difference between  $E_{Cs137}$  and  $E_{RUSLER+EphGEE+ModDirTillEM}$  at each sampling point held a similar pattern. For erosion points,  $E_{Cs137}$  was consistently greater than  $E_{RUSLER+EphGEE+ModDirTillEM}$  under all scenarios, whereas for accumulation points,  $E_{Cs137}$  was consistently lower than  $E_{RUSLER+EphGEE+ModDirTillEM}$ . Similar to the PEI site, a similar pattern was observed for the NB site. Overall,  $E_{Cs137} - E_{RUSLER+EphGEE+ModDirTillEM}$  holds the same pattern with different Cs-137 reference levels.

#### **4.5.3 Model performance based on other validation methods**

In this study, other validation methods can be used to evaluate the performance of the model on the single erosion prediction. To validate the result derived from ephemeral gully erosion models, the appropriate way is to monitor ephemeral gully development, which is to

quantify the change in gully morphology. The traditional and simple approaches (measuring tape, ruler, profile meter) require additional interpolation since the measurements are spatially discontinuous (Capra et al., 2009; Casalí et al., 2006; Castillo et al., 2012; Di Stefano and Ferro, 2011). The well-documented end area method (EAM) is needed to estimate the gully volume (Capra and La Spada, 2015). These methods are unable to represent the entire volume of a gully. The total station survey and ground-based light detection and ranging (LiDAR) scanner survey are able to overcome this shortcoming (Castillo et al., 2012). However, these methods are both time- and cost-consuming. The newly developed technique – photogrammetry has been utilized widely in erosion studies due to its high resolution with relatively low time and cost consumption (Carollo et al., 2015; Castillo et al., 2018; Ciprian Margarint et al., 2019; d'Oleire-Oltmanns et al., 2012). The photogrammetry has been proved to be a reliable tool to reconstruct the surface geometry (Zheng et al., 2020). Therefore, theoretically, the photogrammetry-derived volume should perform better than the manual measurement-estimated volume. In this study, the error of the NB site (19%) was greater than that of the PEI site (8%), which could be associated with the tillage management in the fields. For the NB site, the field was under strip rotation (potato-grain). Hence the field was divided into two sections with a different crop. The section cropped with grain was actually covered with canopy, which caused difficulties for photogrammetry to correctly reconstruct the surface geometry. Whereas for the PEI site, the whole field was under one crop management. Therefore, the tillage management might be one major source of error in the photo interpretation procedure.

The water samples collected at the outlet of fields were designed to validate the sediment estimated from water erosion models (Williams et al., 2016). In this study, the water station was set up at the outlet of the field based on the DEM. However, the DEM was generated about ten to fifteen years ago using LIDAR. With continuous tillage operations and water erosion events, the topography near the outlet had been altered. As a result, waterways were changed. The newly developed waterway delivered mostly runoff water from the field. Therefore, much less runoff water flows through the water gauging station. For an example of the PEI site, no water data was collected from the outlet station. It is better to build the manmade ridge on the field boundary to force the runoff water flowing through the flume. In addition, the model estimated runoff event is based on the long-term (i.e., 20-year) climate data. However, the water station installed in the field only collects short-term data (i.e., 1 to 2-year runoff data). Therefore, the short-term data is unable to represent the climate pattern properly. To better validate the results derived from models, the long-term monitor would be necessary, or the input climate data for the model should be as same as the monitoring period.

#### **4.5.4 Further studies**

From the aspect of model development, particularly for ModDirTilLEM, many improvements can be expected. Firstly, for ModDirTilLEM, the tillage operation has to follow horizontal or vertical directions. The diagonal tillage cannot be operated in the model. Therefore, for the cultivated field, which is not along the true north or east direction, another set of grid points needs to be generated to line up with the field direction. The incorporation of diagonal tillage into the model can help the user to utilize the original DEM (e.g., 5-m

resolution) other than generating the new set of grid points along the field. Secondly, the data used for the interaction component was based on Zheng et al.'s (2021) research. For this research, the single primary implement (chisel) was utilized. Therefore, the interaction component is closely associated with the chisel plough. The design of another primary tillage – mouldboard plough is different from that of a chisel plough. For chisel plough, it breaks up the surface layer of soil, whereas, for mouldboard plough flips the surface soil over and brings up the soil from a deeper layer (Johnson and Moldenhauer, 1979). With respect to erosion, a chisel plough causes less soil erosion when compared to a mouldboard plough. Therefore, different tillage implements could have different impacts on the channel infilling process. Thirdly, the impact of the channel on tillage translocation was not fully tested. For example, for contour tillage, the experiment was only conducted when the tillage direction was perpendicular to the channel direction. However, in reality, the tillage might hit the channel with an angle (e.g., 30 degrees). Therefore, additional data are necessary to fill the knowledge gap. Lastly, for modeling purposes in this study, the cross-section size of the channel was assumed to be 20 cm by 20 cm along the channel. The channel size varied along the channel, which can be estimated using EphGEE. Accounting for the channel size variation, the more sophisticated ModDirTilLEM, considering the complexity of the channel can be developed.

#### **4.6 Conclusion**

Water and tillage erosion has been recognized as the major erosion forms deteriorating the soil in cultivated fields. This chapter is the first one to combine all models of erosion forms that occurred on the cultivated field to estimate total soil erosion. This study uses a 2-

dimensional version of RUSLE2, which is called RUSLER and a newly developed ephemeral gully erosion model (EphGEE), and a modified directional tillage erosion model (DirTilLEM), with an additional component accounting for the interaction effect between water (ephemeral gully) and tillage erosion. These tools rely on 1) detailed topographic elevation data, 2) databases in RUSLE2, 3) runoff, sediment yield, Manning roughness coefficients estimated from RUSLE2, 4) channel critical shear stress and erodibility varying with clay content and time since tillage, 5) tillage management information and 6) detailed tillage implement information. The modeled results indicated that the individual models provide reasonable estimation for the individual erosion processes. For both the PEI and NB sites, the pattern of tillage erosion was better associated with total erosion than water erosion, except for the gully area. For the gully area, the ephemeral gully erosion dominates. The integrated tillage and water erosion models improved the accuracy of the estimation for total soil erosion to some extent. However, the interaction effects (which occurred in the gully area) were difficult to be validated using the current Cs-137 method. Further testing and development of the model for the dynamic erosion process simulation and better validation methods are necessary to improve the performance of models and to approximate observation over a broader range of climate, soil, landscape, and tillage managements in other areas in Canada.

#### **4.7 Acknowledgements**

This study was funded by the Agriculture and Agri-food Canada project "Characterizing and modeling the interactions between water and tillage erosion under potato and cereal production systems" [project number J-000994] (PI: Li) and project "Sustainability measures

to monitor and analyze the environmental impact of Canadian agriculture" [project number J-002316] (PI: McConkey and McDonald) as well as a Canadian Natural Science and Engineering Research Council Discovery Grant (PI: Lobb). The authors would like to thank Dr. Zhisheng Xing, Dr. Yulia Kupriyanovich, Dr. Yefang Jiang and Dr. Dalmo Vieira for their insightful suggestions for the experiment, and Brian Murray, Kang Liang, and Sylvie Lavoie for helping with the field work. We are also grateful to the crew in the farm services unit of the Charlottetown Research and Development Centre for managing the field and conducting the tillage operations.

#### **4.8 References**

- Ahmed, M., Asif, M., Hirani, A.H., Akram, M.N., Goyal, A., 2013. Modeling for agricultural sustainability: a review. Elsevier London.
- Aufrère, L., 1929. Les rideaux: étude topographique, 216 ed. JSTOR, pp. 529-560.
- Bingner, R.L., Theurer, F.D., Yuan, Y., 2003. AnnAGNPS technical processes. USDA-ARS, Washington, D.C.
- Brady, N.C., Weil, R.R., 2016. The nature and properties of soils, 15 ed. Pearson, Columbus, Ohio.
- Capra, A., La Spada, C., 2015. Medium-term evolution of some ephemeral gullies in Sicily (Italy). *Soil Tillage Res.* 154, 34-43. <https://doi.org/10.1016/j.still.2015.07.001>.
- Capra, A., Mazzara, L.M., Scicolone, B., 2005. Application of the EGEM model to predict ephemeral gully erosion in Sicily, Italy. *CATENA* 59, 133-146. <https://doi.org/10.1016/j.catena.2004.07.001>.

- Capra, A., Porto, P., Scicolone, B., 2009. Relationships between rainfall characteristics and ephemeral gully erosion in a cultivated catchment in Sicily (Italy). *Soil Tillage Res.* 105, 77-87. <https://doi.org/10.1016/j.still.2009.05.009>.
- Carollo, F.G., Di Stefano, C., Ferro, V., Pampalone, V., 2015. Measuring rill erosion at plot scale by a drone-based technology. *Hydrol. Processes* 29, 3802-3811. <https://doi.org/10.1002/hyp.10479>.
- Casalí, J., Loizu, J., Campo, M.A., De Santisteban, L.M., Álvarez-Mozos, J., 2006. Accuracy of methods for field assessment of rill and ephemeral gully erosion. *CATENA* 67, 128-138. <https://doi.org/10.1016/j.catena.2006.03.005>.
- Castillo, C., Marín-Moreno, V.J., Pérez, R., Muñoz-Salinas, R., Taguas, E.V., 2018. Accurate automated assessment of gully cross-section geometry using the photogrammetric interface FreeXSapp. *Earth Surf. Process. Landf.* 43, 1726-1736. <https://doi.org/10.1002/esp.4341>.
- Castillo, C., Pérez, R., James, M.R., Quinton, J.N., Taguas, E.V., Gómez, J.A., 2012. Comparing the accuracy of several field methods for measuring gully erosion. *Soil Science Society of America Journal* 76, 1319-1332. <https://doi.org/10.2136/sssaj2011.0390>.
- Chepil, W.S., Siddoway, F.H., Armbrust, D.V., 1962. Climatic factor for estimating wind erodibility of farm fields. *J. Soil Water Conserv.*
- Chow, T.L., Rees, H.W., Daigle, J.L., 1999. Effectiveness of terraces/grassed waterway systems for soil and water conservation: A field evaluation. *J. Soil Water Conserv.* 54, 577-583.

- Ciprian Margarint, M., Niculita, M., Tarolli, P., 2019. Using UAV and LIDAR data for gullies erosion monitoring, EGU General Assembly, Vienna, Austria, p. 8461.
- d'Oleire-Oltmanns, S., Marzloff, I., Peter, K.D., Ries, J.B., 2012. Unmanned Aerial Vehicle (UAV) for monitoring soil erosion in Morocco. *Remote Sens.* 4, 3390-3416. <https://doi.org/10.3390/rs4113390>.
- Dabney, S.M., Vieira, D.A.N., Yoder, D.C., Langendoen, E.J., Wells, R.R., Ursic, M.E., 2015. Spatially distributed sheet, rill, and ephemeral gully erosion. *J. Hydrol. Eng.* 20, C4014009. [https://doi.org/10.1061/\(ASCE\)HE.1943-5584.0001120](https://doi.org/10.1061/(ASCE)HE.1943-5584.0001120).
- Dai, J., Zhang, J., Zhang, Z., Jia, L., Xu, H., Wang, Y., 2020. Effects of water discharge rate and slope gradient on runoff and sediment yield related to tillage erosion. *Archives of Agronomy and Soil Science*, 1-13. <https://doi.org/10.1080/03650340.2020.1766676>.
- De Alba, S., 2003. Simulating long-term soil redistribution generated by different patterns of mouldboard ploughing in landscapes of complex topography. *Soil Tillage Res.* 71, 71-86. [https://doi.org/10.1016/S0167-1987\(03\)00042-4](https://doi.org/10.1016/S0167-1987(03)00042-4).
- Di Stefano, C., Ferro, V., 2011. Measurements of rill and gully erosion in Sicily. *Hydrol. Processes* 25, 2221-2227. <https://doi.org/10.1002/hyp.7977>.
- Erpul, G., Norton, L.D., Gabriels, D., 2002. Raindrop-induced and wind-driven soil particle transport. *CATENA* 47, 227-243. [https://doi.org/10.1016/S0341-8162\(01\)00182-5](https://doi.org/10.1016/S0341-8162(01)00182-5).
- Flanagan, D.C., Nearing, M.A., 1995. USDA-Water Erosion Prediction Project: Hillslope profile and watershed model documentation. Nserl Rep 10, 1-123.

- Gómez, J.A., Nearing, M.A., 2005. Runoff and sediment losses from rough and smooth soil surfaces in a laboratory experiment. *CATENA* 59, 253-266. <https://doi.org/10.1016/j.catena.2004.09.008>.
- Gordon, L.M., Bennett, S.J., Bingner, R.L., Theurer, F.D., Alonso, C.V., 2007. Simulating ephemeral gully erosion in AnnAGNPS. *Transactions of the ASABE* 50, 857-866. <https://doi.org/10.13031/2013.23150>.
- Govers, G., Vandaele, K., Desmet, P., Poesen, J., Bunte, K., 1994. The role of tillage in soil redistribution on hillslopes. *Eur. J. Soil Sci.* 45, 469-478. <https://doi.org/10.1111/j.1365-2389.1994.tb00532.x>.
- Hevia, G.G., Buschiazzo, D.E., Hepper, E.N., Urioste, A.M., Antón, E.L., 2003. Organic matter in size fractions of soils of the semiarid Argentina. Effects of climate, soil texture and management. *Geoderma* 116, 265-277. [https://doi.org/10.1016/S0016-7061\(03\)00104-6](https://doi.org/10.1016/S0016-7061(03)00104-6).
- Johnson, C.B., Moldenhauer, W.C., 1979. Effect of chisel versus moldboard plowing on soil erosion by water. *Soil Science Society of America Journal* 43, 177-179. <https://doi.org/10.2136/sssaj1979.03615995004300010034x>.
- Kachanoski, R.G., Carter, M.R., 1999. Landscape position and soil redistribution under three soil types and land use practices in Prince Edward Island. *Soil Tillage Res.* 51, 211-217. [https://doi.org/10.1016/S0167-1987\(99\)00038-0](https://doi.org/10.1016/S0167-1987(99)00038-0).
- Knisel, W.G., Foster, G.R., 1981. CREAMS [Chemicals, runoff, and erosion from agricultural management systems]: a system for evaluating best management practices [Mathematical models, pollution].

- Knisel, W.G., 1980. CREAMS: A field scale model for chemicals, runoff, and erosion from agricultural management systems. Department of Agriculture, Science and Education Administration.
- Lal, R., 2001. Soil degradation by erosion. *Land Degrad. Dev.* 12, 519-539. <https://doi.org/10.1002/ldr.472>.
- Lentz, R.D., Dowdy, R.H., Rust, R.H., 1993. Soil property patterns and topographic parameters associated with ephemeral gully erosion. *J. Soil Water Conserv.* 48, 354-361.
- Li, S., Lobb, D.A., Lindstrom, M.J., Farenhorst, A., 2008a. Patterns of water and tillage erosion on topographically complex landscapes in the North American Great Plains. *J. Soil Water Conserv.* 63, 37-46. <https://doi.org/10.2489/jswc.63.1.37>.
- Li, S., Lobb, D.A., Lindstrom, M.J., 2007a. Tillage translocation and tillage erosion in cereal-based production in Manitoba, Canada. *Soil Tillage Res.* 94, 164-182. <https://doi.org/10.1016/j.still.2006.07.019>.
- Li, S., Lobb, D.A., Lindstrom, M.J., Farenhorst, A., 2007b. Tillage and water erosion on different landscapes in the northern North American Great Plains evaluated using <sup>137</sup>Cs technique and soil erosion models. *CATENA* 70, 493-505. <https://doi.org/10.1016/j.catena.2006.12.003>.
- Li, S., Lobb, D.A., Lindstrom, M.J., Papiernik, S.K., Farenhorst, A., 2008b. Modeling tillage-induced redistribution of soil mass and its constituents within different landscapes. *Soil Science Society of America Journal* 72, 167-179. <https://doi.org/10.2136/sssaj2006.0418>.

- Li, S., Lobb, D.A., Tiessen, K.H.D., 2009. Modeling tillage-induced morphological features in cultivated landscapes. *Soil Tillage Res.* 103, 33-45. <https://doi.org/10.1016/j.still.2008.09.005>.
- Lindstrom, M.J., Schumacher, J.A., Schumacher, T.E., 2000. TEP: A tillage erosion prediction model to calculate soil translocation rates from tillage. *J. Soil Water Conserv.* 55, 105-108.
- Lobb, D.A., Kachanoski, R.G., Miller, M.H., 1995. Tillage translocation and tillage erosion on shoulder slope landscape positions measured using <sup>137</sup>Cs as a tracer. *Can. J. Soil Sci.* 75, 211-218. <https://doi.org/10.4141/cjss95-029>.
- Lobb, D.A., Lindstrom, M.J., Schumacher, T.E., 2003. Soil erosion processes and their interactions: implications for environmental indicators, *Agricultural Impacts on Soil Erosion and Soil Biodiversity: Developing Indicators for Policy Analysis. Proceedings from an OECD Expert Meeting—Rome, Italy, March*, pp. 325-336.
- MacMillan, R.A., Martin, T.C., Earle, T.J., McNabb, D.H., 2003. Automated analysis and classification of landforms using high-resolution digital elevation data: applications and issues. *CaJRS* 29, 592-606. <https://doi.org/10.5589/m03-031>.
- McConkey, B.G., Lobb, D.A., Li, S., Black, J.M.W., Krug, P.M., 2010. Soil erosion on cropland: introduction and trends for Canada. *Canadian Biodiversity: Ecosystem Status and Trends*.
- Mech, S.J., Free, G.R., 1942. Movement of soil during tillage operations. *Agric. Eng.* 23, 379-382.

- Merritt, W.S., Letcher, R.A., Jakeman, A.J., 2003. A review of erosion and sediment transport models. *Environ. Model. Software* 18, 761-799. [https://doi.org/10.1016/S1364-8152\(03\)00078-1](https://doi.org/10.1016/S1364-8152(03)00078-1).
- Morgan, R.P.C., 2009. *Soil erosion and conservation*, 3rd ed. John Wiley & Sons.
- Nachtergaele, J., Poesen, J., Steegen, A., Takken, I., Beuselinck, L., Vandekerckhove, L., Govers, G., 2001. The value of a physically based model versus an empirical approach in the prediction of ephemeral gully erosion for loess-derived soils. *Geomorphology* 40, 237-252. [https://doi.org/10.1016/S0169-555X\(01\)00046-0](https://doi.org/10.1016/S0169-555X(01)00046-0).
- O'Callaghan, J.F., Mark, D.M., 1984. The extraction of drainage networks from digital elevation data. *Comput. Gr. Image Process.* 28, 323-344.
- Pedersen, H.S., Hasholt, B., 1995. Influence of wind speed on rainsplash erosion. *CATENA* 24, 39-54. [https://doi.org/10.1016/0341-8162\(94\)00024-9](https://doi.org/10.1016/0341-8162(94)00024-9).
- Poesen, J.W., Nachtergaele, J., Verstraeten, G., Valentin, C., 2003. Gully erosion and environmental change: importance and research needs. *CATENA* 50, 91-133. [https://doi.org/10.1016/S0341-8162\(02\)00143-1](https://doi.org/10.1016/S0341-8162(02)00143-1).
- Renard, K.G., 1997. *Predicting soil erosion by water: a guide to conservation planning with the Revised Universal Soil Loss Equation (RUSLE)*. United States Government Printing.
- Römkens, M.J.M., Helming, K., Prasad, S.N., 2002. Soil erosion under different rainfall intensities, surface roughness, and soil water regimes. *CATENA* 46, 103-123. [https://doi.org/10.1016/S0341-8162\(01\)00161-8](https://doi.org/10.1016/S0341-8162(01)00161-8).

- Schnepf, M., Cox, C., 2006. Environmental benefits of conservation on cropland: the status of our knowledge. Soil and Water Conservation Society. Ankeny, Iowa, USA.
- Six, J., Paustian, K., Elliott, E.T., Combrink, C., 2000. Soil structure and organic matter I. Distribution of aggregate-size classes and aggregate-associated carbon. Soil Sci. Soc. Am. J. 64, 681-689. <https://doi.org/10.2136/sssaj2000.642681x>.
- Song, Y., Yan, P., Liu, L., 2006. A review of the research on complex erosion by wind and water. J. Geogr. Sci. 16, 231-241. <https://doi.org/10.1007/s11442-006-0212-1>.
- Sutherland, R.A., 1996. Caesium-137 soil sampling and inventory variability in reference locations: A literature survey. Hydrol. Processes 10, 43-53. [https://doi.org/10.1002/\(SICI\)1099-1085\(199601\)10:1<43::AID-HYP298>3.0.CO;2-X](https://doi.org/10.1002/(SICI)1099-1085(199601)10:1<43::AID-HYP298>3.0.CO;2-X).
- Team, R.C., 2013. R: A language and environment for statistical computing.
- Tiessen, K.H.D., Li, S., Lobb, D.A., Mehuys, G.R., Rees, H.W., Chow, T.L., 2009. Using repeated measurements of <sup>137</sup>Cs and modeling to identify spatial patterns of tillage and water erosion within potato production in Atlantic Canada. Geoderma 153, 104-118. <https://doi.org/10.1016/j.geoderma.2009.07.013>.
- Tiessen, K.H.D, Lobb, D.A., Mehuys, G.R., Rees, H.W., 2007a. Tillage translocation and tillage erosivity by planting, hilling and harvesting operations common to potato production in Atlantic Canada. Soil Tillage Res. 97, 123-139. <https://doi.org/10.1016/j.still.2007.09.005>.

- Tiessen, K.H.D., Lobb, D.A., Mehuys, G.R., Rees, H.W., 2007b. Tillage erosion within potato production in Atlantic Canada: II Erosivity of primary and secondary tillage operations. *Soil Tillage Res.* 95, 320-331. <https://doi.org/10.1016/j.still.2007.02.009>.
- Tiessen, K.H.D., Mehuys, G.R., Lobb, D.A., Rees, H.W., 2007c. Tillage erosion within potato production systems in Atlantic Canada: I. Measurement of tillage translocation by implements used in seedbed preparation. *Soil Tillage Res.* 95, 308-319. <https://doi.org/10.1016/j.still.2007.02.003>.
- USDA-NRCS, 1997. *America's Private Land, A Geography of Hope*. USDA-NRCS, Washington, DC.
- Van Oost, K., Govers, G., De Alba, S., Quine, T.A., 2006. Tillage erosion: a review of controlling factors and implications for soil quality. *Prog Phys Geogr: Earth and Environment* 30, 443-466. <https://doi.org/10.1191/0309133306pp487ra>.
- Van Oost, K., Govers, G., Desmet, P., 2000. Evaluating the effects of changes in landscape structure on soil erosion by water and tillage. *Landscape Ecol.* 15, 577-589. <https://doi.org/10.1023/A:1008198215674>.
- VandenBygaart, A.J., Kroetsch, D., Gregorich, E.G., Lobb, D.A., 2012. Soil C erosion and burial in cropland. *Global Change Biol.* 18, 1441-1452.
- Walling, D.E., He, Q., 1999. Improved models for estimating soil erosion rates from cesium-137 measurements. Wiley Online Library. <https://doi.org/10.2134/jeq1999.00472425002800020027x>.

- Wang, Y., Zhang, J.H., Zhang, Z.H., Jia, L.Z., 2016. Impact of tillage erosion on water erosion in a hilly landscape. *Sci. Total Environ.* 551-552, 522-532. <https://doi.org/10.1016/j.scitotenv.2016.02.045>.
- Williams, M.R., King, K.W., Ford, W., Fausey, N.R., 2016. Edge-of-field research to quantify the impacts of agricultural practices on water quality in Ohio. *J. Soil Water Conserv.* 71, 9A-12A. <https://doi.org/10.2489/jswc.71.1.9A>.
- Wischmeier, W.H., Smith, D.D., 1965. Predicting rainfall-erosion losses from cropland east of the Rocky Mountains. Guide for selection of practices for soil and water conservation (No. 282). Agricultural Research Service, US Department of Agriculture.
- Wischmeier, W.H., Smith, D.D., 1978. Predicting rainfall erosion losses: a guide to conservation planning. Department of Agriculture, Science and Education Administration.
- Woodward, D.E., 1999. Method to predict cropland ephemeral gully erosion. *CATENA* 37, 393-399. [https://doi.org/10.1016/S0341-8162\(99\)00028-4](https://doi.org/10.1016/S0341-8162(99)00028-4).
- Zapata, F., 2002. Handbook for the assessment of soil erosion and sedimentation using environmental radionuclides. Springer.
- Zhang, J.H., Wang, Y., Zhang, Z.H., 2014. Effect of terrace forms on water and tillage erosion on a hilly landscape in the Yangtze River Basin, China. *Geomorphology* 216, 114-124. <https://doi.org/10.1016/j.geomorph.2014.03.030>.
- Zhao, H.L., Yi, X.Y., Zhou, R.L., Zhao, X.Y., Zhang, T.H., Drake, S., 2006. Wind erosion and sand accumulation effects on soil properties in Horqin Sandy Farmland, Inner Mongolia. *CATENA* 65, 71-79. <https://doi.org/10.1016/j.catena.2005.10.001>.

Zheng, F., Lobb, D.A., Li, S., 2021. A plot study on the effects of water eroded channels on tillage translocation. *Soil Tillage Res.* 213, 105118. <https://doi.org/10.1016/j.still.2021.105118>.

Zheng, F., Wackrow, R., Meng, F.R., Lobb, D.A., Li, S., 2020. Assessing the Accuracy and Feasibility of Using Close-Range Photogrammetry to Measure Channelized Erosion with a Consumer-Grade Camera. *Remote Sens.* 12, 1706. <https://doi.org/10.3390/rs12111706>.

Zobeck, T.M., 1991. Soil properties affecting wind erosion. *J. Soil Water Conserv.* 46, 112-118.

#### 4.9 Nomenclature

CAF	channel adjusting function
CV	coefficient variation
DEM	digital elevation model
DirTilLEM	directional tillage erosion model
DR	distance ratio
$E_{Cs137}$	soil erosion estimated from Cs-137 data
$E_{EphGEE}$	soil erosion estimated from EphGEE model
$E_{ModDirTilLEM}$	soil erosion estimated from ModDirTilLEM model
EphGEE	ephemeral gully erosion estimator
$E_{RUSLER}$	soil erosion estimated from RUSLER model
$E_{RUSLER+EphGEE+ModDirTilLEM}$	total soil erosion estimated from the combination of RUSLER, EphGEE and ModDirTilLEM models
$E_{RUSLER+ModDirTilLEM}$	soil erosion estimated from the combination of RUSLER and ModDirTilLEM models
ModDirTilLEM	modified directional tillage erosion model
MR	mass ratio
NB	New Brunswick

PEI	Prince Edward Island
RUSLER	revised universal soil loss equation, version 2 – raster based
SD	standard deviation

## **5. GENERAL CONCLUSIONS**

### **5.1 The context of the research**

Different aspects of the interaction effects between water erosion and tillage erosion were examined in this study: from the effects of the gully on tillage translocation to the effect of channel refilling by tillage on the following water erosion event. The field experiments provided quantitative data for the interaction effects between water and tillage erosion. These data were used to check and upgrade the current tillage erosion and ephemeral gully erosion models, so that the modeling can take into account those aspects of water and tillage erosion interactions examined in the experiments. The upgraded tillage erosion model, coupled with water erosion models, was used to estimate total erosion in two field sites. The total erosion estimates, determined using the Cs-137 method, were used to validate the integrated erosion estimates of water erosion, tillage erosion, and their interactions.

### **5.2 Major findings**

According to the results of the first study, the presence of channels reduced tillage translocation during downslope tillage but increased tillage translocation during upslope tillage. Substantial channel infilling with translocated soil occurred for both downslope and upslope tillage. The soil falling into the channels was mainly from the surface layer for both downslope and upslope tillage, but for downslope tillage, it was mainly from the area away from the channel, whereas for upslope tillage, it was mainly from the area adjacent to the channel. For

contour tillage, the presence of channels increased tillage translocation. The channel was oriented perpendicular to the tillage direction so that tillage was more effective in filling the channel.

The patterns of tillage translocation under different treatments are likely attributed to the relative importance of the trapping effect (channel functions like a trap) versus the energy-intensity-increase effect (greater energy intensity due to less soil being moved with the presence of a channel). If the trapping effect dominates, the overall soil movement, especially forward soil movement, tends to decrease, whereas if the energy-intensity-increase effect dominates, the overall soil movement tends to increase. The relative importance of the trapping effect and the energy-intensity-increase effect is determined by the shape and size of the tillage tool's zone of influence (ZoI). The presence of a channel, its location and orientation relative to the tillage tool, and the tillage direction can all affect the shape and size of the ZoI.

A critical time for channel generation is the period between growing seasons when fields are bare. Farmers usually till fields to effectively eliminate these channels. Both channel, tillage and their combination can affect the subsequent water erosion event. According to the results of the second study, firstly, runoff initiation was accelerated with an existing channel, and runoff discharge and sediment export were increased. Secondly, with a single tillage pass, runoff initiation was delayed, and runoff discharge and sediment export were decreased. Thirdly, when an existing channel was tilled, the effects of tillage dominated so that runoff initiation was delayed and runoff discharge and sediment export are decreased.

The findings of the first two data chapters provided solid evidence that interaction effects between water and tillage erosion can affect the total erosion rates around the channel area in cultivated fields. The knowledge gained from these two chapters can be used to couple tillage and water erosion models, providing more realistic and accurate predictions of tillage erosion and the overall soil erosion on agricultural lands.

In the third study, all erosion processes and the interaction effects between the water-eroded channel and tillage erosion processes were integrated in a modeling framework that uses the same set of topographical, climatic and management data. The model predicted total erosion was validated against total erosion estimated with the Cs-137 measurements. For the non-gully area, the individual models (RUSLER and ModDirTilLEM) provide reasonable estimations for the individual erosion processes (sheet and rill, tillage erosion). Simple addition of the tillage and water erosion models improved the accuracy of the predicted total soil erosion. For the PEI and NB sites, the pattern of total erosion was associated greater with tillage erosion than water erosion, suggesting the strong contribution of tillage erosion towards total erosion. For the gully area, the errors and uncertainties are very high. The interaction effects, modeled in the ModDirTilLEM and EphGEE, were difficult to validate using the current Cs-137 method. This could be due to the dynamic erosion processes in these areas or the low resolution and accuracy of the model input data. In either case, for the total erosion modeling, the gully area is a weak point, and there is an urgent need to integrate water and tillage erosion models at the process level to simulate the dynamic nature of soil redistribution in the gully areas. Based on

the current estimation in the gully area, we could observe a pattern of more soil loss in the gully while more soil accumulation around the boundary of the gully.

### **5.3 Implications for soil and water conservation**

The basic reason for farmers to eliminate water-eroded channels is to control further water erosion and prevent small channels from developing into larger channels, and, ultimately, gullies. Contour tillage is a widely used conservation practice. Chapter 2 confirms that contour tillage can create a smoother surface and fill the water-eroded channel better than downslope and upslope tillage practices. Therefore, we recommend contour tillage for primary tillage (two-way tillage equipment used in this study) when one of the objectives is filling channels.

In Chapter 3, the results suggest that refilling water-eroded channels can reduce water erosion in the short-term. This observation provides a possible tillage management adjustment for the cereal-potato rotation in Atlantic Canada to reduce the risk of water erosion. After the cereal crop, we recommend spring primary tillage over fall primary tillage. There is usually plenty of crop residue left in the field after harvesting. The residue could provide good ground protection from channelized erosion. This protection can last until the primary tillage in the next spring. Even if the channelized erosion occurs after snow melting, the channels can be erased quickly by spring primary tillage. After the potato crop, we recommend primary tillage late in the fall. Residue cover after potato harvesting is poor so the field is not well protected from channelized erosion. Therefore, there is a great chance that channels will be generated in the fall. If channels are not erased, they may develop into gullies later in the fall, causing great soil loss due to gully erosion.

In Chapter 4, for the non-gully area of both sites, the pattern of total erosion was associated with tillage erosion more so than water erosion. Both sites were located in Atlantic Canada, which has a humid coastal climate and rolling landscapes, and high soil disturbance associated with potato cropping. Therefore, conservation measures targeting tillage erosion could have greater impact in reducing total erosion for the non-gully area in potato fields. Soil-landscape restoration could be a useful conservation measure to enhance soil quality in areas subject to tillage erosion. In this practice, the soil is moved from where it accumulates by tillage erosion to where soil is lost by tillage, creating an opportunity for soil quality restoration. For the gully area, the current Cs-137 validation method is not suitable. The density of the sampling points in the gully area (i.e., 1 point per transect) was insufficient to capture the dynamic erosion process occurring in the gully area. Therefore, it was hard to validate the model predicted erosion rates in this area. However, according to our results, the soil loss caused by ephemeral gully erosion was significant. Therefore, it is necessary to apply some conservation practices to reduce gully erosion. For example, grassed waterways, terraces, cover crops, and no-till are proven measures to control gully erosion that could be used.

In the context of sloped fields, the spatial variability of soil is significantly influenced by tillage practices, both in the short-term and the long-term. In the short-term, the immediate consequences of tillage operations, such as plowing, harrowing, or cultivating, trigger alterations in soil distribution. Topsoil is removed from the knolls and accumulating in the depressions. In the medium-term, tillage erosion can escalate to the point of completely removing topsoil from knolls. Simultaneously, depressions accumulate thick layers of topsoil

due to soil build-up. Since the tillage erosion process does not degrade the soil accumulated at depression areas, this soil redistribution can lead to pronounced yield disparities across the landscape. While the soil displaced from hilltops due to tillage erosion doesn't exit the field, it accumulates in the lower portions (depressions). However, these depressions happen to be the focal points of intense ephemeral gully erosion. Consequently, tillage operation supplies the topsoil for water erosion to act upon. This displaced topsoil from hilltops could eventually traverse downstream, becoming linked with water contamination. Additionally, a common practice to restore soil productivity and reduce crop yield variation involves redistributing some of the accumulated topsoil from depressions back to hilltops. However, due to water erosion, portions of this accumulated topsoil can be transported into the water system, thus remaining inaccessible to the hilltops.

Over the long-term, if the tillage erosion is allowed to continue, it will move subsoil from knolls onto the depressions, burying the topsoil underneath. Consequently, productivity in depressions diminishes as well. This extended process leads to a more uniform spatial distribution of soil across the landscape. Subsoil from hilltops starts dominating the soil surface. At this juncture, the sediment carried by channelized erosion in depressions differs from that witnessed during short-term or medium-term tillage events.

Ultimately, understanding the complex interplay between short-term and long-term changes induced by tillage and water erosion is crucial for sustainable land management decisions. The choice of tillage intensity and frequency should be carefully considered to

balance the need for immediate soil preparation with the preservation of desirable spatial variability in the long run.

#### **5.4 Suggestions for future studies**

In this study, the experimental results of both Chapter 2 and Chapter 3 were associated with high variations and errors. The uncertainties of data could be rooted in the variation in experimental conditions (e.g., wind, soil texture, micro-topography, tillage depth, tillage speed etc.). Due to the nature of field experiments, it is difficult to control all conditions in the same strict manner. The in-house soil bin could be a possible option to better control all conditions. In addition, the logistics for in-house experiments are much easier than that for field experiments.

The experimental results of both Chapter 2 and Chapter 3 were designed to be incorporated into erosion models. Ideally, the greater the range and variety in channel sizes and tillage conditions (tillage equipment, tillage speed and depth) included in models, the more accurate the modeling results could be. However, due to resource limitations, the experiments of both chapters only examined one or two channel sizes and one tillage condition. To better understand the variations under real-world conditions, future studies on tillage translocation, runoff discharge and sediment export are needed for broader channel sizes and tillage conditions. These results can be used to model interaction effects between water and tillage erosion more accurately.

Regarding the modeling process, the developed ModDirTilLEM model in this study considered the interaction effect between tillage erosion and gully erosion. The first weak point

of this model is that the tillage operation has to follow horizontal or vertical directions. If the tillage direction is diagonal, a new data point must be extracted from DEMs for tillage erosion modeling. This extraction step could cause additional errors in the results. In addition, some cultivated fields in triangle shape need to be tilled in both diagonal and horizontal/vertical directions for easier operation. Therefore, the incorporation of diagonal tillage into the model is needed for modeling the tillage erosion in different scenarios. Eventually, the goal should be to have any tillage direction be simulated in ModDirTilLEM.

This study assumed a universal channel size for the current version of ModDirTilLEM. The channel size is variable under real-world conditions. When the channel is tilled, the tillage translocation varies due to different channel sizes. The variable channel size can be modeled using EphGEE. The variable channel size can increase the accuracy of modeling interaction effects.

More importantly, the errors and uncertainties of the modeled results are very high around the gully areas. This could be rooted in the dynamic erosion processes in these areas (e.g., the size and location of gullies are not exactly the same from year to year) or the low resolution and accuracy of the model input data. There is an urgent need to integrate water and tillage erosion models at the process level to simulate the dynamic nature of soil redistribution in the gully areas. For example, how the soil at different layers is translocated into the gully areas by tillage. A better understanding of the erosion process and mechanism around the gully areas is required.

A better design of the validation method around the gully area is necessary. Regarding the Cs-137 method, the current sampling point density is insufficient to capture the dynamics of erosion processes in some areas of the landscape. Based on the landform classification, there will be one sampling point close to the ephemeral gully in each transect. It is hard to understand the erosion process with such few sampling points. In addition, the frequency of drone-based air photo taken should be added. In this study, the drone photos were only taken after each major rainfall event. In other words, the surface morphology after tillage operation was missed. Visual observation can help us to better understand the erosion processes.

## APPENDIX

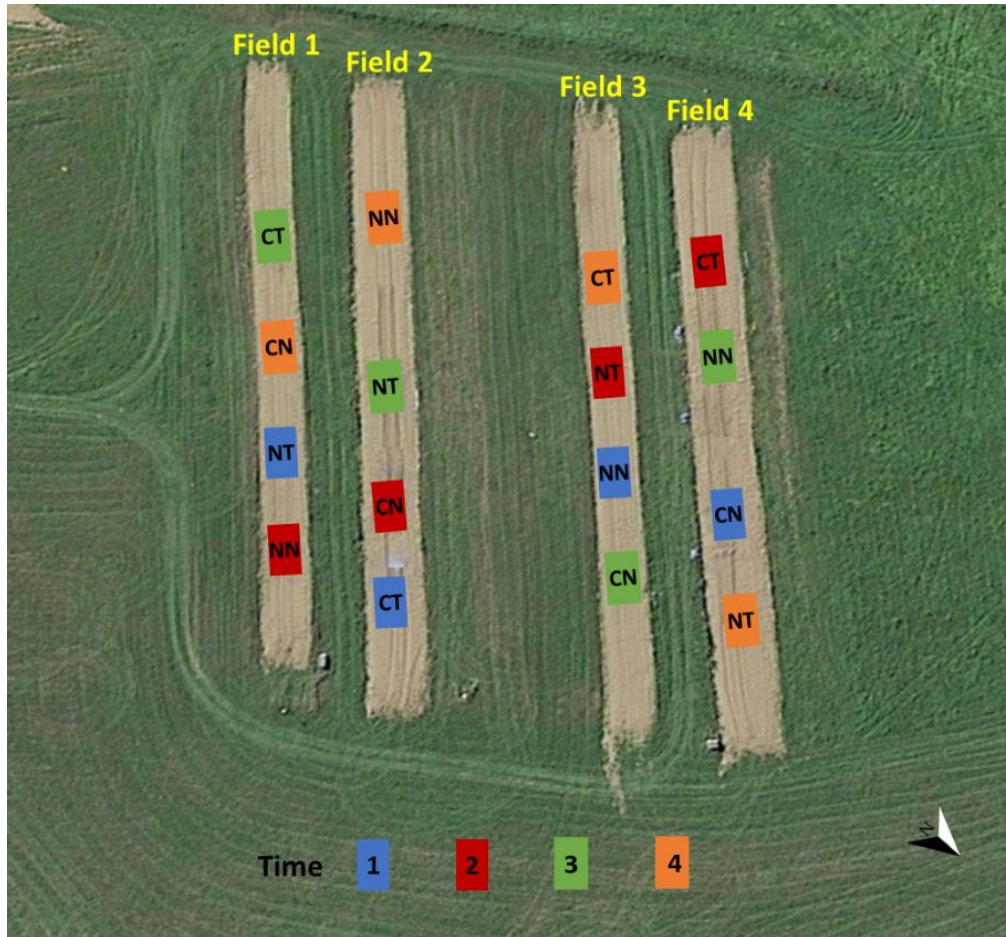


**Figure A.1.** Illustration of plot layout for the field experiment following the Latin Square design. Times of the experiments (shown in different colours) were listed in Table 3.1.

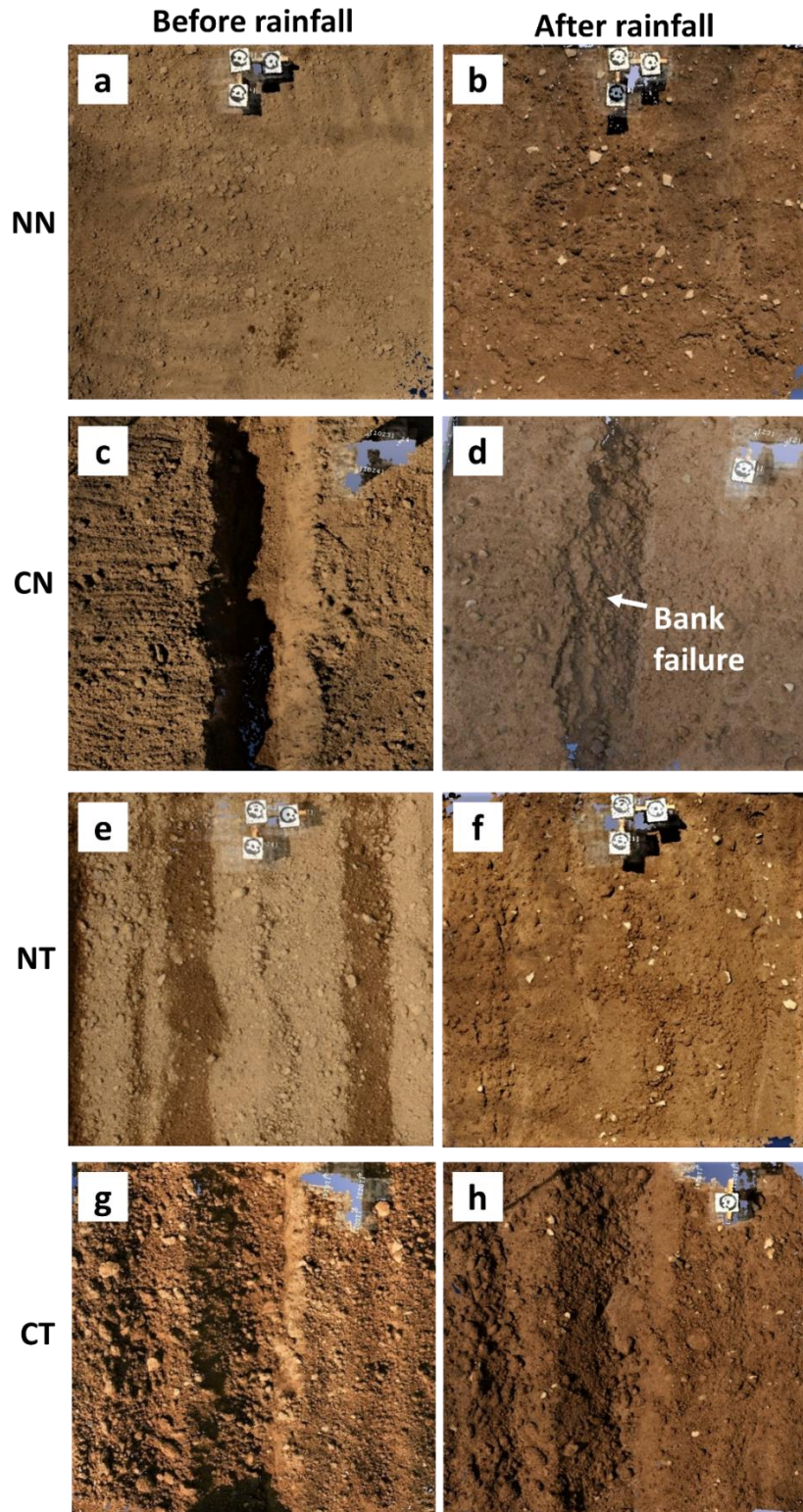


**Figure A.2.** Photos of soil surface before and after the rainfall simulation experiments for the four treatments.

**Table A.1** The p-values of comparisons between paired treatments for runoff flow rate, runoff discharge, sediment yield, total sediment export and sediment concentration obtained from the analysis of covariance (ANCOVA) for the four stages of the rainfall event

		Runoff Flow Rate			Runoff Discharge			Sediment Yield			Total Sediment Export			Sediment Concentration			
		CN	NT	CT	CN	NT	CT	CN	NT	CT	CN	NT	CT	CN	NT	CT	
1	Slope	NN	0.03*	0.22	0.23	0.05†	0.22	0.22	0.05†	0.22	0.23	0.09†	0.22	0.22	N/A	N/A	N/A
		CN	-	0.03*	0.09†	-	0.05†	0.13††	-	0.05†	0.11††	-	0.08†	0.73	-	N/A	N/A
		NT	-	-	0.23	-	-	0.22	-	-	0.22	-	-	0.22	-	-	N/A
	Intercept	NN	0.02*	0.32	0.22	0.06†	0.32	0.30	0.06†	0.32	0.26	0.13††	0.32	0.29	N/A	N/A	N/A
		CN	-	0.02*	0.05*	-	0.06†	0.11††	-	0.06†	0.11††	-	0.12††	0.70	-	N/A	N/A
		NT	-	-	0.22	-	-	0.30	-	-	0.26	-	-	0.29	-	-	N/A
2	Slope	NN	0.89	0.91	0.66	0.90	0.47	0.44	0.58	0.59	0.35	0.48	0.88	0.59	0.07†	0.38	0.02*
		CN	-	0.74	0.40	-	0.43	0.40	-	0.82	0.90	-	0.44	0.37	-	0.70	0.97
		NT	-	-	0.66	-	-	0.96	-	-	0.82	-	-	0.69	-	-	0.21
	Intercept	NN	0.04*	0.19	0.21	0.02*	0.18	0.28	0.06†	0.65	0.26	0.08†	0.55	0.79	0.27	<0.01**	0.08†
		CN	-	<0.001***	<0.001***	-	<0.001***	<0.001***	-	0.03*	0.01*	-	0.05†	0.07†	-	0.25	0.31
		NT	-	-	0.83	-	-	0.64	-	-	0.57	-	-	0.73	-	-	0.38
3	Slope	NN	0.57	0.70	0.95	0.75	0.98	0.93	0.85	0.86	0.60	0.68	0.99	0.92	0.66	0.99	0.81
		CN	-	0.41	0.52	-	0.75	0.59	-	0.93	0.94	-	0.69	0.70	-	0.51	0.35
		NT	-	-	0.62	-	-	0.88	-	-	0.77	-	-	0.93	-	-	0.75
	Intercept	NN	0.56	0.08†	0.21	0.12††	0.08†	0.22	<0.01**	0.89	0.60	0.02*	0.86	0.95	<0.001***	0.17	0.16
		CN	-	0.05*	0.09†	-	<0.01**	<0.01**	-	<0.01**	<0.01**	-	0.02*	0.02*	-	<0.001***	<0.001***
		NT	-	-	0.24	-	-	0.20	-	-	0.73	-	-	0.89	-	-	0.86
4	Slope	NN	0.80	0.70	0.65	0.80	0.79	0.98	0.70	0.86	0.84	0.89	0.84	0.95	0.97	0.99	0.91
		CN	-	0.93	0.97	-	0.61	0.71	-	0.76	0.75	-	0.80	0.85	-	0.95	0.81
		NT	-	-	0.94	-	-	0.74	-	-	0.99	-	-	0.85	-	-	0.80
	Intercept	NN	0.47	0.16	0.05*	0.44	0.07†	0.07†	<0.01**	0.28	0.93	<0.01**	0.50	0.80	<0.001***	0.92	0.14††
		CN	-	0.6	0.45	-	0.02*	0.01*	-	<0.001***	<0.001***	-	<0.01**	<0.01**	-	<0.001***	<0.001***
		NT	-	-	0.90	-	-	0.43	-	-	0.07†	-	-	0.52	-	-	<0.01**

Significance level codes: 0.001 ‘\*\*\*’, 0.01 ‘\*\*’, 0.05 ‘\*’, 0.1 ‘†’, 0.15 ‘††’.